CONSTRAINED STOCHASTIC SIMULATION OF WIND GUSTS FOR WIND TURBINE DESIGN

PROEFSCHRIFT

ter verkrijging van de graad van doctor
aan de Technische Universiteit Delft,
op gezag van de Rector Magnificus prof. dr. ir. J.T. Fokkema,
voorzitter van het College voor Promoties,
in het openbaar te verdedigen
op vrijdag 6 maart 2009 om 12:30 uur

door

Wilhelmus Anna Adrianus Maria BIERBOOMS
natuurkundig ingenieur
geboren te Eindhoven

Dit proefschrift is goedgekeurd door de promotoren:
Prof. dr. G.J.W. van Bussel
Prof. dr. ir. G.A.M. van Kuik

Samenstelling promotiecommissie:
Rector Magnificus, voorzitter
Prof. dr. G.J.W. van Bussel, Technische Universiteit Delft, promotor
Prof. dr. ir. G.A.M. van Kuik, Technische Universiteit Delft, promotor
Prof. dr. A.A.M. Holtslag, Wageningen Universiteit
Prof. dr. J. Mann, Risø DTU, National Laboratory for Sustainable Energy
Prof. dr. J. Peinke, Carl von Ossietzky University Oldenburg
Prof. dr. ir. M. Verhaegen, Technische Universiteit Delft
Dr. ir. P.H.A.J.M. van Gelder, Technische Universiteit Delft
Prof. dr. D.G. Simons, Technische Universiteit Delft, reservelid

Cover design: Wim Bierbooms & Ilma Dekker

CONTENTS

Acknowledgement

First, I am much indebted to Jan Dragt due to his original idea of constrained stochastic simulation. This new concept has been further developed during several national and international projects. I owe thanks to everyone involved in these projects for encouragement and stimulating discussions, especially Po-Wen Cheng.
Furthermore, thanks to the co-authors of the journal papers included in this dissertation: Hans Cleijne and Dick Veldkamp, as well as to the referees for their valuable comments.

A draft text leading to Chapter 6 has been reviewed by several persons. From Laurens de Haan I received instructive remarks on the topic of extreme value theory. Jan Vugts informed me about the probabilistic approach of extreme loading of offshore structures (NewWave).

I want to thank Gijs en Gerard for their patience and the members of the PhD committee for their interest.

Last but not least, this PhD research was not possible if my (former) colleagues did not have *kept me out of the wind* for a very long time.

Summary

This dissertation deals with extreme loads on wind turbines due to turbulence. For the determination of the ultimate loads some specific deterministic, coherent, i.e. constant over the rotor plane, gust shape is specified in the IEC standard. The gust shape is mainly based on a single gust measurement. Some gust amplitude is taken which should represent a 50-year wind condition. Only in case of linear systems one may assume that the 50-year response corresponds to the 50-year input. However, a wind turbine is a non-linear system, so the maximum response could well result from another load case. Another main disadvantage is that the deterministic approach in the standards does not reflect the stochastic nature of turbulence. To overcome these disadvantages an alternative approach is proposed in this thesis. The main idea behind the method is that the extreme responses occur only during severe wind gusts. So, in theory the simulations can be restricted to wind gusts which lead to the extreme response, which saves a lot of simulation time compared to simulation of long term turbulence.

The method of so-called constrained stochastic simulation is introduced. This method specifies how to efficiently generate time series around some specific event in a normal process. All events which can be expressed by means of a linear condition (constraint) can be dealt with. On the basis of the presented theory it can be stated that the stochastic gusts produced in this way are, in a statistical sense, not distinguishable from gusts selected from a (very long) time series. Two examples are given: the generation of stochastic time series around local maxima and the generation of stochastic time series around a combination of a local minimum and maximum with a specified time separation ("extreme rise time gust"). The constrained time series turn out to be a combination of the original process and several correction terms which includes the autocorrelation function and its time derivatives. For the application concerning local maxima it is shown that the presented method is in line with properties of a normal process near a local maximum as found in literature. Simplification of the expression for maximum amplitude gusts leads to an expression that in previous work has been coined *New*Gust. This expression also corresponds to the NewWave expression for the mean shape of an extreme wave in a random sea.

The mean gust shape of maximum amplitude gusts has a rather sharp peak, in contradiction to the gust shape given in standards. The verification of the mean gust shape is done by means of wind measurements from the Cabauw (The Netherlands) site. On the basis of a statistical analysis an expression of the mean gust shape is obtained. This theoretical gust shape is compared with the mean gust shape determined from both simulated and measured turbulence. The resemblance is remarkably good which demonstrates the viability of the method of constrained simulation.

It may be anticipated hat the extreme loading for pitch regulated turbines is caused by gusts with an extreme rise time rather than a local maximum. Constrained stochastic simulation is applied in order to generate the desired gusts. Just as wind field simulation for fatigue purposes it is assumed that turbulence is Gaussian; a possibility is mentioned how to deal with non-Gaussian behavior. An example of a spatial gust as well as the mean spatial gust shape is shown. For a reference turbine the maximum blade root flapping moment have been determined as function of the gust centre in the rotor plane; the maximum response is obtained in case the gust hits one of the rotor blades at 75% of the radius. In case the gust duration is large compared to the integral time constant of the controller, the controller can handle the gust as expected. However even for small rise times it turns out that the maximum flap moment due to the gust is not significantly higher than due to the background turbulence and 1P excitations. This indicates that extreme rise time gusts do not lead to extreme loading of pitch regulated wind turbines.

Next, constrained stochastic simulation is used in order to generate specific wind gusts which will in fact lead to local maxima in the response of (pitch regulated) wind turbines. This is done by considering constraints on the wind input but also on the wind turbine response. For this purpose the power spectrum of turbulence as well as the transfer function from wind input to load is required. The method is demonstrated on basis of a linear model of a wind turbine, inclusive pitch control. The mean gust shape as well as the mean shape of the response, for some gust amplitude, is shown. By performing many simulations (for given gust amplitude) the conditional distribution of the response is obtained. By a weighted average of these conditional distributions over the probability of the gusts the overall distribution of the response (for given mean wind speed) can be obtained. Analytical expressions for the conditional distribution of the response (for given gust amplitude) as well as the overall distribution are specified. These form an ideal test case of tools (e.g. fitting to an extreme value distribution) to be used for non-linear wind turbine models. The analytical expression for the overall distribution of the response turns out to correspond to the Rice distribution of local maxima, which validates the method.

The method described above is applied to a non-linear wind turbine model and not just for one mean wind speed but for several ones in between cut-in and cut-out. The overall distribution of the response is obtained by a weighted average of the distributions for each wind speed bin taking into account the probability of occurrence of those wind speed bins. This overall probabilistic method is demonstrated on the basis of a generic 1 MW stall regulated wind turbine. By first considering a linearised dynamic model of the reference turbine the proposed probabilistic method could again be validated. The determined 50 year response value indeed corresponds to the theoretical value (based on Rice). Next, both constrained and (conventional) unconstrained simulations have been performed for the non linear wind turbine model. For each wind speed bin a number of 100 simulations are performed. For the governing wind speed bins the

number of unconstrained simulations has been increased to 1000 to serve as reference result. For all wind speed bins the results obtained via constrained simulation are better than those using unconstrained simulations in both 50 year estimates as well as uncertainty range of this estimate. The involved computational effort for both methods is about the same.

The required gust statistics of the gust shapes treated in this work (maximum amplitude gust, extreme rise time gust and the specific gust shape leading to an extreme wind turbine response) are specified.

During the employment of the probabilistic method, the contributions of each gust amplitude (or mean wind speed) to the estimation of the tail probability can be established. This provides a rational base for the determination of the required range of gust amplitudes (or mean wind speeds) as well as the discretisation.

The uncertainty range, inherent in the extrapolation from a limited data set to 50 year, is rather large even if 1000 10-min. simulations are performed. It is recommended to mention the uncertainty involved in a 50 year estimate.

For the wind turbine simulations mentioned above, wind gusts are applied which will lead to local maxima in the response. It is shown that in principle any other type of gust could have been applied as well in the probabilistic method. However, if there is no clear correlation between gust and response (i.e. an increase of the gust amplitude leads to higher loads) constrained stochastic simulation has no advantage above conventional, unconstrained simulations.

Comparison between wind turbine load measurements and simulations is complicated by the uncertainty about the wind field experienced by the rotor. By means of constrained simulation wind fields can be generated which encompass measured wind speed series. If the method of constrained wind is used in load verification, the low frequency part of the wind and of the loads can be reproduced well, which makes it possible to compare time traces directly. However from the three load cases for the reference wind turbine investigated here, it appeared that there was no clear improvement in fatigue damage equivalent load ranges.

In future research constrained simulations will also be applied to other current wind turbines and loads. A practical limitation to consider a complete wind field can be the determination of the required transfer functions from wind field (i.e. many points in the rotor plane) to the load of interest. The required number of simulations for each gust amplitude as well as choice of the distribution function (with of without endpoint) may be further investigated. A final validation of any method to come to a 50 year response would be comparison with long term wind turbine load measurements.

Samenvatting

Deze dissertatie behandelt de extreme belastingen op windturbines ten gevolge van turbulentie. In de IEC norm wordt een bepaalde deterministische vlaag, constant over het rotorvlak, voorgeschreven voor de bepaling van de maximale belasting. De betreffende vlaagvorm is grotendeels gebaseerd op een enkele vlaagmeting. De amplitude is zodanig dat het een 50-jaars vlaag moet voorstellen. In geval van een lineair systeem kan er vanuit gegaan worden dat de 50-jaars responsie samenvalt met de 50-jaars vlaag. Een windturbine is echter niet-lineair dus de maximale responsie zou ook tijdens een andere wind situatie kunnen optreden. Een ander nadeel van de deterministische aanpak in de norm is dat het het wezenlijke kenmerk van turbulentie, te weten het is chaotisch, niet in rekening brengt. Om deze nadelen te verhelpen wordt in deze thesis een alternatieve aanpak geïntroduceerd. Het basisidee daarachter is dat extreme responsies alleen optreden gedurende harde windvlagen. In principe kan er dus volstaan worden met het simuleren van deze harde vlagen wat een grote reductie in rekentijd oplevert ten opzichte van simulatie van langdurige turbulentie.

Met de zogenaamde methode van voorwaardelijke stochastische simulatie kunnen bijzondere gebeurtenissen in een normaal stochastisch proces efficiënt gegenereerd worden. Alle gebeurtenissen die te beschrijven zijn met een lineaire conditie (voorwaarde) kunnen behandeld worden. Op grond van de voorgestelde theorie kan gesteld worden dat de zo gegenereerde vlagen statistisch gezien niet te onderscheiden zijn van vlagen die uit een erg lange tijdreeks geselecteerd zijn. Er worden twee voorbeelden gegeven: het genereren van stochastische tijdreeksen rondom een lokaal maximum en het genereren van stochastische tijdreeksen rondom een combinatie van een lokaal minimum en maximum met een bepaald tijdsverschil (kortom vlagen met een snelheidsprong). De uitdrukking voor de voorwaardelijke tijdreeksen blijkt een combinatie te zijn van de oorspronkelijke tijdreeks en enkele correctie termen die de autocorrelatie functie bevatten en tijdsafgeleiden daarvan. Voor de maximale-amplitude-vlagen die met de nieuwe methode zijn gegenereerd, wordt aangetoond dat ze inderdaad de eigenschappen hebben van een normaal proces rondom een lokaal maximum zoals die in de literatuur vermeld worden. Een vereenvoudiging van de uitdrukking voor maximale-amplitude-vlagen leidt tot een uitdrukking die in voorgaand werk *New*Gust is gedoopt. Deze uitdrukking komt ook overeen met de NewWave uitdrukking die de gemiddelde vorm weergeeft van een extreme windgolf in zeegang.

De gemiddelde vlaagvorm van maximale-amplitude-vlagen blijkt in tegenstelling tot de vlaagvorm in normen een nogal scherpe piek te bevatten. De gemiddelde vlaagvorm is geverifieerd op basis van windmetingen te Cabauw (Nederland). Met behulp van een statistische analyse is een uitdrukking voor de gemiddelde vlaagvorm afgeleid. Deze theoretische vlaagvorm is vergeleken met

de gemiddelde vlaagvorm van zowel gesimuleerde als gemeten turbulentie. De overeenkomst is opmerkelijk goed wat de potentie van de methode van voorwaardelijke stochastische simulatie aantoont.

Men kan verwachten dat de maximale belasting van bladhoek geregelde windturbines niet optreedt tijdens maximale-amplitude-vlagen, maar tijdens vlagen met een snelheidsprong. De methode van voorwaardelijke stochastische simulatie is toegepast om vlagen met zo'n snelheidsprong te genereren. Net als bij windveldsimulatie voor vermoeiingsanayse is aangenomen dat turbulentie Gaussisch is. Een mogelijkheid hoe eventeel niet-Gaussisch gedrag meegenomen kan worden, wordt aangestipt. Een voorbeeld van een ruimtelijk vlaag alsook de gemiddelde ruimtelijke vlaag wordt getoond. Voor een referentie windturbine is het maximale klapmoment bij de bladwortel bepaald als functie van de positie van het vlaagcentrum in het rotorvlak. De maximale responsie treedt op als de vlaag een van de rotorbladen treft op driekwart straal. In geval de vlaagduur lang is vergeleken met de integrale tijdsconstante van de regeling, kan de regeling naar verwachting de vlaag wegregelen. Echter ook in geval van een erg snelle snelheidsprong blijkt het maximale klapmoment ten gevolve van de vlaag niet veel groter te zijn dan ten gevolge van gewone turbulentie en 1P excitaties. Dit geeft aan dat vlagen met een sterke helling niet maatgevend zijn voor bladhoekgeregelde windturbines.

Vervolgens is de methode van voorwaardelijke stochastische simulatie toegepast om die specifieke windvlagen te genereren die wel tot lokale maxima in de responsie leiden. Dit is gedaan door niet alleen voorwaarden op te leggen aan de windinvoer maar ook aan de responsie van de windturbine. Om dit te kunnen doen dient het turbulentiespectrum bekend te zijn én de overdrachtsfunctie van windinvoer naar de belasting. De methode is eerst toegepast op een lineair model van een windturbine (inclusief bladhoekregeling). De gemiddelde vlaagvorm en gemiddelde vorm van de responsie, voor een gegeven vlaagamplitude, worden getoond. Door het doen van vele simulaties, voor gegeven vlaagamplitude, kan de voorwaardelijk verdeling van de responsie bepaald worden. Via een gewogen gemiddelde, over de verdeling van de vlaagamplitudes, van deze voorwaardelijke verdelingen kan de verdeling van de responsie bepaald worden (voor een gegeven gemiddelde windsnelheid). Analytische uitdrukkingen voor de (voorwaardelijke) verdeling van de responsie worden gegeven. Deze uitdrukkingen kunnen gebruikt worden voor het testen van hulpmiddelen bij het bepalen van de maximale belastingen van niet-lineaire windturbine modellen, zoals programma's die simulaties (of metingen) passen aan een extreme waarde verdeling. De analytische uitdrukking van de verdeling van de responsie blijkt overeen te komen met de Rice verdeling van lokale maxima. Hiermee is de methode gevalideerd.

De hierboven beschreven methode is toegepast op een niet-lineair windturbine model en niet slechts voor één windsnelheid maar voor meerdere windsnelheden tussen de inschakel- en uitschakelwindsnelheid. De uiteindelijke

verdeling van de responsie wordt verkregen via weging van de verdeling voor elke windsnelheidsinterval met de kans op voorkomen van die windsnelheidintervallen. Deze probabilistische methode is gedemonstreerd aan de hand van een generieke 1 MW overtrekgeregelde windturbine. De probabilistische methode kan weer gevalideerd worden door het eerst toe te passen op een gelineariseerd dynamisch model van de referentie turbine. De bepaalde 50-jaars responsie is inderdaad gelijk aan de theoretische waarde (gebaseerd op Rice). Vervolgens zijn zowel voorwaardelijke stochastische simulaties als (normale) onvoorwaardelijke stochastische simulaties uitgevoerd met het niet-lineaire windturbine model. Voor elke windsnelheidsinterval zijn 100 simulaties gedaan. Voor de bepalende windsnelheidintervallen is dat aantal opgevoerd tot 1000 om als referentie resultaat te kunnen dienen. Voor alle windsnelheidintervallen zijn de resultaten verkregen via voorwaardelijke stochastische simulatie beter dan die via nomale simulaties; de 50-jaars schattingen zijn beter en de onzekerheidsmarge kleiner. De benodigde rekentijd is voor beide methoden ongeveer gelijk.

De benodigde vlaagstatistiek van de in dit werk beschouwde vlagen (maximale-amplitude-vlagen, vlagen met snelheidsprong en de specifieke vlagen die leiden tot een extreme responsie van de windturbine) zijn vermeld.

De bijdragen van elke vlaagamplitude (of gemiddelde windsnelheid) aan de schatting van de staart van de verdeling kan berekend worden tijdens het toepassen van de probabilistische methode. Op basis hiervan kan een rationele afweging gemaakt worden van het benodigde gebied van vlaagamplitudes (of windsnelheden) en de benodigde onderverdeling.

De onzekerheidsband, inherent bij de extrapolatie van een beperkte dataset naar 50 jaar, is nogal groot zelfs als er 1000 10-min. simulaties zijn uitgevoerd. Het wordt aanbevolen om deze onzekerheid te vermelden bij elke 50-jaars schatting.

Voor de bovengenoemde windturbine simulaties zijn de specifieke windvlagen gebruikt die leiden tot een lokaal maximum in de responsie. Er wordt aangetoond dat in principe elke vlaagtype toepast kan worden in de probabilistische methode. Echter als er geen duidelijke correlatie is tussen vlaag en responsie (dus dat bij een toename van de vlaagamplitude de belasting hoger wordt) biedt voorwaardelijke stochastische simulatie geen voordeel ten opzichte van normale simulaties.

De vergelijking tussen gemeten en gesimuleerde windturbine belastingen wordt altijd bemoeilijkt door onzekerheid in het windveld die de rotor voelt. Door voorwaardelijke stochastische simulatie kunnen windvelden gegenereerd worden die de gemeten windtijdreeks(en) bevatten. Het laag frequente deel van de wind en de belastingen blijkt goed gereproduceerd te worden als de methode van voorwaardelijke stochastische simulatie wordt toegepast. Dit maakt het mogelijk om gemeten en gesimuleerde belastings tijdreeksen direct te vergelijken. Echter op grond van drie belastings gevallen voor de onderzochte referentie windturbine blijkt er geen duidelijke verbetering op te treden in de equivalente vermoeiingsbelasting.

In vervolg onderzoek zal voorwaardelijke stochastische simulatie ook toegepast worden op andere huidige windturbines en andere belastingen. Een praktische beperking om een compleet windveld te gebruiken zou kunnen zijn dat de benodigde overdrachtsfuncties van windveld (dus vele punten in het rotorvlak) naar de betreffende belasting niet beschikbaar zijn. Het benodigd aantal simulaties per vlaagamplitude en de keuze van de verdelingsfunctie (met of zonder eindpunt) kan nader onderzocht worden. De ultieme validatie van elke methode om de 50-jaars responsie te bepalen is de vergelijking met langdurige windturbine belastingsmetingen.

Introduction

This dissertation deals with extreme loads on wind turbines. In general the extremes can be due to all kind of wind conditions, internal or external failures (e.g. grid loss) and may also happen during start-up or shut-down. Here we limit ourselves to normal wind conditions during power production (i.e. in between cut-in and cut-out wind speed). So, the extreme loads dealt with can be associated with turbulence. This implies that specific wind conditions like thunderstorms, front passages, downbursts and hurricanes are excluded. The wind speed variations due to a front passage are slower than those due to turbulent gusts. So, with respect to wind turbines a front passage is probably relevant for power balancing but not so much for loads. The wind speeds (averaged over 1-minute) inside a hurricane can be up to 95 m/s, Ref. 6, which is far more than the extreme (10-min.) mean wind speed of 50 m/s mentioned in the IEC standard (IEC 61400-1 Ed. 3, 2005). However, in the hurricane prone country Japan, hurricanes (typhoons) are included in the wind turbine standard. Downbursts are not rare and will perhaps be taken into account in wind turbine standards in the near future. Methods to simulate downbursts are given in Ref. 7 and 8. As mentioned, downbursts are not considered in this work since they require a different modeling approach.

Present wind turbine design packages comprise three components. The first part models wind shear, tower shadow and generates wind fields which resemble the stochastic nature of turbulence. It is common practice to generate all three velocity components covering the rotor disc. The second part concerns the dynamics of the wind turbine including the aerodynamic forces and gravity. The third part is the post processing, like the determination of the ultimate loading and fatigue analysis. The focus of this research is on the generation of wind fields; existing design tools are used to assess the ultimate loads resulting from the generated wind fields. A good introduction to wind field simulation is given by Ref. 1 where Ref. 2 provides an overview of the state-of-the-art.

For the determination of the ultimate loads some specific deterministic, coherent, i.e. constant over the rotor plane, gust shape is specified in the IEC standard: Extreme Operating Gust (EOG). The gust shape is mainly based on a single gust measurement. Some gust amplitude is taken which should represent a 50-year wind condition. Only in case of linear systems one may assume that the 50-year response corresponds to the 50-year input. However, a wind turbine is a non-linear system, so the maximum response could well result from another load case. Another main disadvantage is that the deterministic approach in the standards does not reflect the stochastic nature of turbulence.

To overcome these disadvantages an alternative approach is proposed in this thesis. The main idea behind the method is that the extreme responses occur only during severe wind gusts. So, in theory the simulations can be restricted to wind gusts which lead to the extreme response, which saves a lot of simulation time. In order to do so two questions have to be answered:

1. how to generate these gusts?
2. which gusts are relevant?

Constrained stochastic simulation

The first question is tackled by so-called constrained stochastic simulation. By means of (normal) stochastic simulation wind time series can be generated which resembles turbulence. Nowadays, this is a standard feature of wind turbine design packages. Constrained stochastic simulation is a special kind of stochastic simulation which allows generation of wind gusts which satisfy some specified constraint (condition). E.g. one may generate time series around a local maximum with specified amplitude, or wind gusts which contain a prescribed velocity jump in a specified rise time ('extreme rise time gusts'). These wind gusts are embedded in a stochastic background in such a way that they are, in statistical sense, not distinguishable from real wind gusts (with the same characteristics of the constraint). Constrained stochastic simulation is treated in detail in Chapter 2. As examples maximum amplitude gusts and extreme rise time gusts are dealt with. Simplification of the expression for maximum amplitude gusts, by omitting the constraint that the extreme event has to be a local maximum (i.e. it may also be a local minimum) leads to an expression that in previous work has been coined *New*Gust, Ref. 3. This expression corresponds to the NewWave expression for the mean shape of an extreme wave in a random sea, as used by the offshore industry to assess the extreme wave loads on offshore structures. NewWave is based on the mathematical work of Lindgren, Ref. 4.

For answering the second question a distinction should be made between stall and pitch regulated wind turbines. For the first type of wind turbines it may be anticipated that maximum amplitude gusts are governing the response, see Chapter 3. For pitch regulated turbines extreme rise time gusts are a possible candidate, since the controller may not be able to respond to fast velocity changes. However, wind turbine load simulations show that this is not the case, Chapter 4. The negative result from Chapter 4 necessitates further research on the specific gust shape which indeed leads to an extreme response for pitch turbines. In Chapter 5 a thorough analytical treatment is given on this topic. In order to generate such a gust, the power spectrum of turbulence as well as the transfer function from wind input to load is required. The latter implies that a linearised model of the wind turbine under consideration is needed and that the constrained gust depends on the specific wind turbine and load signal. This linearised wind turbine model is used once for the determination of the gusts; the load calculations should be performed with the original, non-linear model.

Probabilistic method

By performing many simulations (for given gust amplitude) the conditional distribution of the response is obtained. By a weighted average of these conditional distributions over the probability of the gusts the distribution for given mean wind speed is determined. An analytical expression of the required distribution of the gust amplitude is given in Chapter 5. See Chapter 2 for the

statistics of maximum amplitude gusts and extreme rise time gusts. The overall distribution of the response is obtained by a weighted average of the distributions for each wind speed bin taking into account the probability of occurrence of the wind speed bins (Weibull distribution). This probabilistic method is presented in detail in Chapter 6 and demonstrated for a reference turbine. During the employment of the probabilistic method, the contributions of each gust amplitude (or mean wind speed) to the estimation of the tail probability can be established. This provides a rational base for the determination of the required range of gust amplitudes (or mean wind speeds) as well as the discretisation.

Comparison simulated and measured loads

In Chapter 7 constrained stochastic simulation is used in another way. Time domain comparison between simulated and measured wind turbine loads is in practice hindered by the uncertainty of the actual spatial wind field. By application of constrained stochastic simulation, constrained on the measured wind speeds (perhaps of more than 1 anemometer), a wind field can be created which encompass the measured ones. This enables direct comparison of time traces of measured and simulated loads.

Recommendations

Finally, chapter 8 deals with the implementation of the results of this thesis into design standards.

Validation of the method

Verification of any method to determine the long term extreme response is only possible in case long term wind turbine load and wind measurements are available. Since this is not the case validation is the alternative. The method of constrained stochastic simulation is validated by considering maximum amplitude gusts. In Chapter 2 it is shown that it is in line with the properties of a normal process near a local maximum as derived by Lindgren, Ref. 4.

The mean gust shape of maximum amplitude gusts has a rather sharp peak, in contradiction to the gust shape given in standards. The mean gust shape has also been determined on basis of measured wind data from the Cabauw (in the Netherlands) site. The resemblance between the theoretical and experimental curves is treated in Chapter 3.

The probabilistic method to arrive at the 50 year response, as mentioned above, is also applied to a *linearised* model (for each mean wind speed) of the reference turbine. The reason to do so is that a theoretical expression exists for the distribution of local maxima in a normal process, Ref. 5. This makes a validation of the probabilistic method possible since the response of a linear system to a Gaussian input (turbulence) will also be Gaussian. In Chapter 5 it is analytically shown that the distribution of local maxima in the response obtained trough constrained simulation indeed corresponds to the Rice distribution. In Chapter 6 the same is numerically demonstrated by means of wind turbine simulations.

Additional remarks

As stated above it is nowadays common to consider spatial wind fields rather than a coherent one for wind turbine load calculations. Such spatial wind fields have been considered in Chapters 3, 4 and 7. Just for convenience a coherent gust has been taken in the other three Chapters. It should be possible to extent this to spatial ones similar as explained in Chapter 4. In Chapter 4 also the influence of the gust centre, with respect to the rotor plane, on the loading is considered.

A basic assumption of the method presented here is that turbulence is Gaussian (just as is assumed in case of wind field simulation for fatigue analysis). A possible way to take non-Gaussian behavior into account is addressed in Chapter 4.

In Chapter 3 a statistical method has been applied in order to derive a mean gust shape. This expression, Eq. (19), appeared to deviate somewhat from the expression based on constrained stochastic simulation, Eq. (1) from Chapter 3. In the mean time the difference can be explained, see Appendix A.

An attentive reader may notice a typo in Eq. (D.19) in Chapter 5. It should read:

$$f_\eta(\eta) = \eta\sqrt{1-\varepsilon^2}\, e^{-\frac{\eta^2}{2}} \Phi(\frac{\eta\sqrt{1-\varepsilon^2}}{\varepsilon}) + \frac{1}{\sqrt{2\pi}}\varepsilon\, e^{-\frac{\eta^2}{2\varepsilon^2}}$$

Furthermore, the Cabauw met-mast is 213 m tall instead of 240 m as mentioned in Chapter 3.

References

[1] P.S. Veers, Three-dimensional wind simulation, Technical Report SAND88-0152 UC-261, Sandia National Laboratories, 1988.

[2] J. Mann, Simulation of turbulence, gusts and wakes for load calculations, Proceedings of the Euromech Colloquium 464b Wind Energy, 2007.

[3] W. Bierbooms, P.W. Cheng., G. Larsen, B.J. Pedersen, Modeling of extreme gusts for design calculations – *New*Gust FINAL REPORT JOR3-CT98-0239, Delft University of Technology, 2001.

[4] G. Lindgren, Some properties of a normal process near a local maximum, The Annals of Mathematical Statistics, 41, 1870--1883, (1970).

[5] S.O. Rice, Mathematical analysis of random noise, Bell Syst. Techn. J., 23, 282 (1944). [Reprinted in Wax, N. (ed.), Selected papers on noise and stochastic processes, Dover Publ., 1958].

[6] Roland B. Stull, Meteorology for Scientists and Engineers, Brooks/Cole, 2000.

[7] M.T..Chay, F. Albermani, R. Wilson, Numerical and analytical simulation of downburst wind loads, Engineering Structures, 28, 240-254, 2006.

[8] Ahsan Kareem, Numerical simulation of wind effects: a probabilistic perspective, Journal of Wind Engineering and Industrial Aerodynamics, 96, 1472-1497, 2008.

Constrained stochastic simulation—generation of time series around some specific event in a normal process

Wim Bierbooms

Abstract The method of so-called constrained stochastic simulation is introduced. This method specifies how to efficiently generate time series around some specific event in a normal process. All events which can be expressed by means of a linear condition (constraint) can be dealt with. Two examples are given in the paper: the generation of stochastic time series around local maxima and the generation of stochastic time series around a combination of a local minimum and maximum with a specified time separation. The constrained time series turn out to be a combination of the original process and several correction terms which includes the autocorrelation function and its time derivatives. For the application concerning local maxima it is shown that the presented method is in line with properties of a normal process near a local maximum as found in literature. The method can e.g., be applied to generate wind gusts in order to assess the extreme loading of wind turbines.

1. Introduction

Verification of the structural integrity of a wind turbine structure involves analyses of fatigue loading as well as extreme loading. The extreme loading may result during transient operation (start and stop actions), faults and extreme wind events like extreme mean wind speeds, extreme wind shear, extreme wind speed gusts and extreme wind direction gusts. In this paper we restrict ourselves to extreme wind

W. Bierbooms (✉)
Wind Energy Research Group,
Delft University of Technology, Delft, The Netherlands
e-mail: w.a.a.m.bierbooms@tudelft.nl

Springer

gusts. With persistently growing turbines (over 100 m in both rotor diameter and tower height), the extreme loading seems to become relatively more important. The reason for this is that high-frequency wind speed fluctuations, relevant for fatigue, have a limited spatial extent and so will be cancelled out over the rotor plane. In order to assess the fatigue loading generated random 3D wind fields are routinely used in standard wind turbine design packages as used by the wind turbine industry. The stochastic wind fields of typically 10 min of length are generated for different mean wind speeds to cover the wind situations a turbine will meet during its life time. For the stochastic wind field simulation it is assumed that turbulence is a stationary Gaussian process specified by a given (cross) spectral density. The extreme loads are however dealt with in a rather simple way by describing wind gusts as coherent gusts of an inherently deterministic character, e.g., IEC-standard (1998), whereas the gusts experienced in real situation are of a stochastic nature with a limited spatial extension. This conceptual difference may cause substantial differences in the load patterns of a wind turbine when a gust event is imposed. In order to introduce realistic gust load situations of a stochastic nature the *New*Gust method, Dragt and Bierbooms (1996), Bierbooms et al. (2001) and Bierbooms and Dragt (2000), was developed. In this probabilistic method gusts of a given amplitude are generated and used to perform a wind turbine load calculation. A basic assumption of the method is that extreme wind gusts can still be described by means of Gaussian processes. The distribution of the extreme load due to wind gusts (or the 50-years extreme load) can be determined by taking into account all gust amplitudes and all mean wind speeds. The method seems to be fit for stall regulated wind turbines (i.e., with fixed blades) since they are significantly affected by extreme wind speed gusts. For pitch regulated wind turbines it turned out that extreme wind speed gusts did not result in higher loads due to the pitch actions initiated by the control system. Pitch regulated wind turbines may be sensitive to other types of gusts, e.g., extreme rise time gust. The theoretical expression for the mean shape of extreme wind speed gusts has been verified by Bierbooms et al. (2001) and Bierbooms et al. (1999) by comparison with an experimentally derived mean gust shape based on many time records from the Database on Wind Characteristics (http://www.winddata.com). Furthermore the probability of occurrence of gusts has been verified on basis of the same database, Bierbooms et al. (2001).

In the past the stochastic properties of a (normal) process around some specific event have already been frequently studied, especially by means of a Slepian model. This is a random function representation of the process after a level crossing and it consists of one regression term and one residual process. By means of regression approximations it is possible to arrive at e.g., wavelength and amplitude distribution or an approximate density of the response of a random mechanical system, Lindgren and Rychlik (1991). In this paper we are not primarily interested in an approximation of the statistics of the forcing process or response but we will focus on the generation of time series around some specific event in a normal process. The reason for this is that for wind turbine design it is common to consider time domain simulations due to the involved (strong) non-linearities (e.g., the wind force is quadratic in the wind speed; flow separation on the rotor blades). An easy method to generate time series has been denoted constrained stochastic simulation and is dealt with in Section 2. Although the method can be applied for a multivariable normal process just a single normal process will be considered for simplicity. Two examples of events will be shown; in Section 3 local maxima will be considered and

in Section 4 velocity jumps (a non-Slepian process) will be discussed. The treatment of local maxima allows comparison with well known results from literature. Constrained stochastic simulation is already applied in order to generate wind gusts as input for wind turbine design tools to assess the ultimate loads of wind turbines. The overall probabilistic method to determine the extreme response of wind turbines is briefly outlined in Section 5.

2. Constrained stochastic simulation

2.1. Stochastic simulation

In order to describe constrained stochastic simulation we first draw attention to convential stochastic simulation, Shinozuka (1971); as mentioned before the present formulation of the method is restricted to a single normal process. Stochastic time series generators are based on the summation of harmonics with random phase φ (uniformly distributed between 0 and 2π) and amplitudes which follow from the (one-sided) auto power spectral density S:

$$u(t) = \sum_{k=1}^{K} \sqrt{\frac{2\,S_k}{T}} \cos\left(\omega_k t + \varphi\right) \tag{2.1}$$

where t is the (discretised) time, T the total time of the sample and ω_k a set of K equidistant frequencies. For our purpose an alternative description by means of a Fourier series is more appropriate (since the applied theory (Section 2.3) concerns normal random variables):

$$u(t) = \sum_{k=1}^{K} a_k \cos \omega_k t + b_k \sin \omega_k t \tag{2.2}$$

For a normal process $u(t)$, with zero mean, also the Fourier coefficients a_k and b_k will be normal. Their means are zero, they are mutually uncorrelated and their variances are S_k/T.

2.2. Specification of a constraint

One may be interested in specific events in time series of a normal process $u(t)$, e.g., local maxima. A 'brute-force' method to obtain such events is to select these from very long time series of the stochastic process (either measured or stochastically simulated). It will be clear that such an approach is far from practical for events which will occur on average just once in a year or even 50 years. An alternative is to perform a special kind of stochastic simulation during which the desired events are automatically selected. This method has been denoted constrained stochastic simulation.

The applicability of the proposed method is restricted to events which can be expressed as a linear relation:

$$\boldsymbol{y} = \boldsymbol{G}\boldsymbol{x} \tag{2.3}$$

with $\boldsymbol{G}$ a matrix of constants, $\boldsymbol{y}$ a random vector describing the event (constraint) and $\boldsymbol{x}$ a random vector describing the process (e.g., wind velocities at different time

points or the Fourier coefficients). In Sections 3 and 4 G will be specified for the events considered in this paper: local maxima and velocity jumps.

In other words the wind velocities (or the Fourier coefficients) which are normally distributed should satisfy the above conditions (constraints) in order to obtain the desired event. So, selecting some specific event (from a time series) corresponds with considering the matching conditional density.

2.3. Conditional density

Consider normal random vectors x and y with zero means. Suppose that the covariance matrix of the joint random vector $z = \binom{x}{y}$ is:

$$\mathbf{E}[zz^\mathrm{T}] = \begin{pmatrix} M & N^\mathrm{T} \\ N & Q \end{pmatrix} \tag{2.4}$$

i.e.,

$$M = \mathbf{E}[x\,x^\mathrm{T}], \quad Q = \mathbf{E}[y\,y^\mathrm{T}] \text{ and } N = \mathbf{E}[y\,x^\mathrm{T}]$$

The conditional density $f(x|y)$ of x upon observing y is again normal and thus determined by its mean m_c and covariance matrix M_c. The condition y can be a specific value $y = Y$, with Y a constant vector, to be specified later. The mean m_c and covariance matrix M_c can be found in handbooks on statistics, e.g., Rao (1965); sometimes it is denoted as Matrix Inversion Lemma or Sherman-Morrison-Woodbury formula, Mortensen (1987):

$$m_c = N^\mathrm{T} Q^{-1} Y \tag{2.5}$$

$$M_c = M - N^\mathrm{T} Q^{-1} N \tag{2.6}$$

We will consider the special case that y is a linear combination of x, i.e., $y = Gx$ with given weight matrix G. The covariance matrix M_c is now singular. It can be shown that the above relations still hold:

$$m_c = M G^\mathrm{T} Q^{-1} Y \tag{2.7}$$

$$M_c = M - M G^\mathrm{T} Q^{-1} G M \tag{2.8}$$

with

$$Q = G M G^\mathrm{T} \tag{2.9}$$

2.4. Constrained stochastic simulation

The theory explained in Section 2.3 can be applied to either the wind speeds or the Fourier coefficients of Eq. 2.2. We choose for the latter:

$$x = (\,a_1\,a_2\ldots a_k b_1 b_2 \ldots b_K\,)^\mathrm{T} \tag{2.10}$$

~10~

since then the covariance matrix M of x is diagonal with elements S_k/T:

$$M = \mathbf{E}\left[xx^\mathrm{T}\right] = \frac{1}{T} \begin{pmatrix} S_1 & 0 & 0 & 0 & 0 & 0 & 0 \\ 0 & S_2 & 0 & 0 & 0 & 0 & 0 \\ 0 & 0 & \ldots & 0 & 0 & 0 & 0 \\ 0 & 0 & 0 & S_K & 0 & 0 & 0 \\ 0 & 0 & 0 & 0 & S_1 & 0 & 0 \\ 0 & 0 & 0 & 0 & 0 & \ldots & 0 \\ 0 & 0 & 0 & 0 & 0 & 0 & S_K \end{pmatrix} \tag{2.11}$$

The desired event is described by the constraint, Eq. 2.3. The constrained stochastic variable, which satisfies the constraint, is given by:

$$x_c = x + MG^\mathrm{T}Q^{-1}(Y - Gx) \tag{2.12}$$

with M according to Eq. 2.11 and $Q = GMG^\mathrm{T}$ (Eq. 2.9).

This concludes the required theory. In case the Fourier sum is calculated for the Fourier coefficients x, normally distributed with covariance matrix given by Eq. 2.11, a random time series is obtained. In case the Fourier sum is calculated for the Fourier coefficients x_c, according to Eq. 2.12, the desired event is obtained. It is straightforward to implement this in a computer code. In the following Sections 2 examples of events will be considered.

3. Local maxima

3.1. Specification of local maxima

We now make the constrained stochastic simulation, Eq. 2.12, more specific: the simulation of local maxima. By doing so the method can be demonstrated and also verified since local maxima in a normal process have already been extensively studied by others. A local maximum at time t_0 is specified by:

$$\begin{aligned} u(t_0) &= A \\ \dot{u}(t_0) &= 0 \\ \ddot{u}(t_0) &= B < 0 \end{aligned} \tag{3.1}$$

The specification of a local maximum expressed on basis of the Fourier coefficients x equals:

$$Gx = Y \tag{3.2}$$

with

$$G = \begin{pmatrix} \cos\omega_1 t_0 & \cos\omega_2 t_0 & \ldots & \cos\omega_K t_0 & \sin\omega_1 t_0 & \ldots & \sin\omega_K t_0 \\ -\omega_1 \sin\omega_1 t_0 & -\omega_2 \sin\omega_2 t_0 & \ldots & -\omega_K \sin\omega_K t_0 & \omega_1 \cos\omega_1 t_0 & \ldots & \omega_K \cos\omega_K t_0 \\ -\omega_1^2 \cos\omega_1 t_0 & -\omega_2^2 \cos\omega_2 t_0 & \ldots & -\omega_K^2 \cos\omega_K t_0 & -\omega_1^2 \sin\omega_1 t_0 & \ldots & -\omega_K^2 \sin\omega_K t_0 \end{pmatrix} \tag{3.3}$$

and

$$Y = \begin{pmatrix} A \\ 0 \\ B \end{pmatrix} \tag{3.4}$$

3.2. Constrained stochastic simulation of local maxima

On basis of Eq. 2.12 local maxima can be generated; an example of such a time series is shown in Fig. 1. It is also possible to arrive an explicit expression in time domain. Such an expression is convenient in case one wants to use an existing stochastic simulation tool working in time domain. Substitution of Eqs. 3.3 and 2.11 in Eq. 2.9 leads to:

$$Q = \frac{1}{T} \begin{pmatrix} \sum_k S_k & 0 & -\sum_k \omega_k^2 \, S_k \\ 0 & \sum_k \omega_k^2 \, S_k & 0 \\ -\sum_k \omega_k^2 \, S_k & 0 & \sum_k \omega_k^4 \, S_k \end{pmatrix} \tag{3.5}$$

Straightforward application of Eq. 2.12 then leads to the constrained Fourier coefficients:

$$a_{k,c} = a_k + S_k \cos \omega_k t_0 \left(\frac{\sum \omega_k^4 S_k}{N} - \omega_k^2 \frac{\sum \omega_k^2 S_k}{N} \right) (A - u(t_0))$$

$$+ S_k \omega_k \sin \omega_k t_0 \frac{1}{\sum \omega_k^2 S_k} \dot{u}(t_0)$$

$$+ S_k \cos \omega_k t_0 \left(\frac{\sum \omega_k^2 S_k}{N} - \omega_k^2 \frac{\sum S_k}{N} \right) (B - \ddot{u}(t_0)) \tag{3.6}$$
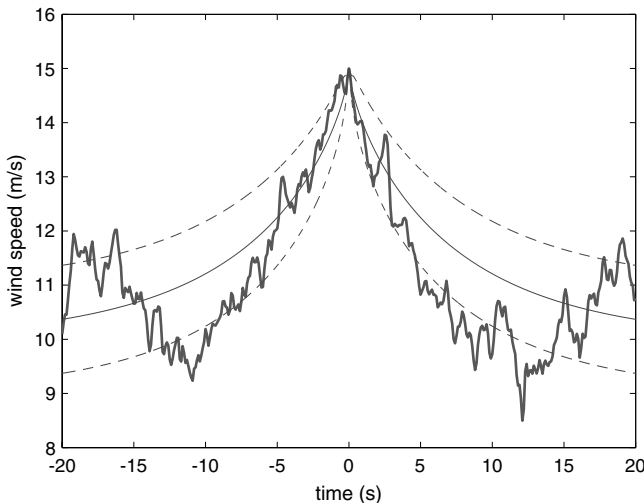
Fig. 1 An example of a gust (local maximum) generated on basis of Eq. 3.8 with value 5 at $t = 0$ s. The *smooth curve* indicates the mean around a local maximum; the *dotted lines* indicate the standard deviation ($r(t)$ based on the von Karman isotropic turbulence spectrum (Appendix A); mean wind speed 10 m/s, standard deviation 1 m/s and maximum frequency 5 Hz)

and

$$
b_{k,c} = b_k + S_k \sin \omega_k t_0 \left(\frac{\sum \omega_k^4 S_k}{N} - \omega_k^2 \frac{\sum \omega_k^2 S_k}{N} \right) (A - u(t_0))
$$

$$
- S_k \omega_k \cos \omega_k t_0 \frac{1}{\sum \omega_k^2 S_k} \dot{u}(t_0)
$$

$$
+ S_k \sin \omega_k t_0 \left(\frac{\sum \omega_k^2 S_k}{N} - \omega_k^2 \frac{\sum S_k}{N} \right) (B - \ddot{u}(t_0)) \tag{3.7}
$$

Doing the Fourier sum, Eq. 2.2, with these constrained Fourier coefficients we obtain:

$$
u_c(t) = u(t) + \left(\frac{\mu}{\mu - \lambda^2} r(t - t_0) + \frac{\lambda}{\mu - \lambda^2} \ddot{r}(t - t_0) \right) (A - u(t_0))
$$

$$
+ \frac{\dot{r}(t - t_0)}{\lambda} \dot{u}(t_0) + \left(\frac{\lambda}{\mu - \lambda^2} r(t - t_0) + \frac{1}{\mu - \lambda^2} \ddot{r}(t - t_0) \right) (B - \ddot{u}(t_0)) \tag{3.8}
$$

with r the (normalized) autocorrelation function:

$$
r(t) = \frac{\sum\limits_k S_k \cos \omega_k t}{\sum\limits_k S_k} \tag{3.9}
$$

and λ and μ the second and fourth order spectral moments, respectively:

$$
\lambda = \frac{\sum\limits_k \omega_k^2 S_k}{\sum\limits_k S_k} = -\ddot{r}(0) \tag{3.10}
$$

$$
\mu = \frac{\sum\limits_k \omega_k^4 S_k}{\sum\limits_k S_k} = \ddddot{r}(0) \tag{3.11}
$$

It is easily verified that $u_c(t)$ indeed satisfies the requested requirements: $u_c(t_0) = A$, $\dot{u}_c(t_0) = 0$ and $\ddot{u}_c(t_0) = B$. The constrained time series $u_c(t)$ is according to Eq. 3.8 a combination of the original process $u(t)$ and three correction terms which include the autocorrelation function and its time derivatives. These correction terms ensures that u_c has the correct value, slope and second derivative at t_0. Note that for increasing heights A the second term in the right hand side of Eq. 3.8 will become more dominant. This implies that the constrained time series will become more and more deterministic in their shape, proportional to the autocorrelation function.

3.3. Mean and variance of the time series around local maxima

Equation 3.8 gives the required recipe to generate a time series around a local maximum with given amplitude A and second derivative B. In order to reflect the behaviour of a normal process around an arbitrary local maximum (with value A)

⌐ Springer

correctly, A can be considered a constant and B should become a random variable (less than zero). By considering the statistics of B, see e.g., Cartwright and Longuet-Higgens (1956), one finds the ensemble mean shape around a local maximum:

$$\bar{u}_c(t) = E[u_c(t)] = Ar(t - t_0) - \frac{F}{A}\text{var}(u) \left\{ r(t - t_0) + \frac{\ddot{r}(t - t_0)}{\lambda} \right\} \qquad (3.12)$$

with

$$F = \frac{\sqrt{2\pi}\gamma e^{\frac{1}{2}\gamma^2}\Phi(\gamma)}{1 + \sqrt{2\pi}\gamma e^{\frac{1}{2}\gamma^2}\Phi(\gamma)} \qquad (3.13)$$

in which Φ is the standard normal cumulative distribution and

$$\gamma = \frac{\lambda A}{\sqrt{\text{var}(u)(\mu - \lambda^2)}} = \frac{A}{\sqrt{\text{var}(u)}} \frac{\sqrt{1 - \varepsilon^2}}{\varepsilon} \qquad (3.14)$$

and var(u) the variance of $u(t)$ and $\varepsilon = \sqrt{\frac{\mu - \lambda^2}{\mu}}$ the bandwidth parameter.

The constant F depends thus on the statistics of the particular random variable $u(t)$. E.g., sea waves is a narrow-banded process (ε less than say 0.7, large γ) resulting in a factor F larger than 0.8 what may be approximated by 1. Atmospheric turbulence is broad-banded (ε larger than 0.7, small γ) and F is in the range of 0.1 to 0.8.

The variance of the constrained stochastic simulations equals:

$$\text{var}(u_c(t)) = \text{var}(u) \left\{ 1 - r^2(t - t_0) - \frac{1}{\lambda}\dot{r}^2(t - t_0) + \left(\frac{(1 - F)\lambda^2}{\mu - \lambda^2} - \left(\frac{F}{A} \right)^2 \text{var}(u) \right) \right. \qquad (3.15)$$

$$\left. \times \left(r(t - t_0) + \frac{1}{\lambda}\ddot{r}(t - t_0) \right)^2 \right\}$$

The mean shape around local maxima plus/minus a standard deviation is already shown in Fig. 1.

Lindgren (1970) has performed a strict mathematical treatment of the properties of a normal process near a local maximum. It is proved that around a local maximum of height A the process $u(t)$ has the same distribution as the process:

$$a(t)A + b(t)B + \Delta(t) \qquad (3.16)$$

with

$$a(t) = \frac{\mu}{\mu - \lambda^2} r(t - t_0) + \frac{\lambda}{\mu - \lambda^2} \ddot{r}(t - t_0)$$
$$b(t) = \frac{\lambda}{\mu - \lambda^2} r(t - t_0) + \frac{1}{\mu - \lambda^2} \ddot{r}(t - t_0)$$

~14~

and $\Delta(t)$ is a non-stationary zero-mean normal process, independent from $b(t)B$, with covariance function (in case $\text{var}(u) = 1$ and $t_0 = 0$):

$$C(s,t) = r(s-t) - \frac{1}{\lambda(\mu-\lambda^2)} \left\{ \lambda\mu r(s)r(t) + \lambda^2 r(s)\ddot{r}(t) + (\mu-\lambda^2)\dot{r}(s)\dot{r}(t) + \lambda^2\ddot{r}(s)r(t) \right.$$

$$\left. + \lambda\ddot{r}(s)\ddot{r}(t) \right\} \tag{3.17}$$

The first two terms of Eq. 3.16 can be considered as regression term and the third one as a residual process. It can be shown that Eq. 3.8 corresponds with the above, so the method presented in this paper is in line with Lindgren (1970); the residual process is given by:

$$\Delta(t) \equiv u(t) - a(t)u(t_0) + \frac{\dot{r}(t-t_0)}{\lambda}\dot{u}(t_0) - b(t)\ddot{u}(t_0) \tag{3.18}$$

A practical advantage of Eq. 3.8, from an engineering point of view, is that it leads to an explicit expression of time series around local maxima. This can be appreciated by comparing Eq. 3.18 to the approximation of the residual process of a Slepian process by means of a Karhunen–Loève expansian in Hasofer (1989). Furthermore the method of constrained stochastic simulation is not restricted to Slepian processes but can be applied to all events in a normal process which can be expressed by means of a linear condition, Eq. 2.3; see for another example the next section.

A method to assess the extreme wave loading of offshore platforms, Taylor et al. (1997) has been based on Lindgren (1970). In fact local extremes rather than maxima are considered in this method. Since it is unlikely that for large A a local minimum is encountered, the third constraint in Eq. 3.1 can be omitted leading to, Taylor et al. (1997) and Bierbooms et al. (2001):

$$u_{c2}(t) = u(t) + r(t-t_0)(A - u(t_0)) + \frac{\dot{r}(t-t_0)}{\lambda}\dot{u}(t_0) \tag{3.19}$$

which can be considered to be the asymptotic form of Eq. 3.8 for large A. Indeed, the mean of u_{c2} equals $A\,r(t-t_0)$ corresponding to the asymptotic form of Eq. 3.12; the variance is $\text{var}(u)\left(1 - r^2(t-t_0) - \dot{r}^2(t-t_0)/\lambda\right)$ in agreement with the asymptotic form of Eq. 3.15. The mean waveform, i.e., $Ar(t-t_0)$, has been coined NewWave by Taylor et al. (1997); the wind gust corresponding to Eq. 3.19 has been denoted *New*Gust by Bierbooms et al. (2001).

4. Gusts with extreme rise times

4.1. Specification of extreme rise time gusts

In the previous section the constrained simulation of local maxima is given. With respect to the extreme loading of stall regulated wind turbines (i.e., with fixed blades) such time series can be used for the load calculation since the extreme loads will most probably be due to gusts with a maximum amplitude (or a simultaneous wind speed gust and wind direction change). For pitch regulated wind turbines (i.e., with blades which can be turned by a control system to accommodate high winds) the extreme

loads may not be connected with extreme wind gusts but with other extreme situations, e.g., gusts with a given extreme rise time rather than amplitude. In this section we will deal with such gusts; this demonstrates the versality of the proposed method. The gust events are now specified by a local minimum and local maximum with a time separation (rise time) Δt and a velocity difference (jump) of ΔU:

$$
\begin{aligned}
\dot{u}(t_0) &= 0 \\
\ddot{u}(t_0) &= B_1 > 0 \\
u(t_0 + \Delta t) - u(t_0) &= \Delta U \\
\dot{u}(t_0 + \Delta t) &= 0 \\
\ddot{u}(t_0 + \Delta t) &= B_2 < 0
\end{aligned} \tag{4.1}
$$

Note that it is not required that the considered minimum and maximum are consecutive; i.e., it is possible that other local minima and maxima are in between. The reason for choosing such a definition for an event is that, with respect for the assessment of extreme loads on wind turbines, it is not a priori known what will cause the highest loads: a modest velocity jump in a (very) short rise time or a large velocity jump in a rather long rise time.

One could opt for considering the 3rd constraint of Eq. 4.1 only, i.e., specifying a velocity jump, but in that case the two points will in general not be a minimum or a maximum. The implication is that the considered gust is just a part of some larger velocity jump; i.e., a gust generated on basis of such a constraint will generally have a larger velocity jump. So load estimates based on such gusts are associated with a whole range of velocity jumps instead of just one value as is the case with Eq. 4.1. Furthermore, specification of just a velocity jump only does not form a countable event, so no expression as Eq. 4.16 can be formulated. This will significantly complicate the probabilistic approach in order to assess extreme wind turbine loading which will be outlined in Section 5.

The specification, Eq. 4.1, can again be expressed in terms of the Fourier coefficients, Eq. 2.10:

$$
\boldsymbol{Gx} = \boldsymbol{Y} \tag{4.2}
$$

with

$$
G = \begin{pmatrix}
-\omega_1 \sin\omega_1 t_0 & -\omega_2 \sin\omega_2 t_0 & \cdots & -\omega_K \sin\omega_K t_0 & \omega_1 \cos\omega_1 t_0 & \cdots & \omega_K \cos\omega_K t_0 \\
-\omega_1^2 \cos\omega_1 t_0 & -\omega_2^2 \cos\omega_2 t_0 & \cdots & -\omega_K^2 \cos\omega_K t_0 & -\omega_1^2 \sin\omega_1 t_0 & \cdots & -\omega_K^2 \sin\omega_K t_0 \\
\cos\omega_1(t_0+\Delta t) - \cos\omega_1 t_0 & \cos\omega_2(t_0+\Delta t) - \cos\omega_2 t_0 & \cdots & \cos\omega_K(t_0+\Delta t) - \cos\omega_K t_0 & \sin\omega_1(t_0+\Delta t) - \sin\omega_1 t_0 & \cdots & \sin\omega_K(t_0+\Delta t) - \sin\omega_K t_0 \\
-\omega_1 \sin\omega_1(t_0+\Delta t) & -\omega_2 \sin\omega_2(t_0+\Delta t) & \cdots & -\omega_K \sin\omega_K(t_0+\Delta t) & \omega_1 \cos\omega_1(t_0+\Delta t) & \cdots & \omega_K \cos\omega_K(t_0+\Delta t) \\
-\omega_1^2 \cos\omega_1(t_0+\Delta t) & -\omega_2^2 \cos\omega_2(t_0+\Delta t) & \cdots & -\omega_K^2 \cos\omega_K(t_0+\Delta t) & -\omega_1^2 \sin\omega_1(t_0+\Delta t) & \cdots & -\omega_K^2 \sin\omega_K(t_0+\Delta t)
\end{pmatrix}
$$

$$\tag{4.3}$$

and

$$
\boldsymbol{Y} = \begin{pmatrix}
0 \\
B_1 \\
\Delta U \\
0 \\
B_2
\end{pmatrix} \tag{4.4}
$$

In order to reflect the behaviour of a normal process around an arbitrary velocity jump correctly, ΔU can be considered a constant and B_1, B_2 are realizations of

stochastic variables. The joint density function of B_1 and B_2 will be determined in Section 4.4.

4.2. Constrained stochastic simulation of extreme rise time gusts

We will not bother to arrive at explicit time domain equations like Eqs. 3.8, 3.12 and 3.15 but restrict ourselves to an implicit description which can easily be evaluated by a simple computer program. For this purpose the equations are reformulated. From Eqs. 2.2, 2.10 and 2.12 we arrive for the constrained wind speed time series at:

$$u_c(t) = u(t) + \boldsymbol{R}(t)(\boldsymbol{Y} - \boldsymbol{y}) \tag{4.5}$$

with $\boldsymbol{Y}$ according to Eq. 4.4,

$$\boldsymbol{y} = \boldsymbol{Gx} = \begin{pmatrix} \dot{u}(t_0) \\ \ddot{u}(t_0) \\ u(t_0 + \Delta t) - u(t_0) \\ \dot{u}(t_0 + \Delta t) \\ \ddot{u}(t_0 + \Delta t) \end{pmatrix} \tag{4.6}$$

and

$$\boldsymbol{R}(t) = [\,\cos \omega_1 t \ldots \cos \omega_K t \, \sin \omega_1 t \ldots \sin \omega_K t\,]\boldsymbol{M}\boldsymbol{G}^{\mathrm{T}}\boldsymbol{Q}^{-1} \tag{4.7}$$

i.e., $\boldsymbol{R}(t)$ is the Fourier sum of $\boldsymbol{M}\boldsymbol{G}^{\mathrm{T}}\boldsymbol{Q}^{-1}$; $\boldsymbol{M}$ according to Eq. 2.11, $\boldsymbol{G}$ given by Eq. 4.3 and $\boldsymbol{Q} = \boldsymbol{GMG}^{\mathrm{T}}$, Eq. 2.9.

Application of Eq. 4.5 will result into the desired gust with velocity jump ΔU with rise time Δt. An example of such constrained stochastic simulation is shown in Fig. 2.
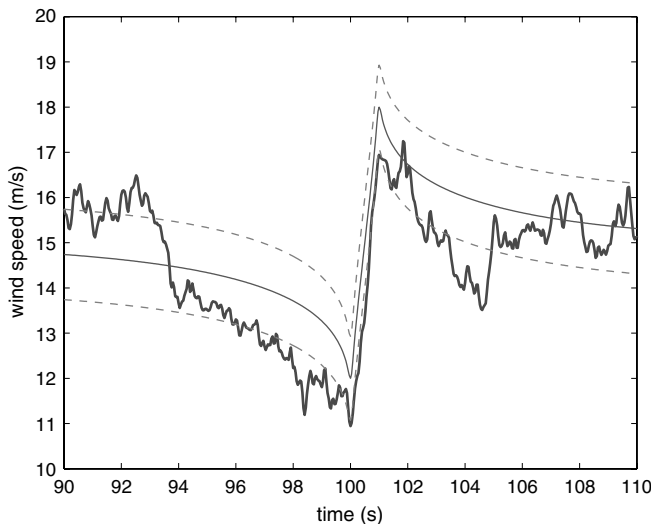
Fig. 2 An example of a gust with a velocity jump from of 6 m/s at $t = 100$ to 101 s. The *smooth curve* indicates the mean gust shape; the *dotted lines* indicate the standard deviation of the gust shape; $r(t)$ based on the von Karman isotropic turbulence spectrum (mean wind speed 15 m/s, standard deviation 1 m/s and maximum frequency 5 Hz)

Springer

4.3. Mean and variance of the time series around extreme rise time gusts

The ensemble mean is given by:

$$\overline{u}_c(t) = \boldsymbol{R}(t)\overline{\boldsymbol{Y}} \tag{4.8}$$

with

$$\overline{\boldsymbol{Y}} = \begin{pmatrix} 0 \\ \overline{B}_1 \\ \Delta U \\ 0 \\ \overline{B}_2 \end{pmatrix} \tag{4.9}$$

The variance equals:

$$\text{var}(u_c(t)) = \text{var}(u(t)) + \boldsymbol{R}(t)(\text{var}(\boldsymbol{Y}) - \boldsymbol{Q})\boldsymbol{R}^{\mathrm{T}}(t) \tag{4.10}$$

with

$$\text{var}(\boldsymbol{Y}) = \begin{pmatrix} 0 & 0 & 0 & 0 & 0 \\ 0 & \text{var}(B_1) & 0 & 0 & \text{cov}(B_1, B_2) \\ 0 & 0 & 0 & 0 & 0 \\ 0 & 0 & 0 & 0 & 0 \\ 0 & \text{cov}(B_1, B_2) & 0 & 0 & \text{var}(B_2) \end{pmatrix} \tag{4.11}$$

For the derivation of Eq. 4.10 use is made of the independence of B_1, B_2 and $u(t)$ and Eqs. 2.2, 2.10, 2.11, 4.6 and 4.7:

$$\mathbf{E}\left[u(\boldsymbol{Ry})^{\mathrm{T}}\right] = \left[\cos\omega_1 t \ldots \cos\omega_K t \ \sin\omega_1 t \ldots \sin\omega_K t\right] \mathbf{E}\left[\boldsymbol{xx}^{\mathrm{T}}\right]\boldsymbol{G}^{\mathrm{T}}\boldsymbol{R}^{\mathrm{T}}$$

$$= \left[\cos\omega_1 t \ldots \cos\omega_K t \ \sin\omega_1 t \ldots \sin\omega_K t\right] \boldsymbol{M}\boldsymbol{G}^{\mathrm{T}}\boldsymbol{R}^{\mathrm{T}} = \boldsymbol{R}\boldsymbol{Q}\boldsymbol{R}^{\mathrm{T}}$$

The mean and standard deviation of the gust shape are shown in Fig. 2; the mean and (co)variance of B_1 and B_2 are determined numerically (based on Eq. 4.18).

4.4. The statistics of extreme rise time gusts

In order to obtain the (joint) statistics of B_1 and B_2 we have to deal with the statistics of gusts as defined by Eq. 4.1. By introducing the following five random variables with zero ensemble means (breakdown of vector $\boldsymbol{y}$, Eq. 4.6):

$$\begin{aligned}
v &= \dot{u}(t_0) \\
w &= \ddot{u}(t_0) \\
x &= u(t_0 + \Delta t) - u(t_0) \\
y &= \dot{u}(t_0 + \Delta t) \\
z &= \ddot{u}(t_0 + \Delta t)
\end{aligned} \tag{4.12}$$

~18~

the probability of occurrence of gusts, with a rise time Δt and a velocity jump of ΔU, equals:

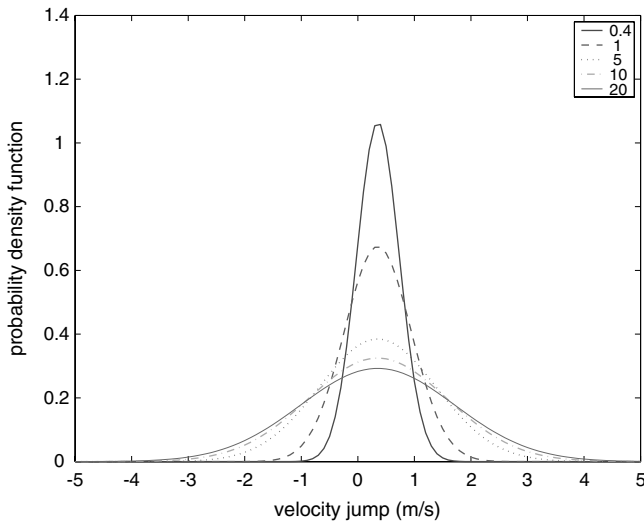$$P_{gusts} = \int_0^{w\,dt} \int_0^{\infty} \int_{\Delta U}^{\Delta U + d(\Delta U)} \int_0^{-z\,d(\Delta t)} \int_{-\infty}^0 f(v, w, x, y, z)\,dv\,dw\,dx\,dy\,dz \quad (4.13)$$

For a given second derivative $w = \ddot{u}(t_0)$ the first time derivative should be in the range between 0 and $w\,dt$ in order to obtain a minimum inside the time interval dt. This explains the integration limits of v; a similar argument holds for the limits of y. The function $f(v,w,x,y,z)$ is a five variate Gaussian probability density function with covariance matrix:

$$\boldsymbol{Q} = \text{var}(u) \begin{bmatrix} \lambda & & & & symmetric \\ 0 & \mu & & & \\ -\dot{r}(\Delta t) & \ddot{r}(\Delta t) + \lambda & 2 - 2r(\Delta t) & & \\ -\ddot{r}(\Delta t) & \dddot{r}(\Delta t) & -\dot{r}(\Delta t) & \lambda & \\ -\dddot{r}(\Delta t) & \ddddot{r}(\Delta t) & \ddot{r}(\Delta t) - \lambda & 0 & \mu \end{bmatrix} \quad (4.14)$$

The mean frequency of gusts $N\Delta_U$, with a velocity jump in the range ΔU to $\Delta U + d(\Delta U)$ and with a rise time in between Δt and $\Delta t + d(\Delta t)$, follows directly from Eq. 4.13:

$$N_{\Delta U} = \frac{P_{gusts}}{dt} \approx d(\Delta U)d(\Delta t) \int_0^{\infty} \int_{-\infty}^0 -wz\, f(0, w, \Delta U, 0, z)\,dw\,dz \quad (4.15)$$

The mean frequency N of all gusts with rise time in between Δt and $\Delta t + d(\Delta t)$ equals:

$$N = d(\Delta t) \int_{-\infty}^{\infty} \int_0^{\infty} \int_{-\infty}^0 -wzf(0, w, \Delta U, 0, z)\,d(\Delta U)\,dw\,dz = d(\Delta t)\frac{\mu}{(2\pi)^2 \lambda} \quad (4.16)$$

The latter identity can be deduced from the following reasoning. Every combination of a local minimum and a local maximum counts as a gust. So the total number of gusts, per unit time, equals the number of local minima, per unit time, times the number of local maxima, per unit time. This holds for every value of the rise time Δt. The mean frequency of local minima is equal to the mean frequency of local maxima and equals: $1/(2\pi)\sqrt{\mu/\lambda}$, Rice (1944).

Finally the density $f(\Delta U)$ of gust events with velocity jump ΔU is obtained:

$$f(\Delta U) = \frac{N_{\Delta U}}{Nd(\Delta U)} = \frac{(2\pi)^2 \lambda}{\mu} \int_0^{\infty} \int_{-\infty}^0 -wzf(0, w, \Delta U, 0, z)\,dw\,dz \quad (4.17)$$

The double integral of the above expression can be evaluated by using the 'completing the square' method, see Appendix B; the density $f(\Delta U)$ is shown in Fig. 3 for several rise times Δt. For a rise time larger than about 10 s the function shape does not change anymore; apparently for large rise times the correlation between the local minimum and local maximum gets so small that the function does not depend any longer on the exact rise time. For a small rise time the function gets more peak shaped; as expected the probability for a large velocity jump decreases for decreasing rise time.

Fig. 3 The probability density function of gusts $f(\Delta U)$ as function of velocity jump ΔU for 5 different values of the rise time Δt (mean wind speed 10 m/s and turbulence intensity 10%)

In conclusion: Eq. 4.5 gives the recipe to generate gusts with a velocity jump ΔU in rise time Δt; B_1 and B_2 should, on basis of Eq. 4.17, be randomly generated according to the following joint 2D density:

$$f(B_1, B_2) = \frac{B_1|B_2|f(0, B_1, \Delta U, 0, B_2)}{\int_0^\infty \int_{-\infty}^0 B_1|B_2|f(0, B_1, \Delta U, 0, B_2)dB_1 dB_2} \tag{4.18}$$

5. Probabilistic method to determine the extreme response of wind turbines

In this section a concise outline is given of a probabilistic method to determine the extreme response of wind turbines. A basic assumption in order to apply constrained stochastic simulation for this purpose is that the extreme response is driven by wind turbulence and that turbulence is Gaussian. Wind gusts generated on basis of Eqs. 3.8 or 4.5 can be used as input for a wind turbine simulation tool. Examples of generated gusts were already shown in Figs. 1 and 2; the autocorrelation function $r(t)$ has been based on the von Karman isotropic turbulence spectrum (Appendix A). A wind turbine design tool determines among other things the internal loads of the wind turbine as function of time; e.g., one may be interested in the maximum bending moment in the rotor blades at the root section. Repetition of application of Eqs. 3.8, 4.5 will lead to different wind gusts and consequently to different responses and maximum rotor blade moments. If several simulations are performed for the same gust amplitude and mean wind speed, a distribution of the extreme loading can be determined. This can be repeated for several gust amplitudes, varying e.g., from 1 to 6 times the standard variation. Each gust amplitude will result in another (cumulative) distribution of the structural loading.

In order to obtain the distribution of the extreme loading, caused by a gust with arbitrary amplitude (for given mean wind speed), the different distributions should

~20~

be convoluted (weighed) with the occurrence probability of the individual gusts. In case of local maxima the probability can by expressed as function of the spectral bandwidth, Cartwright and Longuet-Higgins (1956); in case of extreme rise time gusts the density is given by Eq. 4.17, Fig. 3. Following this procedure, the short-term (say 10 min) distribution of the loading is obtained for some mean wind speed.

In order to determine the long-term distribution the procedure should be repeated for several mean wind speeds. The over-all final distribution is subsequently obtained by weighting with the occurrence probability of the mean wind speeds, i.e., the Weibull distribution or an empirical distribution (histogram) valid for some specific site. The final distribution can be fitted to some extreme value distribution, e.g., Gumbel or Pareto and then finally extrapolated to the desired return period, e.g., 50 years. The long-term distribution of the peak bending moment in the rotor blades shows the probability of exceedance of a certain load level. Instead of an arbitrary value obtained using deterministic analysis (as is presently specified in standards), the designer can chose the level of risk according to the load distribution. Furthermore, using the load distribution and resistance distribution of the structure the probability of failure can be estimated. Together they constitute the tools leading to a more efficient and reliable design of wind turbines. An extensive treatment of other probabilistic methods to determine the extreme wind turbine loading may be found in Cheng (2002).

The theoretical mean gust shape, Eq. 3.12, as well as the gust statistics have been verified by analysis of wind measurements, Bierbooms et al. (1999) and Bierbooms et al. (2001) e.g., from the 'Database on Wind Characteristics' (http://www.winddata.com).

This paper focused on the method of constrained simulation (Section 2) and treated local maxima (Section 3) and rise time gusts (Section 4) as examples. By choosing local maxima as one of the examples comparison with well known results was possible. For reasons of simplicity these examples considered the one point coherent gust (uniform over the rotor plane). In reality a wind turbine will of course encounter spatial gusts (with three velocity components). The extension of the method of constrained stochastic simulation to spatial gusts is given in Bierbooms et al. (2001). Recently, during the review process of this paper, Nielsen et al. (2003) and Bierbooms (2005) have published on this topic. These publications focus on the wind fields and there resulting wind turbine loading. Non-Gaussianity of wind turbulence and how to incorporate it in constrained simulation is also addressed. Nielsen et al. (2003) applied a totally different method, based on variational calculus, in order to simulate gusts. It can be shown that their final results, for a given gust description, are identical to those obtained by constrained simulation. The probability of gusts, needed for the probabilistic approach given above, is not dealt with in Nielsen et al. (2003).

6. Conclusion

Time series around some specific event in a normal process can be generated by means of constrained stochastic simulation. This easy method can be applied for any event which can be expressed as a linear expression of the involved random variables. It has been demonstrated for local maxima and velocity jumps. Time

domain simulations of these events, representing wind gusts, are of practical interest for wind turbine design calculations.

Appendix A: The von Karman isotropic turbulence spectrum

The longitudinal velocity component spectrum S is given by the non-dimensional equation, IEC (1998):

$$\frac{fS(f)}{\text{var}(u)} = \frac{4f\frac{L}{U}}{\left(1 + 70.8\left(f\frac{L}{U}\right)^2\right)^{5/6}} \tag{A1}$$

with

f frequency [Hz]
U mean wind speed [m/s]
$L = 70.7$ m,   the isotropic integral scale parameter and
var(u)   the variance of the longitudinal turbulence component

All expressions for turbulence spectra are for large frequencies inversely proportional to the 5/3 power of the frequency (so-called inertial subrange). This implies that the time derivatives of the autocorrelation function at $t = 0$ are infinite. In order to overcome this problem the spectrum is cut-off above some maximum frequency by means of a Hann window (a rectangular window would introduce oscillations in the autocorrelation function).

Appendix B: Completing the square method

The integrand of the double integral of Eq. 4.17 includes the function $f(0,w,\Delta U,0,z)$, which is a five variate Gaussian probability density function:

$$f(0, w, \Delta U, 0, z) = \frac{1}{(2\pi)^{5/2}\sqrt{\det(\boldsymbol{Q})}} e^{-1/2 y_0^T Q^{-1} y_0} \tag{B1}$$

with

$$\boldsymbol{y}_0 = \begin{pmatrix} 0 \\ w \\ \Delta U \\ 0 \\ z \end{pmatrix} \tag{B2}$$

and det($\boldsymbol{Q}$) the determinant of $\boldsymbol{Q}$, Eq. 4.14.

Via transformation to three new variables it is possible to convert the multinomial of the exponent of $f(0,w,\Delta U,0,z)$ to a sum of perfect squares ('completing the square' method):

$$-\frac{1}{2}\mathbf{y}_0^T\mathbf{Q}^{-1}\mathbf{y}_0 = -\left(k^2 + l^2 + m^2\right) \tag{B3}$$

with

$$\begin{pmatrix} k \\ l \\ m \end{pmatrix} = \mathbf{c}\begin{pmatrix} w \\ z \\ \Delta U \end{pmatrix} = \begin{bmatrix} c_1 & c_2 & c_3 \\ 0 & c_4 & c_5 \\ 0 & 0 & c_6 \end{bmatrix}\begin{pmatrix} w \\ z \\ \Delta U \end{pmatrix} \tag{B4}$$

Equating the six terms of the left hand side of Eq. B3 to the corresponding terms at the right hand side leads to expressions for the six constants. Alternatively one may use Choleski decomposition in order to determine $\mathbf{c}$:

$$\mathbf{c}^T\mathbf{c} = \frac{1}{2}\mathbf{N}^T\mathbf{Q}^{-1}\mathbf{N} \tag{B5}$$

with

$$\mathbf{N} = \begin{bmatrix} 0 & 0 & 0 \\ 1 & 0 & 0 \\ 0 & 0 & 1 \\ 0 & 0 & 0 \\ 0 & 1 & 0 \end{bmatrix}; \text{ i.e., } \mathbf{N}\begin{pmatrix} w \\ z \\ \Delta U \end{pmatrix} = \mathbf{y}_0$$

Through the transformation (B4) the new integration variables become k and l with integration limits (lower and upper resp.):

$$K(l) = \frac{c_2}{c_4}l + \frac{c_3c_4 - c_2c_5}{c_4}\Delta U \tag{B6}$$

$$L = c_5\Delta U \tag{B7}$$

Furthermore:

$$dkdl = c_1c_4dwdz \tag{B8}$$

The transformation allows us to write the two dimensional integral of Eq. 4.17 as a 1D integral which can be solved numerically (strictly speaking it remains a 2D integral since the integrand involves the error function).

$$\int_0^\infty \int_\infty^0 -wzf(0,w,\Delta U,0,z)dwdz = C\int_{-\infty}^L zg(l)e^{-l^2}dl$$
$$= C\int_{-\infty}^L \left(\frac{l}{c_4} - \frac{c_5}{c_4}\Delta U\right)g(l)e^{-l^2}dl \tag{B9}$$

with

$$C = -\frac{1}{(2\pi)^{5/2}\sqrt{det(\mathbf{Q})}c_1c_4}e^{-\left(c_6\Delta U\right)^2} \tag{B10}$$

and

$$g(l) = \int_{K(l)}^{\infty} we^{-k^2}dk = \int_{K(l)}^{\infty} \left\{ \frac{k}{c_1} + h(l) \right\} e^{-k^2}dk = \frac{I_1(l)}{c_1} + h(l)I_2(l) \qquad \text{(B11)}$$

with

$$h(l) = -\frac{c_2}{c_1 c_4}l + \frac{c_2 c_5 - c_3 c_4}{c_1 c_4}\Delta U \qquad \text{(B12)}$$

The factors I_1 and I_2 from Eq. B11 are the following standard integrals:

$$I_1(l) = \int_{K(l)}^{\infty} ke^{-k^2}dk = \frac{1}{2}e^{-K(l)^2} \qquad \text{(B13)}$$

$$I_2(l) = \int_{K(l)}^{\infty} e^{-k^2}dk = \frac{\sqrt{\pi}}{2}\{1 - \text{erf}(K(l))\} \qquad \text{(B14)}$$

with erf the error function.

References

Bierbooms, W.: Investigation of spatial gusts with extreme rise time on the extreme loads of pitch-regulated wind turbines. Wind Energy **8**, 17–34 (2005)

Bierbooms, W., Dragt, J.B.: A Probabilistic Method to Determine the Extreme Response of a Wind Turbine. Delft University of Technology, Delft, (2000)

Bierbooms, W., Dragt, J.B., Cleijne, H.: Verification of the mean shape of extreme gusts. Wind Energy. **2**, 137–150 (1999)

Bierbooms, W., Cheng, P.W., Larsen, G., Pedersen, B.J.: Modelling of Extreme Gusts for Design Calculations—NewGust FINAL REPORT JOR3-CT98-0239. Delft University of Technology, (2001)

Cartwright, D.E., Longuet-Higgins, M.S.: The statistical distribution of the maxima of a random function. Proc. Royal Soc. London Ser. A. **237**, 212–232 (1956)

Cheng, P.W.: A reliability based design methodology for extreme responses of offshore wind turbines, PhD thesis, Delft University Wind Energy Research Institute, (2002)

Database on Wind Characteristics, http://www.winddata.com/

Dragt, J.B., Bierbooms, W.: Modeling of extreme gusts for design calculations. Proceedings European Wind Energy Conference, Göteborg, Sweden, 842–845 (1996)

Hasofer, A.M.: On the Slepian process of a random Gaussian trigonometric polynomial. IEEE Trans. Inf. Theory. **35**, 868–873 (1989)

IEC 61400-1, Ed. 2, Wind Turbine generator Systems. Part 1. Safety Requirements. (1998)

Lindgren, G. Some properties of a normal process near a local maximum. Ann. Math. Stat. **41**, 1870–1883 (1970)

Lindgren, G., Rychlik, I.: Slepian models and regression approximations in crossing and extreme value theory. Int. Stat. Rev. **59**, 195–225 (1991)

Mortensen, R.E.: Random Signals and Systems. Wiley, New York (1987)

Nielsen, M., Larsen, G.C., Mann, J., Ott, S., Hansen, K.S., Pedersen, B.J.: Wind simulation for extreme and fatigue loads, Risø-R-1437(EN), (2003)

Rao, C.R.: Linear Statistical Inference and its Applications. Wiley (1965)

Rice, S.O.: Mathematical analysis of random noise. Bell Syst. Techn. J. **23**, 282 (1944) [Reprinted in Wax, N. (ed.), Selected papers on noise and stochastic processes, Dover, 1958]

Shinozuka, M.: Simulation of multivariate and multidimensional random processess. J. Acoust. Soc. America. 357–368 (1971)

Taylor, P.H., Jonathan, P., Harland, L.A.: Time domain simulation of jack-up dynamics with the extremes of a Gaussian process. J. Vib. Acoust. **119**, 624–628 (1997)

Research Article

Verification of the Mean Shape of Extreme Gusts

Wim Bierbooms* and Jan B. Dragt,† Institute for Wind Energy,
Delft University of Technology, Delft, The Netherlands
Hans Cleijne,‡ TNO-MEP, Apeldoorn, The Netherlands

For design load calculations for wind turbines it is necessary to determine the fatigue loads as well as the extreme loads. An advanced method has been presented previously to incorporate extreme turbulence gusts in wind field simulation, the so-called 'NewGust' method. The gust generator works by constraining the random parameters of a stochastic wind field simulator. The present article deals with the verification of the mean shape of extreme gusts. On the basis of a statistical analysis an expression of the mean gust shape is obtained. This theoretical gust shape is compared with the mean gust shape determined from both simulated and measured turbulence. The resemblance is remarkably good, which demonstrates the viability of the NewGust method. Copyright ©1999 John Wiley & Sons, Ltd.

Introduction

The sophistication of the methods used to carry out wind turbine design calculations has increased enormously over the last two decades.[1] A good example is the treatment of fatigue loads. It is now common practice to consider for the fatigue analysis a complete representation of both the temporal and spatial structure of the turbulence. The applied wind field simulation methods are based on a stochastic description of turbulence (i.e. the auto- and cross-spectra of all three turbulence components).

The situation for the determination of extreme loads is totally different. Up to now, only simple deterministic gusts (e.g. a cosine gust) have been used to determine the extreme operating response, instead of applying a stochastic description of the wind (as is the case for fatigue analysis). Quoted from reference 1: 'Turbulence models of the form described above are now widely used for the calculation of fatigue loads for design purposes. For calculation of extreme loads, however, it is standard practice to base calculations on deterministic descriptions of extreme wind conditions. Current design standards and certification rules specify extreme events in terms of discrete gusts, wind direction changes and wind shear transients. The form, amplitude and time period specified for these discrete events remain rather arbitrary and largely unvalidated. The development of more reliable methods for the evaluation of extreme design loads, based possibly on the use of probabilistic analysis, requires considerable effort but is crucially important in the context of refining wind turbine design analysis'. Such a new method has been proposed by the Institute for Wind Energy and presented at EUWEC '96.[2] This method, which has been given the name 'NewGust', is based on constrained simulation and described in Reference 2; a more comprehensive description of constrained simulation is given in Reference 3.

*Correspondence to: Wim Bierbooms, Institute for Wind Energy, Delft University of Technology, Stevinweg 1, NL-2628 CN Delft, The Netherlands. Email: w.bierbooms@ct.tudelft.nl
†Emeritus Professor of Wind Energy.
‡Current address: KEMA Power Generation & Sustainable, Arnhem, The Netherlands.

The present article will focus on the gust shape and is partly based on the work performed during a Dutch project.[4] In order to motivate our prime interest in the mean gust shape, we start with a brief overview of the *New*Gust method.

Motivation and Background

As (most) gusts are part of the turbulence, they also should be accounted for in a stochastic fashion. In Reference 2 we investigated that by a method similar to a technique for peak wave loading of offshore structures by random sea waves. The principle is as follows.

Random turbulence simulations are made generally by random number generators for Fourier coefficients, using power spectrum (or, equivalently, correlation function) specifications of the real atmosphere turbulence. A small fraction of those simulations will contain high gusts that are relevant for peak load evaluation. One can of course select these rare events from a (very) large number of simulations in order to study peak loads, but it is much more convenient to restrict oneself to simulations with random number sets which have been preselected to produce the wanted gusts. This requires a form of constrained simulation. It was shown in Reference 2 that a method to perform such a simulation is mathematically equivalent to taking an arbitrary simulation and applying certain adaptations to either the Fourier coefficients (in the frequency domain) or adaptations in the time domain. The time domain formula for a peak of height A at time t_0 reads

$$u_{\text{constr}}(t) = u_{\text{simul}}(t) + r(t - t_0)\,(A - u_{\text{simul}}(t_0)) + \frac{\dot{r}(t - t_0)\,\dot{u}_{\text{simul}}(t_0)}{\lambda} \tag{1}$$

where $u_{\text{simul}}(t)$ is any random simulation, $r(t)$ is the normalized autocorrelation function and λ is a (constant) measure for the randomness of the turbulence (see also (12)). This formula accounts for the time dependence only, but it was shown to be extendable to space-dependent gust simulations also, where the spatial correlation function enters. We called this method *New*Gust. It is shown that the gusts according to (1) are, in a statistical sense, not distinguishable from gusts selected from a very long stochastic time series. Many load calculations for a wind turbine rotor have been made in order to see what the effect is of this theoretically more appropriate way of dealing with turbulent gust loading. In Reference 2 we found the following, preliminary, effects.

- The shape of the gust (second term of (1)) is much sharper than the usual cosine shape. The effect of the shape difference on the peak load is limited. Only very flexible blades with low damping give a significant dynamic overshoot.
- More important is the embedding of the gusts in a stochastic environment (first term in (1)). This may increase the peak loads up to several tens of per cents.
- The space dependence of the gusts considerably lowers the peak loads of large rotors compared with uniform (over the rotor plane) gusts.
- The effects are of the same order of magnitude as safety factors in design standards. Thus they are important enough to deserve further study.

Although based on (largely) empirical turbulence specifications, the *New*Gust method is rather theoretical. Thus there is a need for experimental verification. The most peculiar aspect is the shape of the gusts, very different from what has been common up to now. If that shape can be confirmed from real wind turbulence measurements, it will be a strong indication that the *New*Gust method is viable. To make that verification is the aim of the present article.

Thus the article will focus on the shape of the gust. For the moment the longitudinal turbulence component only will be considered. Please note that our prime goal is not the determination of the mean gust shape in a meteorological sense but with respect to the extreme loading on wind turbines. In the next

section a general statistical method is presented in order to derive an analytical expression for the mean gust shape. The succeeding two sections will treat the comparison of the theoretical mean gust shape with the mean gust shape determined from simulated and measured wind respectively. We made the analysis for simulated wind in order to verify the method of gust analysis, while the analysis of the measured wind data gives the real 'proof of the pudding'.

The Theoretical Mean Gust Shape

General Statistical Method

A general method to determine the statistical means of certain parameters of a stationary stochastic process has been given by Middleton.[5] In order to present this method, it is inevitable to use a lot of equations. The reader is encouraged to put some effort into understanding them in order to grasp the elegance and strength of the statistical method. The method can be divided into the following steps.

● Specify the events of interest (e.g. zero crossing or maximum). Determine a series of mathematical operations (differentiation, time shift, rectifier, step function, etc.; see also Figure 1) which transfers the original time series $u(t)$ into a series of delta functions at the time instants of the specific events:

$$p(t) = \sum_i \delta(t - t_i) \tag{2}$$

with $p(t)$ a (possibly non-linear) function of $u(t)$, $u(t + \tau)$, $\dot{u}(t)$, etc.

● The number of events for a specific time series in the time interval T equals

$$N = \int_0^T p(t) \mathrm{d}t \tag{3}$$

The expectation value of the number of events equals

$$E[N] = E\left[\int_0^T p(t)\mathrm{d}t\right] = \int_0^T E[p(t)]\mathrm{d}t = T\, E[p(t_0)] \tag{4}$$

for any t_0 (owing to the stationarity of the stochastic process).

● The sum of the signals in the neighbourhood of the events is

$$S(\tau) = \sum_i u(t_i + \tau) = \sum_i \int_0^T u(t + \tau)\, \delta(t - t_i)\, \mathrm{d}t = \int_0^T u(t + \tau)p(t)\mathrm{d}t \tag{5}$$
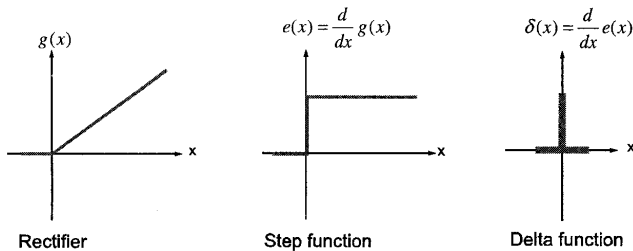

Figure 1. Some basic mathematical operations

for some range of τ (both positive as well as negative values are allowed; the range must be small compared with T). The expectation value of this sum of the signals in the neighbourhood of the events is

$$E[S(\tau)] = \int_0^T E[u(t + \tau)\ p(t)]\ \mathrm{d}t = T\ E[u(t_0 + \tau)\ p(t_0)] \tag{6}$$

Notice that this is a function of τ only.

- The mean signal in the neighbourhood of the events equals (for one sample time series)

$$\bar{u}(\tau) = \frac{S(\tau)}{N} \tag{7}$$

The expectation value equals

$$E[\bar{u}(\tau)] = \frac{E[S(\tau)]}{E[N]} = \frac{E[u(t + \tau)\ p(t)]}{E[p(t)]} \tag{8}$$

The above expectation values can be evaluated if the (multidimensional) density function of $u(t)$, $u(t + \tau)$, $\dot{u}(t)$, etc. which occur in $p(t)$ is known. Please note that in principle it is not required that the density function be Gaussian. In practice, however, the expectation value can be analytically determined if the density function is Gaussian and is of limited dimension only.

It is a subject of further research whether it is possible to determine the expectation value in the case of a non-Gaussian (multidimensional) distribution function, if such a function can be specified anyway, by means of Monte Carlo integration.

Example Application

The above method will be illustrated by the determination of the expected number of (positive) zero crossings in a stationary Gaussian (wind) signal. In Figure 2 it is shown by which operations the (positive) zero crossings may be selected from a (wind) signal $u(t)$:

$$p(t) = \delta(u(t))\ g(\dot{u}(t)) \tag{9}$$

with $g(t)$ the rectifier function. The expected number of (positive) zero crossings per time period equals, according to (4),

$$\frac{E[N]}{T} = E[p(t)] = \int\int \mathrm{d}u\ \mathrm{d}v\ \delta(u)\ g(v)\ P(u, v) \tag{10}$$
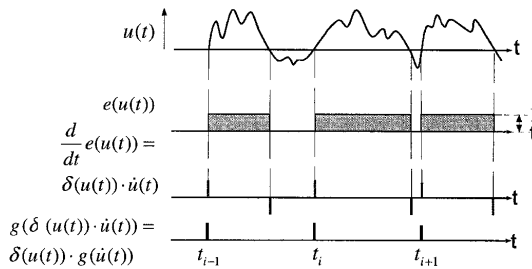

Figure 2. Mathematical operations which select (positive) zero crossings from a stochastic signal

The multidimensional density function of $u(t)$ and $\dot{u}(t)$ is here denoted by $P(u,v)$ and assumed to be joint normal. The covariance matrix equals

$$\Lambda = \sigma^2 \begin{pmatrix} 1 & 0 \\ 0 & \lambda \end{pmatrix} \tag{11}$$

with

$$\lambda = -\ddot{r}(0) \tag{12}$$

where r denotes the normalized autocorrelation function and σ is the standard deviation. The inverse of the covariance matrix equals

$$Q = \frac{1}{\sigma^2} \begin{pmatrix} 1 & 0 \\ 0 & 1/\lambda \end{pmatrix} \tag{13}$$

and thus

$$P(u, v) = \frac{1}{2\pi\sigma^2 \sqrt{\lambda}} \, e^{-(1/2\sigma^2)(u^2 + v^2/\lambda)} \tag{14}$$

Substitution gives

$$\frac{E[N]}{T} = \int_{-\infty}^{\infty} \mathrm{d}v \, g(v) \, P(0, v) = \frac{1}{2 \pi \sigma^2 \sqrt{\lambda}} \int_{0}^{\infty} v e^{-v^2/(2 \sigma^2 \lambda)} \mathrm{d}v \tag{15}$$

Note that the delta function in the integrand is elevated by setting u equal to zero, and $g(v)$ may be replaced by v and setting the lower limit of integration equal to zero.

By substitution of

$$z = \frac{v^2}{2 \sigma^2 \lambda} \tag{16}$$

we finally obtain

$$\frac{E[N]}{T} = \frac{\sqrt{\lambda}}{2 \pi} \int_{0}^{\infty} e^{-z} \mathrm{d}z = \frac{\sqrt{\lambda}}{2 \pi} \tag{17}$$

with

$$\lambda = -\ddot{r}(0) \tag{18}$$

This is the famous formula of Rice.[6]

Mean Gust Shape

We now direct our attention to the topic of extremes. In an analogous manner the following expression for the mean shape of an extreme (maximum or minimum) between levels A and $A + \mathrm{d}A$ may be derived (see Figure 3 and Appendix A):

$$\frac{\bar{u}(\tau)}{\sigma} = \frac{A}{\sigma} r(\tau) - \frac{\sigma}{A} \left(r(\tau) + \frac{\ddot{r}(\tau)}{\lambda} \right) \tag{19}$$
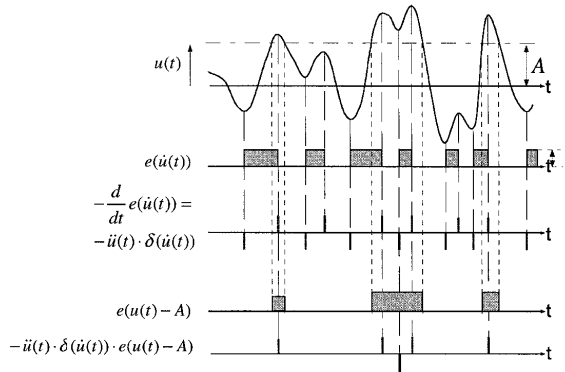
Figure 3. Mathematical operations which select extremes above level A from a stochastic signal

Notice that local minima are also taken into account (but counted as -1). The advantage is the treatment of a peak with a small dip, which will regularly occur in a stochastic time series. In this way such a peak is counted as 2 maxima and 1 minimum and thus in total as $2 - 1 = 1$ extreme (instead of 2 maxima). In other words, a peak with a small dip will have about the same effect on the average peak shape as a peak without a dip. Furthermore, a dip (near the threshold A) in a flank of some higher peak, which is of no interest for our purpose, will have only a minor effect on the mean gust shape, as it is treated as 1 maximum and 1 minimum and thus as 0 extremes.

The theoretical expression of the autocorrelation function of turbulence has a sharp peak at $\tau = 0$. The second derivative at $\tau = 0$, which is required for the evaluation of (19), is infinite (in the hypothetical case that the spectrum does not drop off in the dissipation range); this is due to the fact that the turbulence spectrum for large frequencies is inversely proportional to the 5/3 power of the frequency ('inertial subrange').

In the situation of measurements this will not be the case owing to the involved rounding off. Firstly, the anemometer has some dynamic properties. Secondly, the measurements should have been filtered according to the applied sample frequency, e.g. in the case of a 2 Hz-sampled wind signal a filter of 1 Hz should have been applied. For the verification of the mean gust shape this may have a considerable influence if the sample frequency is low.

See Figure 4 for the theoretical mean gust shape for two filter time constants. This implies that for verification the filter time constant (or sampling frequency) should be taken into account.

Our interest concerns extreme gusts, so large values of the amplitude A. In this case the first term of (19), $(A/\sigma)r(\tau)$, is dominating, which corresponds with the expression of *New*Gust[2] based upon constrained simulation. Note that it is not yet clear why the above expression (19) deviates from expression (1) of *New*Gust for small amplitudes caused by the second term; this deviation does not have any practical consequence however, because it is restricted to small amplitudes.

In the literature a similar expression to (19) can be found for the extreme loads on offshore platforms due to hydrodynamic excitation by means of waves;[7] this expression is based on the general work on extremes by Lindgren.[8] The (small) difference between (19) and the expression given in Reference 8 is due to the fact that there only maxima are considered without correction for small dips; both expressions converge again for large amplitudes.

So far the (extreme) wind speed at one point in space has been considered. In fact an extreme gust has a spatial extension (thus non-uniform over the rotor plane) as given in Reference 2. In practice it will be difficult or even impossible to determine the position of the centre of some gust with the aid of a limited
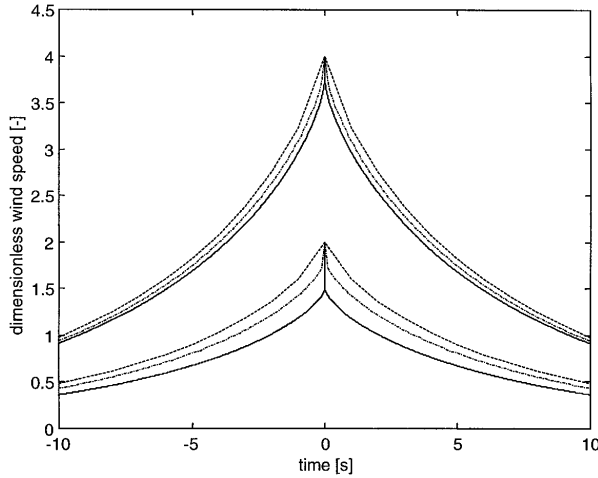
Figure 4. Theoretical mean gust shapes for two different time constants of sampling filter (T = 1 s, broken lines; T = 0·1 s, chain lines) compared with theoretical curves (full lines), for gust amplitudes of 4 σ (upper curves) and 2σ (lower curves)

number, say six to eight, of anemometers. This implies that a statistical analysis of a large number of gusts is the only way possible. For this purpose an analogous derivation to that given in Appendix A has been carried out, leading to the following (theoretical) expression for the 'spatial gust shape', which is the shape of the wind at height 2 around the time instant of an extreme at height 1 (with amplitude A):

$$\frac{\overline{u_{\text{gust}}}(\tau)}{\sigma} = \frac{A}{\sigma}\rho(\tau) - \frac{\sigma}{A}\left(\rho(\tau) - \frac{\ddot{\rho}(\tau)}{\ddot{r}(0)}\right) \tag{20}$$

with ρ the cross-correlation function. Equation (20) is a generalization of (19).

Verification of the Gust Shape by Means of Simulated Wind

In this section the mean gust shape from simulated wind will be compared with the theoretical expression given in the previous section in order to verify the method of gust analysis. The advantage of simulated wind is that the correlation function required in (19) is known, for it is used as input for the wind field simulation. With the aid of the wind field simulation package SWING3,[9] time series are generated for mean wind speeds 10 and $20\,\text{m s}^{-1}$ at two heights (40 and 80 m) with a duration of more than 10 min (16,384 time steps of 0·04 s). For each of these simulations, 100 realizations have been generated in order to increase the number of gusts. The expressions according to the isotropic turbulence theory are used (see Appendix B).

The following steps, according to the analysis method described in the previous section, are applied in order to determine the mean gust shape.

● Search in the simulated wind time series $u(t)$ for time instants of local maxima or minima (thus no condition on the second derivative) and for which the wind speed u is between levels A and $A + \text{d}A$. Four classes have been investigated: between $0·5\,\sigma$ and $1·5\,\sigma$, between $1·5\,\sigma$ and $2·5\,\sigma$, between $2·5\,\sigma$ and $3·5\,\sigma$, and larger than $3·5\,\sigma$.
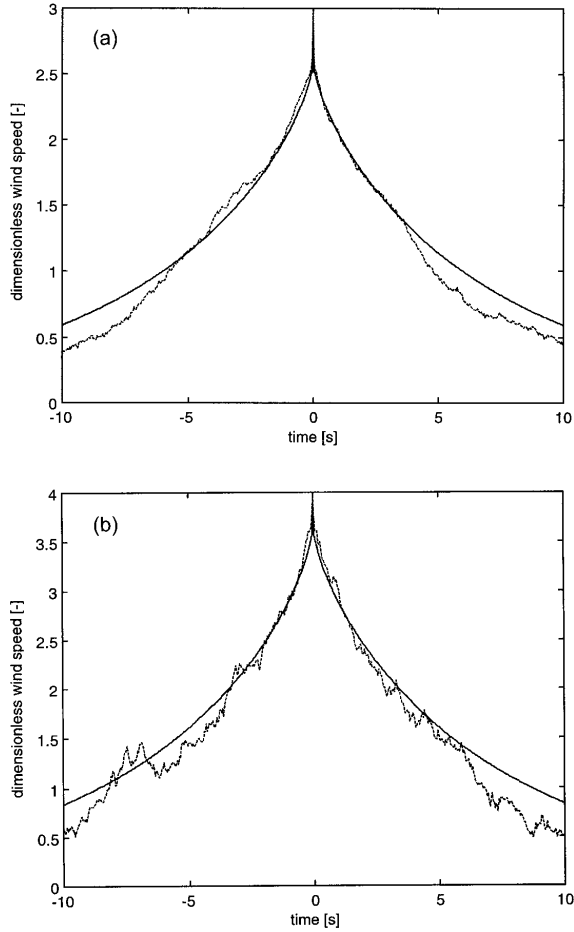
Figure 5. (a) Comparison of mean gust shape according to theory (full line) and derived from simulated wind (broken line), with amplitude of 3 σ and mean wind speed of 10 m s⁻¹. The number of gusts equals 479. (b) Comparison of mean gust shape according to theory (full line) and derived from simulated wind (broken line), with amplitude of 4 σ and mean wind speed of 10 m s⁻¹. The number of gusts equals 26

- Take the pieces of the wind time series around the extremes found (e.g. 10 s before until 10 s after the extreme).
- Average all found pieces; a maximum is counted as +1 and a minimum as −1.

As can be seen from Figure 5, the agreement between the theoretical gust shape and the ones derived from the time series is remarkably good. The small deviations are due to the stochastic nature of turbulence.
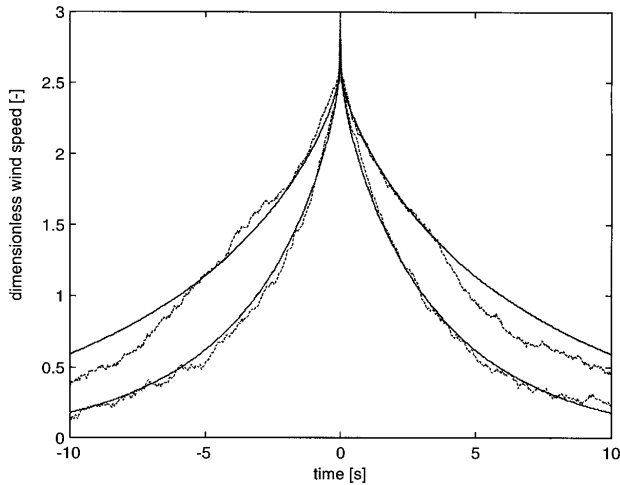
Figure 6. Comparison of mean gust shapes according to theory (full lines) and derived from simulated wind (broken lines), with amplitude of 3 σ and wind speeds of 10 m s^{-1} (upper curves) and 20 m s^{-1} (lower curves)

In Figure 6 the mean gust shapes are given for two different mean wind speeds; it can be seen that it is necessary to do the verification for each mean wind speed separately. From a similar comparison (not shown here) the importance of the specific auto- and cross-correlation functions can be demonstrated.

The theoretical method can also be applied to determine the spatial shape. The method is as follows.

- Search in the simulated wind at height 1 for extremes.
- Determine the pieces of the wind time series at height 2 around the found time instants.
- Average all these pieces.

The agreement between the mean spatial gust shape according to the time series and the theoretical curves is also very good (Figure 7). The fact that the mean spatial gust shape from the time series is lower than the theoretical curve is due to the relatively large width of the amplitude range: all gusts between 2.5σ and 3.5σ are counted as 3σ gusts. The gusts with smaller amplitude will occur more often than larger gusts; this implies that averaging over all gusts will lead to a mean spatial gust shape with a smaller amplitude.

Verification of the Gust Shape by Means of Measured Wind

In this section the mean temporal and spatial gust shapes are determined experimentally and compared with the theoretical expressions derived previously. The wind data analysed here have been measured at the 240 m tall meteorological tower of Cabauw. Cabauw is situated near Utrecht in the Netherlands and surrounded by farmland with an average terrain roughness of 0·03 m. The data set contains approximately 700 h of data recorded at five different heights (20, 40, 80, 140 and 200 m) and measured at a sample frequency of 2 Hz. The measurements have been made during periods when wind speeds higher than 10 m s^{-1} were expected. The average wind speed of the complete data set is 10 m s^{-1}. For the verification process the wind data from 40 and 80 m heights have been selected, as these are relevant to wind turbine design. The gust shape was derived from the measurements at 40 m height. The data from
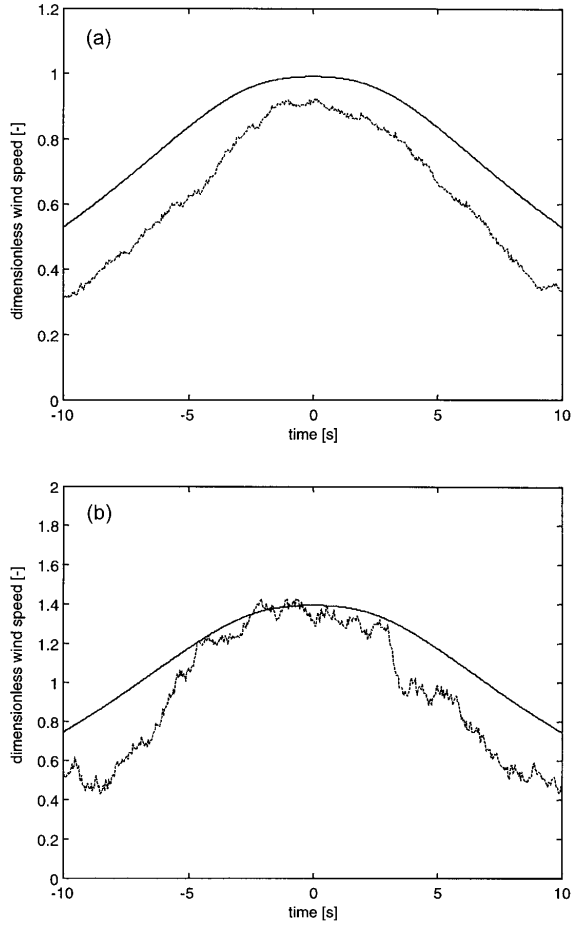
Figure 7. (a) Comparison of mean spatial gust shape according to theory (full line) and derived from simulated wind (broken line), with amplitude of 3 σ (1897 gusts). (b) Comparison of mean spatial gust shape according to theory (full line) and derived from simulated wind (broken line), with amplitude of 4 σ (115 gusts)

80 m height have been used to verify the spatial gust shape, i.e. the wind signal at 80 m, given a wind maximum at 40 m height. For the data processing the following process was used.

- For every record of 10 min, average properties were calculated: average wind speed and standard deviation.
- The wind speed was normalized using these average properties.
- Minima and maxima of the 40 m signal having an amplitude larger than 1.5σ were extracted and stored, together with 30 s before and after the extreme.
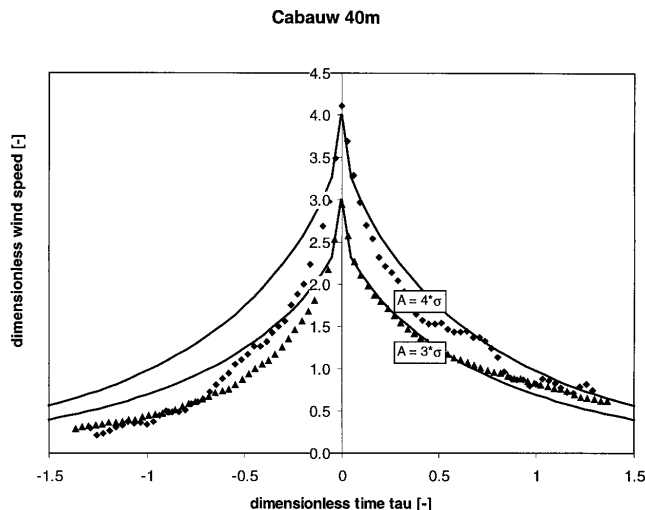- For the same time period the 80 m wind signal was stored.

Cabauw 40m

Figure 8. *Comparison of mean gust shapes according to theory (lines) and derived from measured wind (symbols), for amplitudes of 3 σ and 4 σ*

● Using ensemble averaging, the average maximum gust and the gust shape at 80 m were calculated.

The total number of gusts used for averaging was approximately 1700.

Figure 8 shows the gust shape at 40 m height for two different amplitudes, i.e. $3\,\sigma$ and $4\,\sigma$. The time axis has been normalized with the longitudinal length scale L (i.e. the $^{x}L_{u}$ of ESDU[10]) and the average wind speed V: $\tilde{\tau} = 0\cdot747\,V\tau/L$.

Figure 9 shows the average gust shape of the wind speed at 80 m, measured simultaneously with the 40 m maximum. The maximum value is lower than that of the 40 m maximum gust, reflecting the non-perfect lateral coherence. For comparison the theoretical gust shapes have been plotted. The expressions for the auto- and cross-correlation functions were taken from ESDU.[10] The small dip at $\tau = 0$ in Figure 9 is due to the dependence of the compound lateral length scale on τ, by application of the Taylor hypothesis on 'frozen turbulence'.

The agreement between the measurements and the theoretical curves is remarkably good. Both the shape and magnitude of the gusts are predicted well by the theoretical curves, although the real wind speeds are not strictly Gaussian. The existing small deviations between the theoretical and measured data might be partially due to the fact that for the theoretical curves the auto- and cross-correlation functions from ESDU were taken rather than the ones derived from the actual site measurements.

Note that the wind signal exhibits a time asymmetry. A possible explanation for this effect is the asymmetric behaviour of cup anemometers, which accelerate fast but decelerate much slower. The maximum of the 80 m gust seems to have shifted to negative time values. This suggests that there is an effect of wind shear, which has not been accounted for in the theoretical expressions.

Conclusions

An analytical expression for the mean shape of extreme gusts is presented assuming that turbulence is a stationary stochastic process. According to this expression, the gust has a rather sharp peak, in contradiction to the gust shape given in standards.
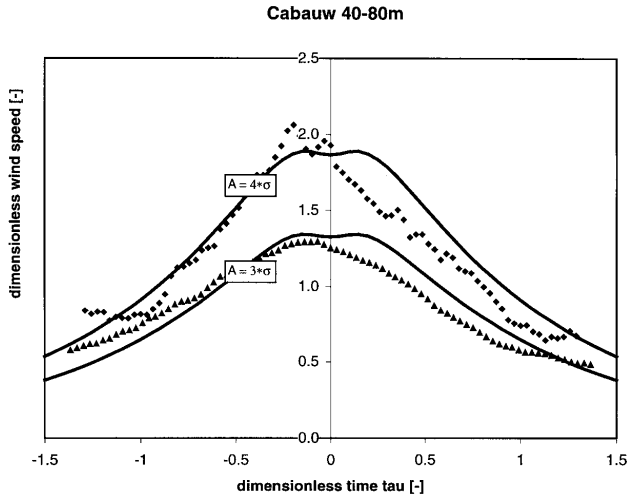
Cabauw 40-80m

Figure 9. Comparison of mean spatial gust shapes according to theory (lines) and derived from measured wind (symbols), for amplitudes of 3 σ and 4 σ

The theoretical mean gust shape has been verified by means of simulated and measured wind data. The resemblance between the theoretical and experimental curves is good, in particular for the shape in time. Some possible reasons have been indicated for the still existing small deviations. This demonstrates the viability of a new advanced method (*New*Gust[2]) for the determination of the extreme response. In the framework of a European project[11,12] this method will be extended and demonstrated for present wind turbines.

Acknowledgements

References

1. D. C. Quarton, 'The evolution of wind turbine design analysis—a twenty year progress review', *Wind Energy*, **1**, 5–24 (1998).
2. J. B. Dragt and W. Bierbooms, Modelling of extreme gusts for design calculations, *European Union Wind Energy Conf*., Göteborg, May, 1996, pp. 842–845.
3. J. B. Dragt and W. Bierbooms, Constrained simulation, to be published.
4. W. Bierbooms, J. W. Cleijne and P. Cheng, Uitbreiding en verificatie van methode voor extreme windbelastingen, *Novem Project 224.720-9740*, June, 1999.
5. D. Middleton, *An Introduction to Statistical Communication Theory*, McGraw-Hill, New York, 1960.
6. S. O. Rice, 'Mathematical analysis of random noise', *Bell Syst. Tech. J.*, **23**, 282 (1944), Reprinted in N. Wax (ed.), *Selected Papers on Noise and Stochastic Processes*, Dover, New York, 1958.

Wind Energ., **2**, 137–150 (1999)

7. P. H. Taylor, P. Jonathan and L. A. Harland, 'Time domain simulation of jack-up dynamics with the extremes of a Gaussian process', *J. Vibration and Acoustics* **119**, 624–628 (1997).
8. G. Lindgren, 'Some properties of a normal process near a local maximum', *Ann. Math. Statist.*, **41**, 1870–1883 (1970).
9. W. A. A. M. Bierbooms and J. B. Dragt, The choice of atmospheric turbulence models for stochastic rotor load calculations, *European Wind Energy Conf.*, Thessaloniki, October, 1994, pp. 648–653.
10. ESDU, 'Engineering Sciences Data', *Wind Engineering; Volume 1a; Wind Speeds and Turbulence*, ESDU International, London, 1975.
11. W. Bierbooms, Determination of the loading due to extreme gusts for design calculations, *European Wind Energy Conf.*, Dublin, October, 1997, pp. 622–625.
12. W. Bierbooms, P. W. Cheng, G. Larsen, B. J. Pedersen and K. Hansen, Modelling of extreme gusts for design calculations (*New*Gust), *European Wind Energy Conf.*, Nice, March, 1999, pp. 1001–1004 [see also appendix].
13. A. Heck, *Introduction to Maple*, Springer, New York, 1993.

Appendix A: Peaks above Some Threshold A in a Stationary Gaussian Wind Signal

In this appendix, peaks above some threshold A are investigated. For this situation the function $p(t)$ is as follows (see also Figure 3):

$$p(t) = -\ddot{u} \; \delta(\dot{u}(t)) \; e(u(t) - A) \tag{21}$$

with $e(t)$ the unit step function at $t = 0$ (Heaviside function).

As remarked before, the local minima are also taken into account (but counted as -1). The advantage is the treatment of a peak with a small dip, which will regularly occur in a stochastic time series. In this way such a peak is counted as 2 maxima and 1 minimum and thus in total as $2 - 1 = 1$ extreme (instead of 2 maxima). In other words, a peak with a small dip will have about the same effect on the average peak shape as a peak without a dip. Furthermore, a dip (near the threshold A) in a flank of some higher peak, which is of no interest for our purpose, will have only a minor effect on the mean gust shape, as it is treated as 1 maximum and 1 minimum and thus as 0 extremes. Another advantage of this approach is that it simplifies the analytical derivation.

The expectation value of u around these peaks according to (8) is

$$E[\bar{u}(\tau)] = \frac{E[-u(t + \tau) \; \ddot{u}(t) \; \delta(\dot{u}(t)) \; e(u(t) - A)]}{E[-\ddot{u}(t) \; \delta(\dot{u}(t)) \; e(u(t) - A)]} \tag{22}$$

The multidimensional distribution function of $u(t)$, $\dot{u}(t)$, $\ddot{u}(t)$ and $u(t + \tau)$ will be denoted by $P(u,v,w,z)$. The shape of a gust above level A can now be expressed as

$$\overline{u_{>A}}(\tau) = \frac{\int \int \int \int du \; dv \; dw \; dz \; (-z \; w \; \delta(v) \; e(u - A)) \; P(u, v, w, z)}{\int \int \int \int du \; dv \; dw \; dz \; (-w \; \delta(v) \; e(u - A)) \; P(u, v, w, z)} \tag{23}$$

The delta function in the integrand can be evaluated by setting v equal to zero. Furthermore, the Heaviside function can be eliminated by adapting the limits of integration, so we obtain

$$\overline{u_{>A}}(\tau) = \frac{-\int_{A}^{\infty} du \int_{-\infty}^{\infty} dw \int_{-\infty}^{\infty} dz \; P(u, 0, w, z) \; w \; z}{-\int_{A}^{\infty} du \int_{-\infty}^{\infty} dw \int_{-\infty}^{\infty} dz \; P(u, 0, w, z) \; w} \tag{24}$$

The above expression gives the mean of all peaks above level A. In order to derive an expression for the mean shape of a peak between levels A and $A + \mathrm{d}A$, the denominator and numerator should be differentiated with respect to A:

$$\overline{u_A}(\tau) = \frac{\int_{-\infty}^{\infty} \mathrm{d}w \int_{-\infty}^{\infty} \mathrm{d}z \; P(A, 0, w, z) \; w \; z}{\int_{-\infty}^{\infty} \mathrm{d}w \int_{-\infty}^{\infty} \mathrm{d}z \; P(A, 0, w, z) \; w} \tag{25}$$

The probability density function $P(u,v,w,z)$ is a 4D normal distribution with zero means and covariance matrix

$$\Lambda = \sigma^2 \begin{pmatrix} 1 & 0 & -\lambda & r(\tau) \\ 0 & \lambda & 0 & -\dot{r}(\tau) \\ -\lambda & 0 & \mu & \ddot{r}(\tau) \\ r(\tau) & -\dot{r}(\tau) & \ddot{r}(\tau) & 1 \end{pmatrix} \tag{26}$$

In principle the required integrals can now be evaluated. In practice this will be difficult, because the inverse of the covariance matrix is needed. For this purpose one may use special tools for formula manipulation, e.g. Maple.[13] After performing these mathematical derivations, expression (19) will be obtained without further approximations. In Reference 4 another route is followed by introducing conditional probabilities, which reduces the dimension of the problem.

In an analogous manner, expression (20) can be derived for the 'spatial' mean gust shape.

Appendix B: Auto- and Cross-correlation Functions Based on the Isotropic Turbulence Theory

The (normalized) autocorrelation function for the longitudinal turbulence component equals[10]

$$r(\tau) = 0 \cdot 592 \; \tilde{\tau}^{1/3} K_{1/3}(\tilde{\tau}) \tag{27}$$

with K the modified Bessel function of the second kind and $\tilde{\tau}$ the dimensionless time:

$$\tilde{\tau} = 0 \cdot 747 \; \frac{V\tau}{L} \tag{28}$$

with V the mean wind speed and L the longitudinal length scale.

The cross-correlation function for the longitudinal velocity component (for a distance D perpendicular to the longitudinal velocity component) equals[10]

$$\rho(D, \tau) = (f(\tilde{\tau}) - g(\tilde{\tau})) \frac{\Delta s^2}{\Delta r^2} + g(\tilde{\tau}) \tag{29}$$

with

$$f(\tilde{\tau}) = 0 \cdot 592 \; \tilde{\tau}^{1/3} K_{1/3}(\tilde{\tau}), \qquad g(\tilde{\tau}) = 0 \cdot 592 \; (\tilde{\tau}^{1/3} K_{1/3}(\tilde{\tau}) - 0 \cdot 5 \; \tilde{\tau}^{4/3} K_{2/3}(\tilde{\tau})) \tag{30}$$

and

$$\Delta s = \tau V, \qquad \Delta r = \sqrt{(\Delta s)^2 + D^2}, \qquad \tilde{\tau} = \frac{0 \cdot 747}{L} \Delta r \tag{31}$$

with V the mean wind speed and L the longitudinal length scale.

The first and second derivatives of these functions may be obtained in an analytical or numerical way.

Research Article

Investigation of Spatial Gusts with Extreme Rise Time on the Extreme Loads of Pitch-regulated Wind Turbines

Wim Bierbooms*, Section Wind Energy, Delft University of Technology, Delft, The Netherlands

It is assumed that the extreme loading of pitch-regulated turbines is caused by gusts with an extreme rise time rather than an extreme gust amplitude. A special kind of wind field simulation, so-called constrained stochastic simulation, is dealt with in order to generate the desired gusts. Just as in wind field simulation for fatigue purposes, it is assumed that turbulence is Gaussian; a possibility is mentioned of how to deal with non-Gaussian behaviour. On the basis of the presented theory it can be stated that the stochastic gusts produced in this way are, in a statistical sense, not distinguishable from gusts selected from a (very long) time series. An example of a spatial gust as well as the mean spatial gust shape is shown. For a reference turbine the maximum blade root flapping moment has been determined as a function of the gust centre in the rotor plane; the maximum response is obtained in the case where the gust hits one of the rotor blades at 75% of the radius. When the gust duration is large compared with the integral time constant of the controller, the controller can handle the gust as expected. However, even for small rise times it turns out that the maximum flap moment due to the gust is not significantly higher than that due to the background turbulence and 1P excitations. This may indicate that perhaps extreme rise time gusts do not lead to extreme loading of pitch-regulated wind turbines. For a final judgement a proper probabilistic approach is necessary; an outline of such an approach has been sketched. Furthermore, it is recommended to do research on other gust types in order to find out the type which leads to the extreme wind turbine loading. Copyright © 2004 John Wiley & Sons, Ltd.

Introduction

Verification of the structural integrity of a wind turbine structure involves analyses of fatigue loading as well as extreme loading arising from the wind climate. With persistently growing turbines (over 100 m in both rotor diameter and tower height), the extreme loading seems to become relatively more important. The reason for this is that high-frequency wind speed fluctuations, relevant for fatigue, have a limited spatial extent and so will be cancelled out over the rotor plane. In order to assess the fatigue loading generated, random 3D wind fields are routinely used in standard wind turbine design packages employed by the wind turbine industry. Stochastic wind fields of typically 10 min length are generated for different mean wind speeds to cover the wind situations a turbine will meet during its lifetime. For the stochastic wind field simulation it is assumed that turbulence is a stationary Gaussian process specified by a given (cross-)spectral density. The extreme loads, however, are dealt with in a rather simple way by describing wind gusts as coherent gusts of an inherently

*Correspondence to: W. Bierbooms, Section Wind Energy, Delft University of Technology, Delft, The Netherlands.
E-mail: W.Bierbooms@lr.tudelft.nl

deterministic character (see e.g. Reference 1), whereas the gusts experienced in real situations are of a stochastic nature with a limited spatial extension.

This conceptual difference may cause substantial differences in the load patterns of a wind turbine when a gust event is imposed. In order to introduce realistic gust load situations of a stochastic nature, the *New*Gust method[2] has been launched. It has been inspired by NewWave, a method to generate extreme waves based on the mathematical work of Lindgren,[3] but it differs in methodology. In the probabilistic approach of *New*Gust, gusts of given amplitude are generated and used to perform a wind turbine load calculation. The distribution of the extreme load (or the 50 year extreme load) can be determined by taking into account all gust amplitudes and all mean wind speeds. The method turned out to be fit for stall-regulated wind turbines: the mean theoretical gust shape has been verified[2,4] by comparison with an experimentally derived mean gust shape based on many time records from the database on wind characteristics.[5] Furthermore, the probability of occurrence of gusts has been verified on the basis of the same database.[2]

For pitch-regulated wind turbines it is assumed that the extreme response is associated with gusts with an extreme rise time. In Reference 6, coherent gusts with extreme rise time have been dealt with. In this article we will extend the method to spatial gusts.

The method to generate gusts has been denoted constrained stochastic simulation and is dealt with in the third section. In the next section we start with a brief overview of wind field generation in general. Examples of spatial gusts with extreme rise time are shown in the fourth section. The consequence of these gusts on the loading of wind turbines is outlined in the fifth section. Finally, the sixth section treats a probabilistic approach to determine the overall extreme loading of wind turbines, and in the seventh section some remarks on non-Gaussianity are made.

Recently a report[7] has been published in which a totally different method, based on variational calculus, is applied in order to simulate gusts. It can be shown that the final results, for a given gust description, based on the method of constrained stochastic simulation (third section) and the method used in Reference 7 are identical.

Simulation of Stochastic Wind Fields

Stochastic time series generators are based on the summation of harmonics with random phase φ (uniformly distributed between 0 and 2π) and amplitudes which follow from the (two-sided) auto power spectral density S:[8]

$$u(t) = \sum_{k=-K}^{K} A_k \cos(\omega_k t + \varphi_k) \tag{1}$$

with

$$A_k = \sqrt{S_k \Delta f}$$

where t is the (discretized) time, $\Delta f = 1/T$ is the frequency step, T is the total time of the sample and ω_k is a set of $2K$ equidistant frequencies ($k = 0$ excluded).

In most wind field generators implemented in wind turbine design tools, a 3D generalization of equation (1) is used; the square root is then replaced by a matrix decomposition. A practical disadvantage is that for a full 3D wind field the matrix gets very large, with corresponding high computional demand and required memory use. A more fundamental disadvantage is that no consistent set of cross-spectra exists for all velocity components (longitudinal, lateral and vertical) for all points in space. A way to overcome this problem is to generate a 3D wind field in some box in space (at one point in time) rather than as function of time:

$$\mathbf{u}(\mathbf{r}) = \sum_{spq} \mathbf{A}_{spq} \cos(\mathbf{k}\mathbf{r} + \varphi_{spq}) \tag{2}$$

with

$$\mathbf{A}\mathbf{A}^{\mathrm{T}} = \mathbf{E}(\mathbf{k})\Delta k$$

(vectors and matrices are indicated by bold symbols)

The summation of equation (2) is now over whole (circular) wavenumber space ($k = 2\pi/\lambda$, with λ the wavelength, the equivalent of $\omega = 2\pi/T$; the indices s, p and q correspond respectively to the k_x, k_y and k_z directions) rather than over frequency space. The tensor $\mathbf{E}(\mathbf{k})$ is the 3D Fourier transform of the correlation tensor $\mathbf{Q}(\mathbf{r})$, so it describes all second-order moments of turbulence:

$$\mathbf{Q}(\mathbf{r}_2 - \mathbf{r}_1) = E\left[\begin{pmatrix} u(\mathbf{r}_1) \\ v(\mathbf{r}_1) \\ w(\mathbf{r}_1) \end{pmatrix} (u(\mathbf{r}_2)\ \ v(\mathbf{r}_2)\ \ w(\mathbf{r}_2))\right] \qquad (3)$$

$$\mathbf{E}(\mathbf{k}) = \frac{1}{(2\pi)^3} \int \mathbf{Q}(\mathbf{r}) \mathrm{e}^{-ikr} \mathrm{d}\mathbf{r} \qquad (4)$$

For isotropic turbulence the spectrum tensor is known and can be decomposed analytically. The decomposition is not unique, so different choices can be made (see e.g. References 9 and 10).

With respect to the geometry of a wind turbine rotor it is natural to apply polar co-ordinates. In Reference 10, equation (2) is therefore rewritten in cylindrical co-ordinates in both wavenumber and real space. The obtained expression for the velocity vector is periodic in azimuth angle (with period 2π; recall that a wind field is generated for one time instant) and can thus be expanded in a Fourier series. It turns out that the Fourier coefficients can be expressed in terms of Bessel functions (of the first kind). Next the x-axis is transformed into a time axis by application of Taylor's frozen turbulence hypothesis: $x = -Ut$ (and $k_x = -2\pi f/U$); the plane of the wind turbine rotor is chosen to be the r–φ (y–z) plane. This all leads to a 2D FFT over frequency and azimuthal mode. In fact, in the wind field generator Swing4[11,12] a 1D FFT only is performed and the azimuthal Fourier coefficients are stored. The remaining Fourier summation is done in the wind turbine design tool, as the azimuth angles of the rotor blades are calculated at each time step. The advantage of this approach is that it makes interpolation superfluous: the wind velocities are generated at the blade section locations and the correct azimuthal positions. In this article we will generate 3D wind fields in a fixed frame of reference, so a 2D FFT is performed. A (wavenumber-dependent) correction is applied just before the FFT in order to correct for the anisotropy of atmospheric turbulence.

A physically more appropriate way to correct for anisotropy is treated in Reference 9. By application of the linearized Navier–Stokes equation and consideration of the lifetime of eddies a 'sheared' spectral tensor is obtained. Next a wind field is generated through a 3D FFT in Cartesian co-ordinates. It should be possible to apply this sheared tensor also in the method presented in this article.

Constrained Stochastic Simulation

Uniform wind gusts

In this subsection a concise overview is given of generation of gusts at one point (or alternatively, coherent gusts, constant over the rotor plane) with an extreme rise time.[6] In the context of this article, such a gust is specified by a local minimum and a local maximum with a time separation (rise time) Δt and a velocity difference (jump) ΔU:

$$\begin{aligned} \dot{u}(t_0) &= 0 \\ \ddot{u}(t_0) &= B_1 > 0 \\ u(t_0 + \Delta t) - u(t_0) &= \Delta U \\ \dot{u}(t_0 + \Delta t) &= 0 \\ \ddot{u}(t_0 + \Delta t) &= B_2 < 0 \end{aligned} \qquad (5)$$

Since we assume turbulence to be Gaussian, the first and second time derivatives exist. Note that it is not required that the minimum and maximum concerned are consecutive, i.e. it is possible that other local minima and maxima are in between. The reason for choosing such a definition for an event is that, with respect to the assessment of extreme loads on wind turbines, it is not known *a priori* what will cause the highest loads: a modest velocity jump in a (very) short rise time or a large velocity jump in a rather long rise time.

One could opt for considering the third constraint of equation (5) only, i.e. specifying a velocity jump, but in that case the two points will in general not be a minimum or a maximum. The implication is that the considered gust is just a part of some larger velocity jump, i.e. a gust generated on the basis of such a constraint will generally have a larger velocity jump. Thus load estimates based on such gusts are associated with a whole range of velocity jumps instead of just one value as is the case with equation (5). Furthermore, specification of just a velocity jump does not form a countable event. This will significantly complicate the probabilistic approach which will be outlined in the sixth section.

A remark on the actual values for B_1 and B_2 will be given at the end of this subsection.

A 'brute force' method to obtain wind gusts, with a rise time inside a small range around a desired value Δt and with a velocity jump inside a small range around ΔU, is to select these from very long time series of turbulence (either measured or stochastically simulated). It will be clear that such an approach is far from practical for extreme gusts which will occur on average just once in a year or even 50 years. Furthermore, sufficiently long measured time series, with a high enough sampling rate of say 5 Hz and at several space points, do not exist.

An alternative is to perform a special kind of stochastic simulation during which the desired gusts are automatically selected. This method has been denoted constrained stochastic simulation. The starting point of constrained stochastic simulation is stochastic simulation, equation (1). In fact, for our purpose an alternative description by means of a Fourier series is more appropriate:

$$u(t) = \sum_{k=1}^{K} a_k \cos(\omega_k t) + b_k \sin(\omega_k t) \tag{6}$$

As already mentioned, for wind field simulation routinely performed in order to assess wind turbine fatigue loads, it is assumed that turbulence is Gaussian. The same assumption is applied for constrained stochastic simulation; in the seventh section some ways of dealing with non-Gaussianity will be discussed. For normally distributed wind speed fluctuations also the Fourier coefficients a_k and b_k will be normal. Their means are zero, they are mutually uncorrelated and their variances are S_k/T, where S is the one-sided auto power spectral density of the wind speed fluctuations.

For ease of notation we rewrite equation (6) as

$$u(t) = \mathbf{\Psi}(t)c \tag{7}$$

with row vector

$$\mathbf{\Psi}(t) = (\cos(\omega_1 t) \; \cdots \; \cos(\omega_K t) \; \sin(\omega_1 t) \; \cdots \; \sin(\omega_K t)) \tag{8}$$

and column vector **c** consisting of the Fourier coefficients:

$$c = (a_1 \; a_2 \; \cdots \; a_K \; b_1 \; \cdots \; b_K)^{\mathrm{T}} \tag{9}$$

The specification of a wind gust, equation (5), can now also be done on the basis of the Fourier coefficients a_k and b_k:

$$\mathbf{a} = \mathbf{A} \tag{10}$$

The random vector **a** is a linear relation of **c** defined by

$$\mathbf{a} = \mathbf{Gc} = \begin{pmatrix} \dot{u}(t_0) \\ \ddot{u}(t_0) \\ u(t_0 + \Delta t) - u(t_0) \\ \dot{u}(t_0 + \Delta t) \\ \ddot{u}(t_0 + \Delta t) \end{pmatrix}$$ (11)

with $\mathbf{G}$ a matrix of constants:

$$\mathbf{G} = \begin{pmatrix} \dot{\boldsymbol{\Psi}}(t_0) \\ \ddot{\boldsymbol{\Psi}}(t_0) \\ \boldsymbol{\Psi}(t_0 + \Delta t) - \boldsymbol{\Psi}(t_0) \\ \dot{\boldsymbol{\Psi}}(t_0 + \Delta t) \\ \ddot{\boldsymbol{\Psi}}(t_0 + \Delta t) \end{pmatrix}$$ (12)

The vector $\mathbf{A}$ equals the right-hand side of equation (5), i.e.

$$\mathbf{A} = \begin{pmatrix} 0 \\ B_1 \\ \Delta U \\ 0 \\ B_2 \end{pmatrix}$$ (13)

In other words, the Fourier coefficients a_k and b_k which are normally distributed should satisfy the above conditions in order to obtain the desired wind gust. Thus selecting some specific gust (from a time series) corresponds to considering the matching conditional density of the Fourier coefficients.

The conditional density $f(\mathbf{c}|\mathbf{a} = \mathbf{A})$ of $\mathbf{c}$ upon observing $\mathbf{a} = \mathbf{A}$ is again normal and thus determined by its mean $\mathbf{m}_c$ and covariance matrix $\mathbf{M}_c$. The mean and covariance matrix can be found in handbooks on statistics (see e.g. Reference 13):

$$\mathbf{m}_c = \mathbf{MG}^T\mathbf{Q}^{-1}\mathbf{A}$$ (14)

$$\mathbf{M}_c = \mathbf{M} - \mathbf{MG}^T\mathbf{Q}^{-1}\mathbf{GM}$$ (15)

with

$$\mathbf{M} = \mathrm{E}[\mathbf{cc}^T]$$ (16)

$$\mathbf{Q} = \mathrm{E}[\mathbf{aa}^T] = \mathbf{GMG}^T$$ (17)

The above equations are valid for normal random variables, which explains our choice of equation (6) instead of equation (1); furthermore, equation (6) with Gaussian coefficients is more correct than equation (1).

The conditional random vector $\mathbf{c}_c$, corresponding to the conditional density $f(\mathbf{c}|\mathbf{a} = \mathbf{A})$ is

$$\mathbf{c}_c = \mathbf{c} - \mathbf{MG}^T\mathbf{Q}^{-1}(\mathbf{Gc} - \mathbf{A})$$ (18)

If $\mathbf{c}$ satisfies the original unconstrained statistics, then $\mathbf{c}_c$, the conditional random vector satisfying $\mathbf{Gc}_c = \mathbf{A}$, has the mean $\mathbf{m}_c$ and covariance $\mathbf{M}_c$ of the constrained process, equations (14) and (15). This can be verified by writing out the equations for the mean and covariance. Equation (18) provides the required recipe for transforming any realization of the unconstrained process $\mathbf{c}$ into a constrained realization $\mathbf{c}_c$.

The above equations for conditional random vectors are general valid, so they can be applied for the vectors **c** and **a** as given in equations (9) and (11). The covariance matrix **M** of **c**, the Fourier coefficient vector, is diagonal with elements S_k/T:

$$\mathbf{M} = \frac{1}{T} \begin{pmatrix} S_1 & 0 & 0 & 0 & 0 & 0 & 0 \\ 0 & S_2 & 0 & 0 & 0 & 0 & 0 \\ 0 & 0 & \cdots & 0 & 0 & 0 & 0 \\ 0 & 0 & 0 & S_K & 0 & 0 & 0 \\ 0 & 0 & 0 & 0 & S_1 & 0 & 0 \\ 0 & 0 & 0 & 0 & 0 & \cdots & 0 \\ 0 & 0 & 0 & 0 & 0 & 0 & S_K \end{pmatrix} \tag{19}$$

The constraint is that there is a gust, i.e. a velocity jump ΔU within rise time Δt, at t_0. The corresponding equation in vector notation is already given as equation (10). The constrained stochastic variable, which satisfies the constraint, can now be generated on the basis of equation (18) with **M** from equation (19), **G** from equation (12), **Q** from equation (17) and **A** from equation (13).

This concludes the required theory. In the case where the Fourier sum is calculated for the Fourier coefficients **c** normally distributed with covariance matrix given by equation (19), a random wind time series (turbulence) is obtained. In the case where the Fourier sum is calculated for the Fourier coefficients $\mathbf{c}_c$ according to equation (18), the desired gust (with velocity jump ΔU within rise time Δt) is obtained:

$$u_c(t) = u(t) - \mathbf{R}(t)(\mathbf{a} - \mathbf{A}) \tag{20}$$

with **A** given by equation (13), **a** by equation (11) and

$$\mathbf{R}(t) = \mathbf{\Psi}(t)\mathbf{M}\mathbf{G}^{\mathrm{T}}\mathbf{Q}^{-1} \tag{21}$$

i.e. $\mathbf{R}(t)$ is the Fourier sum of $\mathbf{M}\mathbf{G}^{\mathrm{T}}\mathbf{Q}^{-1}$

In the case where the number of constraints is limited, it should be possible to extend equation (20) into some explicit expression. For example, in the case of a maximum amplitude gust ($u(t_0) = A$, $\dot{u}(t_0) = 0$) an explicit expression is given in Reference 2 which includes the autocorrelation function and its first time derivative.

It is straightforward to implement this in a computer code. An example of such constrained stochastic simulation is shown in Figure 1.

The mean gust shape is given by

$$\bar{u}_c(t) = \mathbf{R}(t)\overline{\mathbf{A}} \tag{22}$$

with

$$\overline{\mathbf{A}} = \begin{pmatrix} 0 \\ \overline{B}_1 \\ \Delta U \\ 0 \\ \overline{B}_2 \end{pmatrix} \tag{23}$$

The variance is

$$\mathrm{var}(u_c(t)) = \mathrm{var}(u(t)) + \mathbf{R}(t)\,(\mathrm{var}(\mathbf{A}) - \mathbf{Q})\,\mathbf{R}^{\mathrm{T}}(t) \tag{24}$$
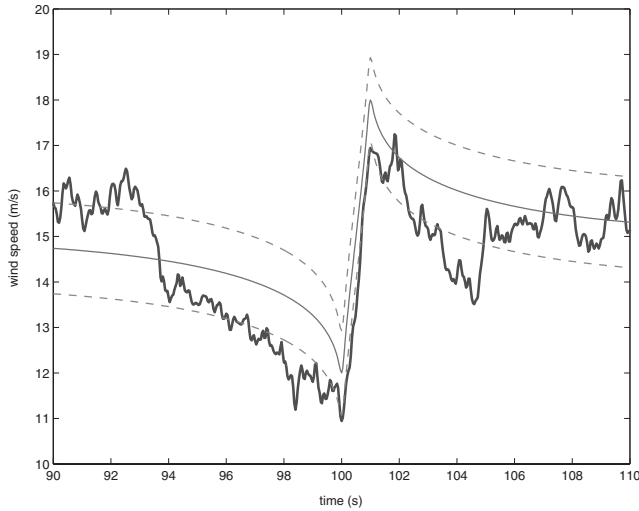
with

Figure 1. An example of a gust with a velocity jump of 6 m s^{-1} at t = 100 to 101 s. The smooth curve indicates the (theoretically) mean gust shape; the broken lines indicate the standard deviation of the gust shape

$$\text{var}(\mathbf{A}) = \begin{pmatrix} 0 & 0 & 0 & 0 & 0 \\ 0 & \text{var}(B_1) & 0 & 0 & \text{cov}(B_1, B_2) \\ 0 & 0 & 0 & 0 & 0 \\ 0 & 0 & 0 & 0 & 0 \\ 0 & \text{cov}(B_1, B_2) & 0 & 0 & \text{var}(B_2) \end{pmatrix} \tag{25}$$

The theoretical mean gust shape has been verified by analysis of wind measurements[6] on the basis of the database on wind characteristics.[5]

We will conclude this subsection with a remark on the values of B_1 and B_2. Equation (20) gives the required recipe to generate a time series around a gust ΔU in Δt with some specific values of the second derivatives: B_1 and B_2. In order to reflect the behaviour of turbulence (assumed to be Gaussian) around an arbitrary gust ΔU in Δt, B_1 and B_2 should become random variables. The corresponding probability density functions (B_1 positive values only, B_2 negative values only) can be deduced from the gust statistics (dealt with in the sixth section). For the wind turbine loads the actual values turned out to be of minor importance. Thus, for simplicity, B_1 and B_2 were set to their mean values (which can be determined numerically) in the preparation of Figure 1 (and also in the remainder of this article).

Spatial wind gusts

For spatial gusts[14] we have to specify some wind speeds, say N, in the rotor plane (assumed to be perpendicular to the mean wind speed). For reasons of simplicity the results for the longitudinal component only will be dealt with in this subsection. The velocity fluctuations at these N points form a column vector $\mathbf{u}(t)$, so equation (6) becomes

$$\mathbf{u}(t) = \sum_{k=1}^{K} \mathbf{a}_k \cos(\omega_k t) + \mathbf{b}_k \sin(\omega_k t) \tag{26}$$

The Fourier coefficients $\mathbf{a}_k$ and $\mathbf{b}_k$ can, analogously to equation (9), be put into one large column vector $\mathbf{c}_s$ (subscript 's' indicates spatial) with $2KN$ elements:

$$\mathbf{c}_s = (\mathbf{a}_1^T \ \mathbf{a}_2^T \ \cdots \ \mathbf{a}_K^T \ \mathbf{b}_1^T \ \cdots \ \mathbf{b}_K^T)^T \tag{27}$$

Like equation (7), we can now rewrite equation (26) as

$$\mathbf{u}(t) = \mathbf{\Psi}_s(t)\mathbf{c}_s \tag{28}$$

with matrix

$$\mathbf{\Psi}_s(t) = (\cos(\omega_1 t)\mathbf{I} \ \cdots \ \cos(\omega_K t)\mathbf{I} \ \sin(\omega_1 t)\mathbf{I} \ \cdots \ \sin(\omega_K t)\mathbf{I}) \tag{29}$$

where $\mathbf{I}$ indicates the $N \times N$ unit matrix.

The mean of vector $\mathbf{c}_s$ is again zero and the covariance matrix follows from the covariances of the Fourier coefficients. They are independent for different frequencies, and for the same frequency the following relation holds:

$$\mathrm{E}[\mathbf{a}_k \mathbf{a}_k^T] = \mathrm{E}[\mathbf{b}_k \mathbf{b}_k^T] = \frac{1}{T}\mathbf{S}_k \tag{30}$$

with $\mathbf{S}_k$ the matrix of the cross-power spectral densities of the wind speed fluctuations at the different space points. They are found from the auto power spectral densities (the same as in the previous subsection) and the coherence function γ:

$$\mathbf{S}_k = S_k \begin{pmatrix} 1 & \gamma_{21} & \cdots & \gamma_{N1} \\ \gamma_{21} & 1 & \cdots & \gamma_{N2} \\ \cdots & \cdots & \cdots & \cdots \\ \gamma_{N1} & \gamma_{N2} & \cdots & 1 \end{pmatrix} \tag{31}$$

The coherence function is specified in e.g. standards.

The covariance matrix $\mathbf{M}_s$ of $\mathbf{c}_k$ is thus a block diagonal matrix with the matrices $(1/T)\mathbf{S}_k$ on the main diagonal (compare with equation (19)).

Next the constraints have to be specified. This time it can be required that a velocity jump is present somewhere in the wind field. Therefore a unit (column) vector $\mathbf{e}$ is used to specify the constraints:

$$\begin{aligned} \mathbf{e}^T \dot{\mathbf{u}}(t_0) &= 0 \\ \mathbf{e}^T \ddot{\mathbf{u}}(t_0) &= B_1 > 0 \\ \mathbf{e}^T (\mathbf{u}(t_0 + \Delta t) - \mathbf{u}(t_0)) &= \Delta U \\ \mathbf{e}^T \dot{\mathbf{u}}(t_0 + \Delta t) &= 0 \\ \mathbf{e}^T \ddot{\mathbf{u}}(t_0 + \Delta t) &= B_2 < 0 \end{aligned} \tag{32}$$

Supposing the rotor centre corresponds to the ith wind speed element, one has to choose $\mathbf{e}$ to be the ith unit vector $\mathbf{e}_i$, i.e. the ith element is 1 if a gust in the centre of the rotor is required. The constraint $5 \times 2KN$ matrix $\mathbf{G}_s$ becomes

$$\mathbf{G}_s = \begin{pmatrix} \mathbf{e}^T \dot{\mathbf{\Psi}}(t_0) \\ \mathbf{e}^T \ddot{\mathbf{\Psi}}(t_0) \\ \mathbf{e}^T (\mathbf{\Psi}(t_0 + \Delta t) - \mathbf{\Psi}(t_0)) \\ \mathbf{e}^T \dot{\mathbf{\Psi}}(t_0 + \Delta t) \\ \mathbf{e}^T \ddot{\mathbf{\Psi}}(t_0 + \Delta t) \end{pmatrix} \tag{33}$$

The desired spatial gust is now given by

$$\mathbf{u}_c(t) = \mathbf{u}(t) - \mathbf{R}_s(t)(\mathbf{a} - \mathbf{A}) \tag{34}$$

with

$$\mathbf{R}_s(t) = \mathbf{\Psi}_s(t)\mathbf{M}_s\mathbf{G}_s^{\mathrm{T}}\mathbf{Q}^{-1} \tag{35}$$

It seems that the equations are getting too clumsy, but, owing to the structure of the $\mathbf{M}_s$ and $\mathbf{G}_s$ matrices, the result for the constraint velocity at each space point (with index i running from 1 to N) is similar to the result for the coherent gust, equation (20):

$$u_{c,i}(t) = u_i(t) - \mathbf{R}_i(t)(\mathbf{a} - \mathbf{A}) \tag{36}$$

with $\mathbf{a}$ and $\mathbf{A}$ the left- and right-hand sides respectively of equation (32) and

$$\mathbf{R}_i(t) = \mathbf{\Psi}(t)\mathbf{M}_2\mathbf{G}^{\mathrm{T}}\mathbf{Q}^{-1} \tag{37}$$

where $\mathbf{G}$ is given by equation (12) (i.e. for the coherent gust) and $\mathbf{M}_2$ is a $2K \times 2K$ diagonal matrix with elements $S_k \, \gamma_{in}/T$, with n the index of the gust centre. Thus, compared with the equation for the coherent gust, a factor γ_{in} is introduced; note that this factor is frequency dependent.

It is not necessary to calculate $\mathbf{Q}$ via the matrix multiplication of equation (17), since it can be directly evaluated through its definition as the covariance matrix of $\mathbf{a}$ (see equation (40)).

In the next section, examples of spatial gusts derived on the basis of equation (36) will be given.

The equations for the mean and variance of spatial gusts are similar to the ones for coherent gusts, equations (22) and (24).

Instead of equation (32), it would also be possible to specify a gust by constraints at several points in the rotor plane. However, it would become very difficult to determine the statistics of such gusts (see the sixth section), since the dimension of the involved integral, equation (39), becomes too large.

Spatial Gusts with Extreme Rise Time

The method described in the previous section has been applied to generate spatial gusts. As an example, a gust is generated with a velocity jump of $\Delta U = 4 \cdot 8$ m s^{-1} and a rise time of $\Delta t = 1 \cdot 2$ s. The gust minimum (maximum) is at 30 s (31·2 s) and the gust centre is eccentric with respect to the rotor plane: at a radial position of 15 m and azimuth angle 0 (the mean wind speed equals 10 m s^{-1} and for the standard deviation 1 m s^{-1} is taken). In Figure 2 the wind speeds as a function of time (with respect to the mean wind speed) are shown for several azimuthal positions and a radial position of 15 m; also the mean gust shape is given.

The wind speed at the position of the gust centre resembles the result for the coherent gust, Figure 1. Note that the gust shape will be different if another realization of $u(t)$ is used in equation (20). Figure 3 shows a 3D representation of the same gust as a function of time. It turns out that the spatial extent of this extreme rise time gust is limited to say 30 m × 30 m.

The gust statistics will be dealt with later (see the sixth section and Figure 8).

Wind Turbine Loading due to Spatial Gusts with Extreme Rise Time

Two pitch-regulated reference turbines will be considered. The first is a three-bladed 2 MW turbine with a rotor diameter of 80 m. With respect to the limited spatial extension of the gust (see previous section) it can be anticipated that the maximum response will occur in the case where the gust centre is located near one of the blades. The maximum root blade flapping moment of the first blade (in upward vertical position, as shown in Figure 4) as a function of the position of the gust centre is shown in Figure 4 by means of a contour plot (mean wind speed 25 m s^{-1}, turbulence intensity 8%, velocity jump of 4·8 m s^{-1} in 0·8 s). The plot was obtained through simulation with the simulation tool Bladed (Garrad Hassan), using as input the mean gusts shown on the left in Figure
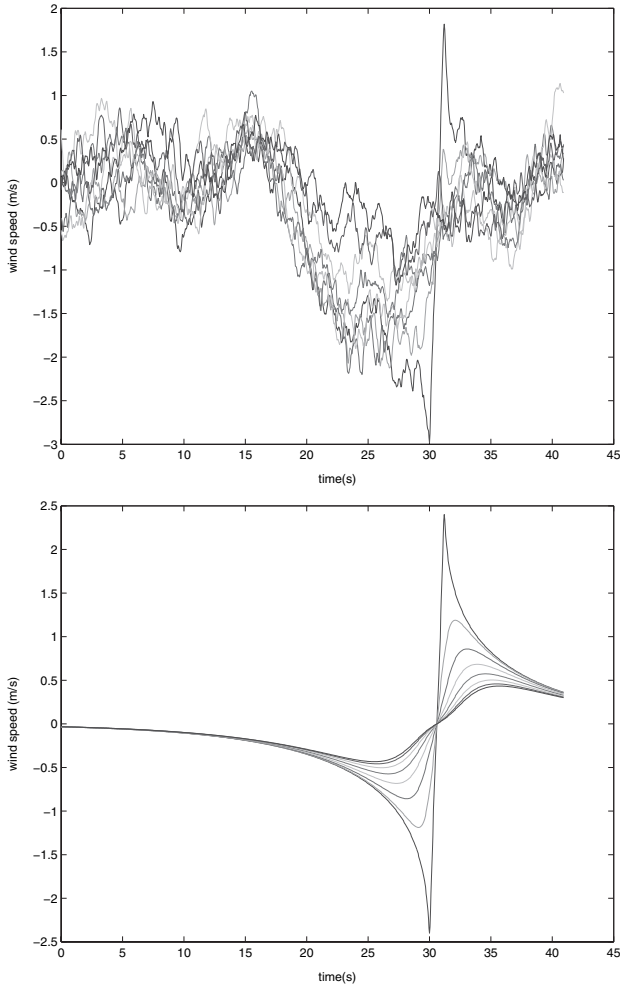
Figure 2. An example of a spatial gust with a velocity jump of 4·8 m s⁻¹ at t = 30 to 31·2 s for points on a circle (radius r = 15 m, azimuth angles 0, π/8, . . . , 7π/8; the gust centre is at an azimuth angle of 0). Top: gusts. Bottom: mean gust shapes

3. Bladed is a state-of-the-art wind turbine design tool which includes, relevant for our purpose, dynamic stall and dynamic inflow. The maximum loading occurs when the gust centre is at a lateral position of 0 m and a vertical position of 30 m (i.e. at three-quarters of the radius). In this situation the gust is in line with the wind shear and covers the outer part of the rotor blade, which contributes most to the flapping moment.

An example of the response of the reference wind turbine as a function of time is presented in Figure 5.

The controller is designed to keep the power constant above rated wind speed; the reduction of loads was not an explicit objective. However, the controller (with an integral time constant of 2·4 s) does a great job in
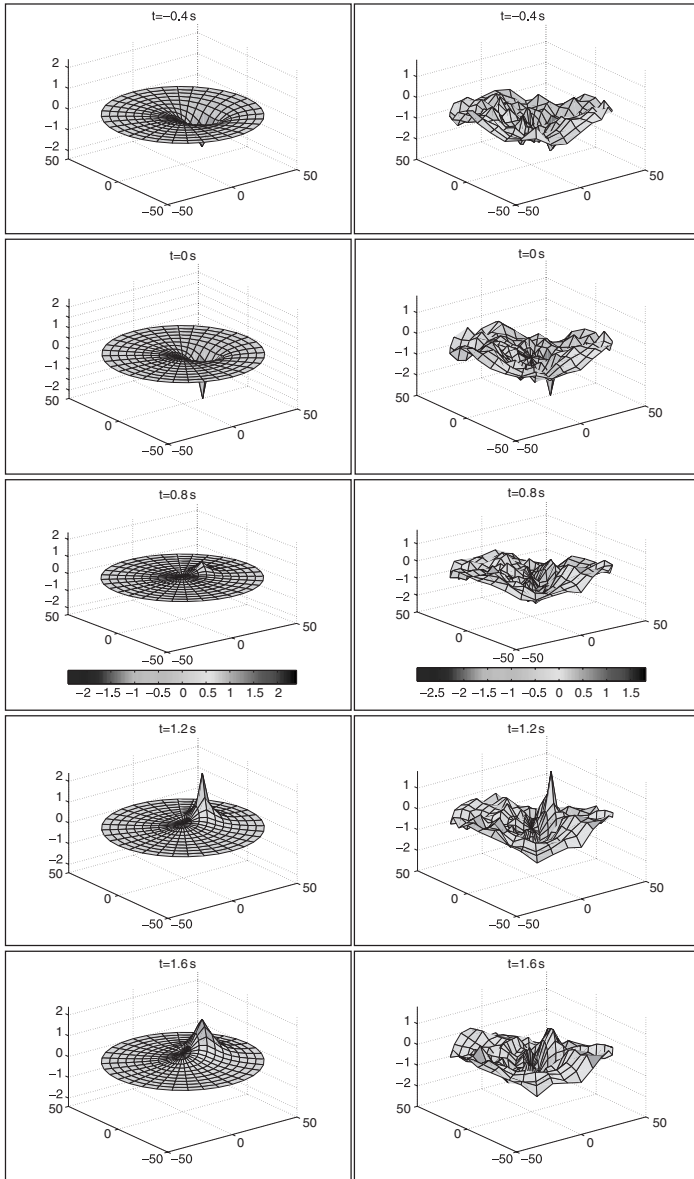
Figure 3. An example of a spatial gust with a velocity jump of 4·8 m s⁻¹; the gust centre is at a radial position of 15 m and an azimuth angle of 0. From top to bottom: time t = −0·4, 0 (gust minimum), 0·8, 1·2 (gust maximum) and 1·6 s. Right: gusts. Left: mean gust shapes
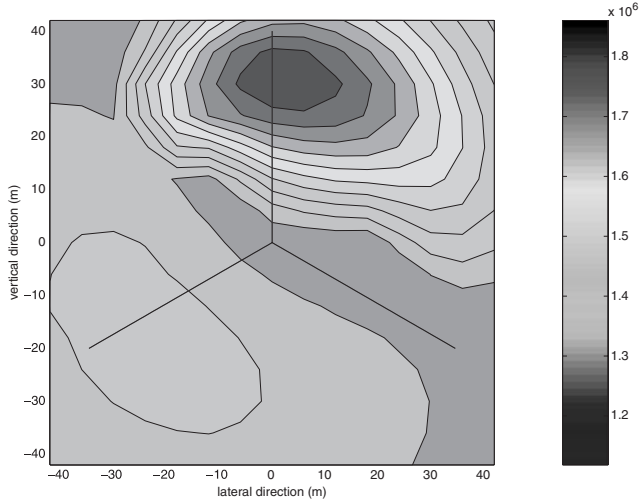
Figure 4. *Influence of the position of the gust centre on the maximum blade root flapping moment (N m) of the first blade (vertical upward position)*
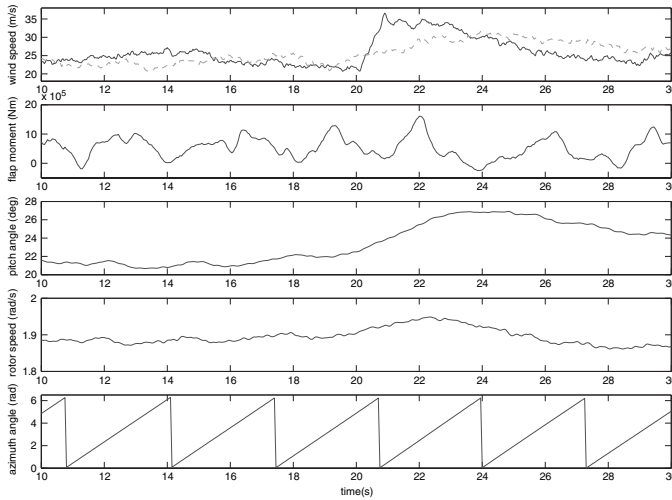

Figure 5. *Wind turbine response on a spatial gust (velocity jump of 16 m s^{-1} in 0·8 s, mean wind speed 25 m s^{-1}, turbulence intensity 8%). The gust centre is located at a lateral position of 0 m and a vertical position of 36 m; the wind speed at hub height is indicated by the broken line in the top graph. At zero azimuth angle the blade is pointing vertically upwards*
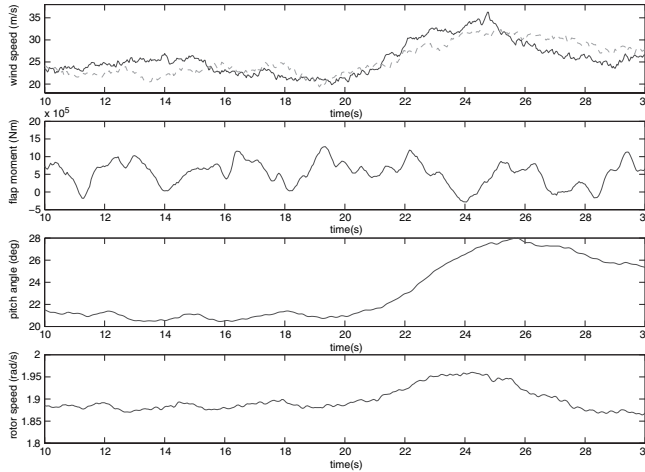
Figure 6. Wind turbine response on a spatial gust (velocity jump of 16 m s⁻¹ in 4·6 s; mean wind speed 25 m s⁻¹, turbulence intensity 8%). The gust centre is located at a lateral position of 0 m and a vertical position of 36 m; the wind speed at hub height is indicated by the broken line in the top graph

reducing the flap moment; in spite of the severe gust (a velocity jump of eight times the standard deviation) the maximum flap moment is not significantly higher than the other local maxima (due to the background turbulence and $1P$ excitations such as tower shadow and gravity). A similar simulation is shown in Figure 6 in the case of a gust rise time of 4·6 s.

The gust duration is now large compared with the integral time constant of the controller, so, as expected, the controller can deal with the gust. In fact the flap moment due to the gust is even lower than the other local maxima in the flap moment.

It is no use to compare the above results with the wind turbine response on the IEC EOG (extreme operating gust), since the latter has an assumed return period of 1 or 50 years and the first are just random examples. It would of course be possible to consider an extreme rise time gust with a return period of 1 or 50 years,[6] but such an approach is not recommended: in general a 50 year gust will not lead to a 50 year load. Thus it is preferable to extrapolate the wind turbine response on gusts instead of the gusts themselves. If the response of say the flapping moment is extrapolated to 1 or 50 years, a proper comparison can be made with the IEC EOG load. This probabilistic approach is outlined in the next section; however, the analysis has not yet been performed for spatial gusts.

The second reference turbine is a 2·75 MW turbine (92 m rotor diameter) with pitch control/variable speed. Using the Flex5 wind turbine code, the response is calculated on a gust with a velocity jump of 13 m s⁻¹ in 0·45 s (gust centre at 32 m, mean wind speed 20 m s⁻¹, turbulence intensity 13%), see Figure 7.

For clarity this time the mean gust shape of extreme rise time gusts has been used as wind input. Again the effect on the maximum flap moment is rather limited with respect to the severity of the gust (a velocity jump of five times the standard deviation).

Owing to these results, it seems not worthwhile to consider gusts with other velocity jumps, as is required in the probabilistic approach outlined in the next section. Instead an investigation on the particular gust shape which leads to extreme loads is recommended. For the time being a preliminary conclusion can be drawn that maybe an extreme rise time gust (above rated wind speed) does not lead to extreme loads of pitch-regulated wind turbines.
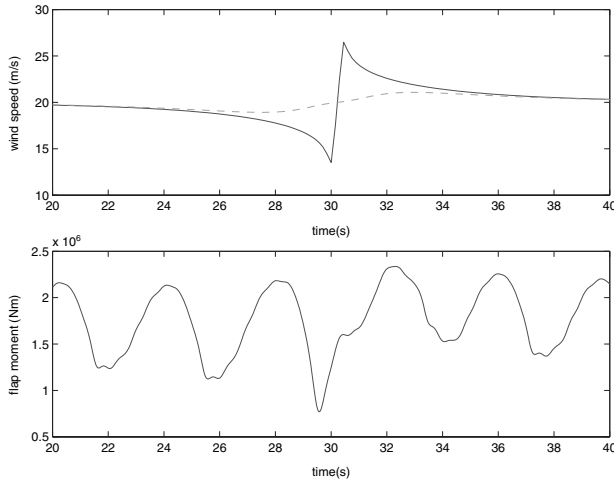
Wind Energ. 2005; **8**:17–34

Figure 7. Response of the second reference wind turbine on a spatial gust (velocity jump of 13 m s⁻¹ in 0·45 s, mean wind speed 20 m s⁻¹, turbulence intensity 13%). The gust centre is located at a lateral position of 0 m and a vertical position of 32 m; the wind speed at hub height is indicated by the broken line in the upper graph

A Probabilistic Approach to Determine the Extreme Loading of Wind Turbines

In this section a concise outline is given of a probabilistic method to determine the extreme response of wind turbines. Wind gusts generated on the basis of equation (36) can be used as input for a wind turbine simulation tool. Such a tool determines among other things the internal loads of the wind turbine as a function of time; e.g. one may be interested in the maximum bending moment in the rotor blades at the root section. Repeated application of equation (36) will lead to different wind gusts and consequently to different responses and maximum rotor blade moments. If several simulations are performed for the same gust amplitude and mean wind speed, a distribution of the extreme loading can be determined. This can be repeated for several gust amplitudes, varying e.g. from one to six times the standard variation. Each gust amplitude will result in another (cumulative) distribution of the structural loading. In order to obtain the distribution of the extreme loading, caused by a gust with an arbitrary amplitude (for given mean wind speed), the different distributions should be convoluted (weighed) with the occurrence probability of the individual gusts, which will be dealt with in the next subsection. Following this procedure, the short-term (say 10 min) distribution of the loading is obtained for some mean wind speed.

In order to determine the long-term distribution, the procedure should be repeated for several mean wind speeds. The overall final distribution is subsequently obtained by weighting with the occurrence probability of the mean wind speeds, i.e. the Weibull distribution or an empirical distribution (histogram) valid for some specific site. The final distribution can be fitted to some extreme value distribution, e.g. Gumbel or Pareto and then finally extrapolated to the desired return period, e.g. 50 years. The long-term distribution of the peak bending moment in the rotor blades shows the probability of exceedance of a certain load level. Instead of an arbitrary value obtained using deterministic analysis (as is presently specified in standards), the designer can choose the level of risk according to the load distribution. Furthermore, using the load distribution and resistance distribution of the structure, the probability of failure can be estimated. Together they constitute tools leading to more efficient and reliable design of wind turbines.
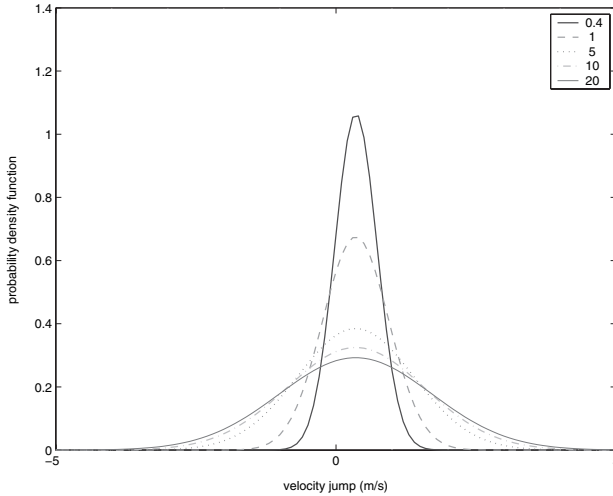
Gust statistics

By introducing five random variables with zero means (breakdown of vector **a**, equation (11)), namely

$$
\begin{aligned}
v &= \dot{u}(t_0) \\
w &= \ddot{u}(t_0) \\
x &= u(t_0 + \Delta t) - u(t_0) \\
y &= \dot{u}(t_0 + \Delta t) \\
z &= \ddot{u}(t_0 + \Delta t)
\end{aligned}
\tag{38}
$$

the probability of occurrence of gusts with a rise time Δt and a velocity jump ΔU is

$$
P_{\text{gusts}} = \int_0^{wdt} \int_0^\infty \int_{\Delta U}^{\Delta U + d(\Delta U) - zd(\Delta t)} \int_0^0 \int_{-\infty}^0 f(v, w, x, y, z) \, dv \, dw \, dx \, dy \, dz
\tag{39}
$$

For a given second derivative $w = \ddot{u}(t_0)$ the first time derivative should be in the range between 0 and wdt in order to obtain a minimum inside the time interval dt. This explains the integration limits of v; a similar argument holds for the limits of y. The function $f(v, w, x, y, z)$ is a five-variate Gaussian probability density function with covariance matrix (identical to the one given in equation (17))

$$
Q = \text{var}(u) \begin{bmatrix}
\lambda & & & \text{symmetric} & \\
0 & \mu & & & \\
-\dot{r}(\Delta t) & \ddot{r}(\Delta t) + \lambda & 2 - 2r(\Delta t) & & \\
-\ddot{r}(\Delta t) & \dddot{r}(\Delta t) & -\dot{r}(\Delta t) & \lambda & \\
-\dddot{r}(\Delta t) & r^{(4)}(\Delta t) & -\ddot{r}(\Delta t) - \lambda & 0 & \mu
\end{bmatrix}
\tag{40}
$$

where r is the normalized autocorrelation function, $\lambda = \ddot{r}(0)$ is the second-order spectral moment and $\mu = r^{(4)}(0)$ is the fourth-order spectral moment.

The mean frequency $N_{\Delta U}$ of gusts with a velocity jump in the range from ΔU to $\Delta U + d(\Delta U)$ and with a rise time between Δt and $\Delta t + d(\Delta t)$ follows directly from equation (39):

$$
\begin{aligned}
N_{\Delta U} &= \frac{P_{\text{gusts}}}{dt} \\
&\approx d(\Delta U)d(\Delta t) \int_0^\infty \int_{-\infty}^0 -wz \, f(0, w, \Delta U, 0, z) dw dz
\end{aligned}
\tag{41}
$$

The mean frequency N of all gusts is

$$
\begin{aligned}
N &= d(\Delta t) \int_{-\infty}^\infty \int_0^\infty \int_{-\infty}^0 -wz \, f(0, w, \Delta U, 0, z) d(\Delta U) dw dz \\
&= d(\Delta t) \frac{\mu}{(2\pi)^2 \lambda}
\end{aligned}
\tag{42}
$$

The last identity can be deduced from the following reasoning. In this article a gust is given by a combination of a local minimum and a local maximum as defined by equation (5). This implies that it is not required that the minimum and maximum are consecutive. In other words, every combination of a local maximum and a local minimum counts as a gust. Since a gust is given by a combination of a minimum and a maximum, we have to consider two time intervals with time separation Δt. The first is the interval around the local minimum with width dt and the second is the interval around the local maximum with width d(Δt). The mean frequency of local minima is equal to the mean frequency of local maxima, namely $[1/(2\pi)] \sqrt{\mu / \lambda}$; this leads to equation (42).

Finally the density $f(\Delta U)$ of gust events with velocity jump ΔU is obtained:

Figure 8. Probability density function of gusts, f(ΔU), as a function of velocity jump ΔU for five different values of the rise time Δt (mean wind speed 10 m s⁻¹, turbulence intensity 10%)

$$f(\Delta U) = \frac{N_{\Delta U}}{N\mathrm{d}(\Delta U)}$$

$$= \frac{(2\pi)^2 \lambda}{\mu} \int_0^\infty \int_{-\infty}^0 -wz\, f(0, w, \Delta U, 0, z)\mathrm{d}w\mathrm{d}z \qquad (43)$$

Via transformation to three new variables it is possible to convert the multinomial of the exponent of $f(u, 0, w, \Delta U, 0, z)$ to a sum of perfect squares ('completing the square' method). This allows us to write the two-dimensional integral of equation (43) as a 1D integral which can be solved numerically (strictly speaking it remains a 2D integral, since the integrand involves the error function).

The function $f(\Delta U)$ is shown in Figure 8 for several rise times Δt. For a rise time larger than about 10 s the function shape does not change anymore; apparently for large rise times the correlation between the local minimum and the local maximum gets so small that the function does not depend any longer on the exact rise time. For a small rise time the function gets more peak shaped; as expected, the probability of a large velocity jump decreases with decreasing rise time.

The gust statistics have been verified by analysis of wind measurements.[6]

Non-Gaussianity

A basic assumption of the method described in the third and fourth sections is that turbulence is Gaussian. The general opinion nowadays is that this it not correct, especially for time derivatives. Methods to generate non-Gaussian turbulence can be found in e.g. Reference 7. One of these methods starts with the generation of a Gaussian time series $x(t)$ which is transformed with a proper function to take into account the required non-Gaussian target distribution

$$u = g(x) \qquad (44)$$

If a monotonically increasing function is chosen, local extremes are not affected (in time) by the transformation, so it is possible to express the constraint in terms of the Gaussian variable:

$$u(t_0) = A \quad \Leftrightarrow \quad x(t_0) = g^{\mathrm{inv}}(A)$$
$$\dot{u}(t_0) = 0 \quad \Leftrightarrow \quad \dot{x}(t_0) = 0 \tag{45}$$
$$\ddot{u}(t_0) = B \quad \Leftrightarrow \quad \ddot{x}(t_0) = g^{\mathrm{inv}}(B)$$

This implies that constraints as treated in the third section can be handled.

The influence of non-Gaussianity, however, should not be overestimated; the mean shapes of uniform wind gusts, equation (22), compare very well (for non-complex terrain) with mean gust shapes based on wind measurements.[6]

With respect to the gust statistics (see previous section) it is not a problem at all to replace the Gaussian expression, equation (43) and Figure 8, with an empirical, non-Gaussian, one in order to derive the overall distribution of the wind turbine loading.

Conclusions

A probabilistic method has been outlined in order to determine the long-term distribution of the extreme response of pitch-regulated wind turbines. The probabilistic method relies on a quick determination of the response caused by a single spatial gust, with a given velocity jump in a given rise time (at some desired point in space), by means of so-called constrained simulation. If several wind turbine simulations are performed for the same velocity jump and mean wind speed, a distribution of the loading can be determined. In order to obtain the distribution of the loading caused by a gust with an arbitrary velocity jump (and given mean wind speed), the distributions for different gust amplitudes should be weighted with the occurrence probability of the individual gusts. The overall final distribution is obtained by weighting with the occurrence probability of the mean wind speed (Weibull) and can subsequently be extrapolated to the desired return period, e.g. 50 years.

A basic assumption of the above method is that turbulence is Gaussian (just as is assumed in the case of wind field simulation for fatigue analysis). A possible way to take non-Gaussian behaviour into account is mentioned in the article.

The above analysis has not yet been performed for spatial gusts with an extreme rise time. However, simulations with some severe spatial gusts for two reference turbines have shown that they did not lead to significantly high loads in the blade root flapping moment. Thus it is possible that extreme rise time gusts might not be governing the extreme loading of pitch-regulated wind turbines. Therefore it is recommended to investigate other types of wind gusts as well.

Acknowledgements

References

1. International Electrotechnical Commission. *Wind Turbine Generator Systems—Part 1: Safety Requirements*. IEC 61400-1, 1998.
2. Bierbooms W, Cheng PW, Larsen G, Pedersen BJ. Modelling of extreme gusts for design calculations—*New*Gust. *Final Report JOR3-Ct98-0239, IW-00170R*, Delft University of Technology, 2001.

3. Lindgren G. Some properties of a normal process near a local maximum. *The Annals of Mathematical Statistics* 1970; **41**: 1870–1883.
4. Bierbooms W, Dragt JB, Cleijne H. Verification of the mean shape of extreme gusts. *Wind Energy* 1999; **2**: 137–150.
5. Database on wind characteristics. [Online]. Available: http://www.winddata.com/.
6. Bierbooms W. The effect of gusts with extreme rise time on the extreme loads of wind turbines. *EWEC '03*, Madrid, 2003.
7. Nielsen M, Larsen GC, Mann J, Ott S, Hansen KS, Pedersen BJ. Wind simulation for extreme and fatigue loads. *Risø-R-1437(EN)*, 2003.
8. Shinozuka M. Simulation of multivariate and multidimensional random processes. *The Journal of the Acoustical Society of America* 1971; **49**: 357–368.
9. Mann J. Wind field simulation. *Probabilistic Engineering Mechanics* 1998; **13**: 269–282.
10. Dragt JB. Three-component wind field simulation in a wind turbine rotor plane, using polar coordinates. *IW-96100R*, Delft University of Technology, 1996.
11. Dragt JB, Bierbooms WAAM. Transverse wind velocity fluctuations and their effect on a wind turbine rotor. *European Wind Energy Conference*, Thessaloniki, 1994; 654–660.
12. Bierbooms W. Swing4 user guide. *IW-98133R*, Delft University of Technology, 1998.
13. Mortensen RE. *Random Signals and Systems*. Wiley: New York, 1987.
14. Bierbooms W, Dragt JB. A probabilistic method to determine the extreme response of a wind turbine. *IW-00168R*, Delft University of Technology, 2000.

Specific gust shapes leading to extreme response of pitch-regulated wind turbines

Wim Bierbooms

Delft University Wind Energy Research Institute (DUWIND), Kluyverweg 1, 2629 HS Delft, The Netherlands

E-mail: W.A.A.M.Bierbooms@tudelft.nl

Abstract. Via so-called constrained stochastic simulation gusts can be generated which satisfy some specified constraint. Constrained stochastic simulation is based on conditional densities of normal random variables and it has previously been applied to generate maximum amplitude gusts and velocity jumps. In this paper it is used in order to generate specific wind gusts which will lead to local maxima in the response of (pitch-regulated) wind turbines. The method is demonstrated on basis of a linear model of a wind turbine, inclusive pitch control. The mean gust shape as well as the mean shape of the response, for some gust amplitude, is shown. By performing many simulations (for given gust amplitude) the conditional distribution of the response is obtained. By a weighted average of these conditional distributions over the probability of the gusts the overall distribution of the response can be obtained. Analytical expressions for the conditional distribution of the response (for given gust amplitude) as well as the overall distribution are specified. These form an ideal test case of tools (e.g. fitting to an extreme value distribution) to be used for non-linear wind turbine models. The application of the above method on a non-linear model of a wind turbine has still to be done.

1. Introduction

In order to arrive at the 50-years extreme response of wind turbines it would be ideal to have available the wind data, at the specific location of the wind farm, over a period of say 500 year and unlimited computational power. The 50-years response could than be determined on basis of simple statistical analysis of the simulated response. Both conditions do of course not apply in practice. Instead in standards some deterministic gust shape is provided which should represent the 50 years extreme situation, [8]. However both the gust shape as well as amplitude is rather arbitrary. Furthermore the deterministic gust does not reflect the stochastic nature of turbulence. An alternative is to do simulations, as long as practical feasible, and extrapolate the results to the desired return period of 50 years applying extreme value theory.

Here we will consider another alternative. In [1] so called constrained stochastic simulation is treated which allow to generate wind gusts which satisfy some specified constraint. E.g. one may generate time series around a local maximum with specified amplitude, or wind gusts which contain a prescribed velocity jump in a specified rise time. These wind gusts are embedded in a stochastic background in such a way that they are, in statistical sense, not distinguishable from real wind gust (with the same characteristics of the constraint). Constrained stochastic simulation enables us to limit the simulation to situations which contributes to the extreme response and skip all others. This

potentially saves a lot of computational time and limit the required extrapolation (and accompanying uncertainty) to the required return period.

Maximum amplitude gusts have been successfully applied for stall-regulated turbines; furthermore the mean gust shape is validated against wind measurements, [3]. For pitch-regulated turbines it has been presumed that velocity jumps (specified by a local minimum and local maximum with a time separation (rise time) Δt and a velocity difference ΔU) will lead to extreme response. However in [4] it is shown that the control system is able to handle such kind of gusts. In this paper we will focus on the particular gust shapes which will lead to the extreme response. In order to determine these gusts a linear model of a wind turbine will be used.

It is assumed that turbulence is Gaussian. An idea to extend the methodology to the non-Gaussian case is given in [4]. For convenience the wind speed at one point only will be considered; it should be possible to extend the method to a 3 D wind field. This paper will focus on the (theoretical) method rather than the application. The required statistical analysis is given, as much as possible, in separate appendices.

2. Determination of the specific gust shape

Constrained stochastic simulation is based on conditional densities, see Appendix A. As introduction of the method maximum amplitude gusts are treated first. The following (zero mean normal) random variables (RV) are considered: $x = u(t)$, $y_1 = u(0)$ and $y_2 = \dot{u}(0)$ with u(t) representing the stochastic wind on a wind turbine. The (co)variances of these RV's are, see also Appendix B:

$$M = R_{uu}(0) \tag{2.1}$$

$$\mathbf{Q} = \begin{bmatrix} R_{uu}(0) & 0 \\ 0 & -\ddot{R}_{uu}(0) \end{bmatrix} \tag{2.2}$$

$$\mathbf{N}^{\mathrm{T}} = \begin{bmatrix} R_{uu}(t) & -\dot{R}_{uu}(t) \end{bmatrix} \tag{2.3}$$

A local extreme of level A in the wind at t=0 is given by the constraint:

$$y_1 = A; \quad y_2 = 0 \tag{2.4}$$

Application of Eq. (A.5) leads to the desired gust shape (already presented in earlier work, e.g. [3]):

$$u_c(t) = u(t) + \frac{R_{uu}(t)}{R_{uu}(0)}(A - u(0)) - \frac{\dot{R}_{uu}(t)}{\ddot{R}_{uu}(0)}\dot{u}(0) \tag{2.5}$$

This gust represents an extreme in the wind. For large gust amplitudes A the mean gust shape resembles the autocorrelation function (ACF). In case local maxima only are considered one have to add an extra constraint (2nd derivative less than 0). The resulting expression for such gust can be found in [1].

We now focus on the gust which will lead to the governing ultimate response of a pitch-regulated wind turbine. Here it is assumed that the governing response is given by a local maximum related to e.g. the ultimate compression (or tension) stress at some critical location (e.g. blade root or tower base) or related to the maximum blade tip deflection (to prevent tower collision). For this purpose the wind input u(t) as well as the response r(t) has to be considered. The concerned event is specified by a local maximum in the response (of arbitrary value) at t=0 and the value of the wind input. In fact the wind input is not considered at t=0 but somewhat earlier, $t = -\delta$. The mathematical reason for this will be explained shortly; since there will always be some time delay between the wind input and response of the wind turbine it is also natural to do so. So the following RV are involved: $x = u(t)$, $y_1 = u(-\delta)$, $y_2 = \dot{r}(0)$ and $y_3 = \ddot{r}(0)$. The (co)variances are:

$$M = R_{uu}(0) \tag{2.6}$$

$$\mathbf{Q} = \begin{bmatrix} R_{uu}(0) & 0 & \ddot{R}_{ur}(\delta) \\ 0 & -\ddot{R}_{rr}(0) & 0 \\ \ddot{R}_{ur}(\delta) & 0 & \ddot{R}_{rr}(0) \end{bmatrix} \tag{2.7}$$

$$\mathbf{N}^{\mathrm{T}} = \begin{bmatrix} R_{uu}(t+\delta) & -\dot{R}_{ru}(t) & \ddot{R}_{ru}(t) \end{bmatrix} \tag{2.8}$$

The time difference $-\delta$ has been chosen such that $\dot{R}_{ru}(-\delta) = 0$; this result in a less complex structure for the required inverse of $\mathbf{Q}$. Straightforward application of Eq. (A.5) again provides the gust which leads to an extreme in the response:

$$u_c(t) = u(t) + \frac{1}{\Delta}\{\ddot{R}_{rr}(0)R_{uu}(t+\delta) - \ddot{R}_{ur}(\delta)\ddot{R}_{ru}(t)\}(A - u(-\delta))$$

$$- \frac{\dot{R}_{ru}(t)}{\ddot{R}_{rr}(0)}\dot{r}(0) + \frac{1}{\Delta}\{-\ddot{R}_{ur}(\delta)R_{uu}(t+\delta) + R_{uu}(0)\ddot{R}_{ru}(t)\}(B - \ddot{r}(0)) \tag{2.9}$$

with $\Delta = R_{uu}(0)\ddot{R}_{rr}(0) - \ddot{R}_{ur}^{\,2}(\delta)$

The expression for the response follows from the fact that the response of a linear system to the ACF of the input equals the cross correlation function (CCF) and the response to the CCF equals the ACF of the output (see Appendix B).

$$r_c(t) = r(t) + \frac{1}{\Delta}\{\ddot{R}_{rr}(0)R_{ur}(t+\delta) - \ddot{R}_{ur}(\delta)\ddot{R}_{rr}(t)\}(A - u(-\delta))$$

$$- \frac{\dot{R}_{rr}(t)}{\ddot{R}_{rr}(0)}\dot{r}(0) + \frac{1}{\Delta}\{-\ddot{R}_{ur}(\delta)R_{ur}(t+\delta) + R_{uu}(0)\ddot{R}_{rr}(t)\}(B - \ddot{r}(0)) \tag{2.10}$$

with r(t) the response to u(t).

It is easily verified that the above expressions indeed satisfy the constraint:

$$u_c(-\delta) = A; \quad \dot{r}_c(0) = 0; \quad \ddot{r}_c(0) = B \le 0 \tag{2.11}$$

By taking the time difference $-\delta$ such that $\dot{R}_{ru}(-\delta) = 0$ ensures that $R_{ru}(-\delta) = R_{ur}(\delta)$ is a local extreme and as a result $r_c(0)$ is a local maximum, as expressed by Eq. (2.11). In case another choice had been made for δ still correct expressions could have been obtained, but they would be more complicated than Eq. (2.9) and (2.10).

3. Simulations based on a linear model of the wind turbine

For a linear system it is known that the response to a Gaussian signal is also Gaussian. This implies that the distribution of the local maxima in the response is given by the Rice distribution, [2]. In other words it is useless to apply constrained stochastic simulation to a linear system since the final answer is already known. Here we will nevertheless use a linear model of a wind turbine, just in order to demonstrate the probabilistic method. In fact the theoretical solution allows us to verify the probabilistic method.

Since design packages does not standard offer a possibility to determine a linear model the model described in [6] has been used instead. This model describes the behavior of a typical 3-bladed pitch regulated wind turbine of 3 MW around the operating point of a mean wind speed of 16 m/s (the rotor speed is 17.25 rpm). Use is made of so-called Coleman transformation in order to obtain equations of motion without azimuth dependent terms. The consequence is that for the input the blade effective wind speed should be used. This is the wind speed as observed by a rotating blade at some radial position (so inclusive 1P and higher harmonics due to rotational sampling). The pitch control system concerns a simple PI system with as input the generator speed. As example the blade root flap moment
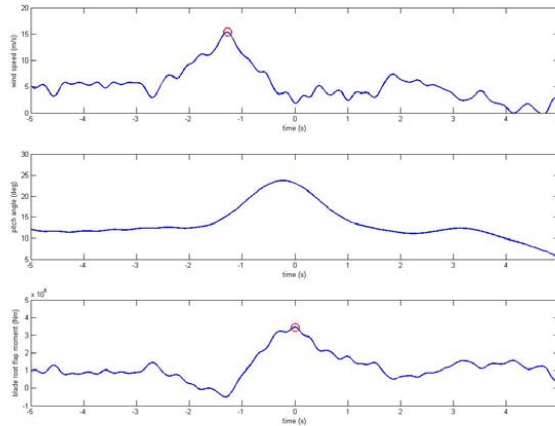
Figure 1. An example of constrained stochastic simulation; $A = 6\sigma_u$. Top: wind speed; middle: pitch angle; bottom: blade root flap moment (all variables with respect to their working point values).

is taken as reference load, but any other load could have been taken as well. The transfer function H between wind speed and root flap moment follows from the state space description of the linear model mentioned above. The required cross correlation function R_{ru} is obtained via a Fourier Transform of the cross spectrum S_{ru} (see also Eq. (B.13)):

$$S_{ru} = H^* S_{uu} \qquad (3.1)$$

with S_{uu} the spectrum of turbulence and the asterisk denotes the complex conjugate. The ACF's of the input and response are obtained via the Fourier Transform of the corresponding spectra.

Based on Eq. (2.9) gusts have been generated for a value of A equal to 6 times the standard deviation. The wind speed u(t) is created by an ordinary stochastic wind field generator. The value of B has been drawn randomly based on its distribution (Appendix C); see Appendix B for the determination of the other required parameters. An example of such a gust is shown in Fig. 1. For this example the time shift equals $\delta = 1.27\,\mathrm{s}$; the constraint $u_c(-\delta) = A$ is also indicated in the figure. In general this constraint will not coincide with a local maximum in the wind speed.

The response at t=0 is indicated by a circle; it is always a local maximum (due to the constraints $\dot{r}_c(0) = 0$ and $\ddot{r}_c(0) = B \le 0$) but it is not necessarily the maximum inside the whole time series (a simulation length of 200 s is taken). In total 100 simulations have been performed, the averages of these simulations are depicted in Fig. 2.

The theoretical mean gust shape of constrained simulations follows from Eq. (2.9); the mean value of B can be determined from its density function, see Appendix C. For our reference case it turns out that the mean gust shape almost resembles the auto correlation function of the wind (shifted in time over δ). In general the mean gust shape will be different for other wind turbines, mean wind speeds and/or type of response considered (e.g. tower base moment instead of blade root moment). Note that
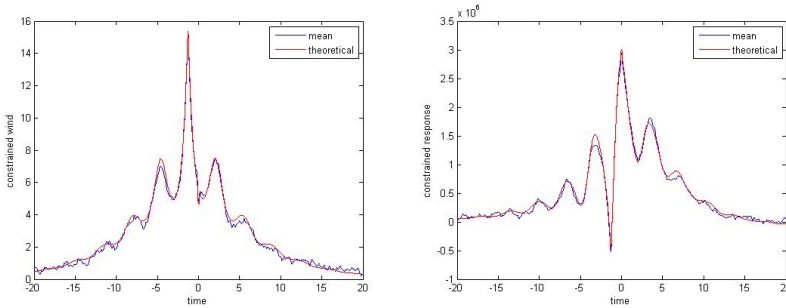
Figure 2. The mean wind speed (left) and the mean blade root flap moment (right) of 100 constrained stochastic simulations; A $=6\,\sigma_u$

for the reference case the wind concerns the blade effective wind speed; the rotational modes are clearly visible (compare with e.g. Fig. 5.18 from [7]). For these reasons it makes not so much sense to directly compare the gust shape of Fig. 2 to e.g. velocity jumps treated in [4] since the latter are given in a fixed frame of reference and are applied to some other reference turbine.

The mean shape of the response is shown in Fig. 2, right. Figure 2 is based on constrained simulations, but the same result would have been obtained by selecting all local maxima from the response of an ordinary simulation over a long time period and performing an average (after first shifting all local maxima to t=0 and selecting only the local maxima for which in the corresponding wind input $u_c(-\delta)$ lies in a small range around A). The mean shape of the response is, in this case,
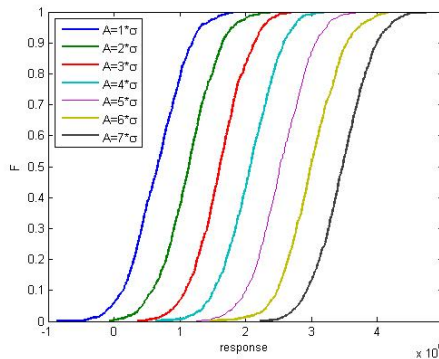
Figure 3. The conditional distributions of the blade root flap moment for different values for A (based on 1000 constrained stochastic simulations for each A).

dominated by the cross correlation function (shifted in time over δ); in general it will depend on the specific wind turbine and type of response.

In order to obtain the overall extreme load constrained stochastic simulations have to be performed for different values for A (and repeated for different mean wind speeds, turbulence intensities). In Fig. 3 the results for A ranging from $1\,\sigma_u$ to $7\,\sigma_u$ are given. The empirical conditional distributions of Fig. 3

are obtained by sorting the values of the response (at t=0) to magnitude (order statistics) and appoint to each value:

$$F_e = \frac{i}{n+1} \tag{3.2}$$

with n the total number of simulations for each A (here n=1000) and i ranging from 1 to n.

Finally, by a weighted average of these distributions over the probability of the gusts (i.e. distribution of A) the overall distribution of the response could be obtained (for given mean wind speed and turbulence intensity), see also Eq. (D.16). As already mentioned this overall distribution of the local maxima in the response should be given by the Rice distribution. In Appendix D it is proven that this is indeed the case which is some kind of verification of the given derivations. An extensive treatment of the overall probabilistic method can be found in [9].

A nice side effect of dealing with a linear system is that a theoretical expression for the conditional distribution can be obtained, see Eq. (D.13). The conditional distribution in case of $A = 6\sigma_u$ is shown in Fig. 4. Since we are interested in the extreme values the tails are of importance. In order to emphasize the tails also –log(1-F) is plotted. This can be interpreted as log(T) with T the return period (expressed in the number of local maxima in the response). For the reference case the 50-year value corresponds to:

$$T_{50} = 50 * 365 * 24 * 3600 * N_{tot} = 3 \ 10^9 \tag{3.3}$$

with N_{tot} the mean frequency of local maxima, see Eq. (D.4). For the reference wind turbine model N_{tot}=2 Hz, so log(T_{50}) equals 21.9 (indicated by a dotted line). In case of 1000 simulations the highest response value corresponds to a return period of about T=1000, so log(T)=6.9. The theoretical curve is compared with two empirical distributions; the first one based on 1000 constrained stochastic simulations (similar to Fig. 3) and the other based on 50 year of simulations. The agreement turns out to be excellent which validates the theoretical expressions given in Appendix D.
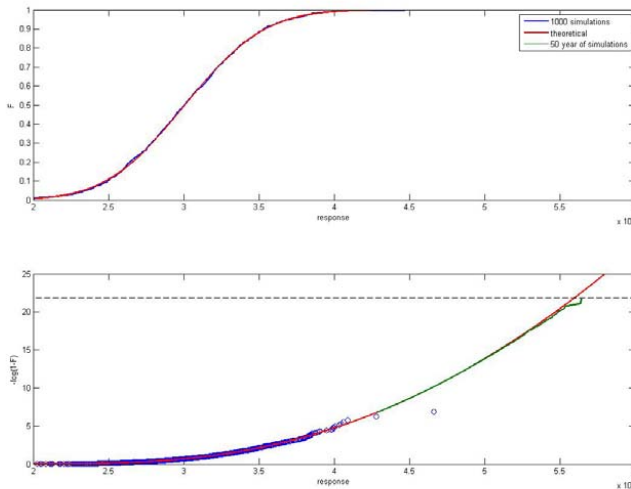
Figure 4. The conditional distributions of the blade root flap moment for A =6 σ_u ; comparison between 1000 constrained simulations, the theoretical distribution and 50 years of simulations. The dotted line indicates the 50 year return value.

4. Conclusions and outlook

A method has been presented to generate specific wind gusts. These so-called constrained stochastic simulations can be used in order to determine the 50-year return value of the wind turbine load. To this end gusts have to be generated for different amplitudes (for each mean wind speed). The overall distribution of the load is obtained by averaging over all amplitudes (and mean wind speeds).

The specific gusts are based on a linear model of a (pitch-regulated) wind turbine and are such that they will lead to local maxima in the response. However it makes no sense to apply the above mentioned method on the linear model itself since in that case an analytical expression for the distribution of extremes is already available, [2]. Instead the gusts should be applied on a non-linear model of a wind turbine (which still has to be done). It is of course not certain that the specified gusts will also lead to extreme response in that situation but it is expected that the proposed method is an improvement compared to deterministic extreme gusts as specified in standards. Furthermore it should be realized that uncertainty is inherent in extreme value analysis. Even in case of simulations based on ordinary generated stochastic wind fields (or measured wind records), one can not guarantee that gusts which dominate the 50-year response are present during the simulation period.

For application of the method with standard wind turbine design packages the formulation of Eq. (2.9) should be generalized to the 3 D case; this can be done similar to [4].

A nice side effect of dealing with a linear system is that analytical expressions for the conditional distribution of the response (for given gust amplitude) as well as the overall distribution exist. These form an ideal test case of tools (e.g. fitting to an extreme value distribution) to be used for non-linear wind turbine models.

Acknowledgement

References

[1]   Wim Bierbooms, Constrained Stochastic Simulation – Generation of Time Series around some specific Event in a Normal Process, Extremes, Vol 8, p 207–224, 2006.
[2]   Rice, S.O., Mathematical analysis of random noise, Bell Syst. Techn. J., 23, 282 (1944). [Reprinted in Wax, N. (ed.), Selected papers on noise and stochastic processes, Dover Publ., 1958].
[3]   Bierbooms, W., Cheng, P. W., Larsen, G. and Pedersen, B. J., Modelling of Extreme Gusts for Design Calculations - NewGust, Publishable final report JOR3-CT98-0239, Delft University of Technology, IW-00171R, 2001.
[4]   Wim Bierbooms, Investigation of spatial gusts with extreme rise time on the extreme loads of pitch regulated wind turbines, Wind Energy, Vol 8, p 17-34, 2005.
[5]   Cartwright, D.E. and Longuet-Higgins, M.S., The statistical distribution of the maxima of a random function, Proc. Royal Soc. London Ser. A 237, 212--232, (1956).
[6]   T.G. van Engelen, Design model and load reduction assessment for multi-rotational mode individual pitch control (higher harmonics control), EWEC 2006.
[7]   Tony Burton et al., Wind Energy Handbook, Wiley, 2001.
[8]   IEC 61400-1, Ed. 3: Wind turbines - Part 1: Design requirements, 2005.
[9]   Wim Bierbooms, Determination of the extreme value in the response of wind turbines by means of constrained stochastic simulation, submitted to 27th ASME Wind Energy Symposium, 2008.

Appendix A: Conditional distribution

In the paper multiple times use is made of the properties of conditional distributions of normal random variables (RV). The conditional density $f_c(x\,|\,y)$ of **x** upon observing **y** is again normal and thus determined by its mean μ_c and covariance matrix M_c. The condition **y** can be some specific value **y**=**Y**, with **Y** a constant vector. The expressions for the mean and covariance matrix can be found in handbooks on statistics (the T stands for transpose):

$$\boldsymbol{\mu}_c = \mathbf{N}^T \mathbf{Q}^{-1} \mathbf{Y} \tag{A.1}$$

$$\mathbf{M}_c = \mathbf{M} - \mathbf{N}^T \mathbf{Q}^{-1} \mathbf{N} \tag{A.2}$$

The matrices **M**, **N** and **Q** follow from the covariance matrix of the joint random vector $\begin{pmatrix}\mathbf{x}\\\mathbf{y}\end{pmatrix}$:

$$\mathrm{E}[\begin{pmatrix}\mathbf{x}\\\mathbf{y}\end{pmatrix}\begin{pmatrix}\mathbf{x}^T & \mathbf{y}^T\end{pmatrix}] = \begin{pmatrix}\mathbf{M} & \mathbf{N}^T\\\mathbf{N} & \mathbf{Q}\end{pmatrix} \tag{A.3}$$

i.e.: **M**=E[**x x**^{T}], **Q**=E[**y y**^{T}] and **N**=E[**y x**^{T}]. Vector notation is used since in general the random variables **x** and **y** can be vectors.

The conditional density $f_c(x\,|\,y)$ can also be expressed in terms of the joint density $f(x,y)$ and marginal density $f_{xy}(y)$:

$$f_c(x\,|\,y) = \frac{f_{x,y}(x,y)}{f_y(y)} \tag{A.4}$$

As example the case is treated that the covariance matrix of the joint random vector is given by: $\begin{pmatrix}3 & 1.5\\1.5 & 2\end{pmatrix}$; i.e. the variance of x is 3, the variance of y is 2 and the correlation coefficient equals about 0.6. The condition Y equal to 1.2 is taken, see Fig. A1 (left).
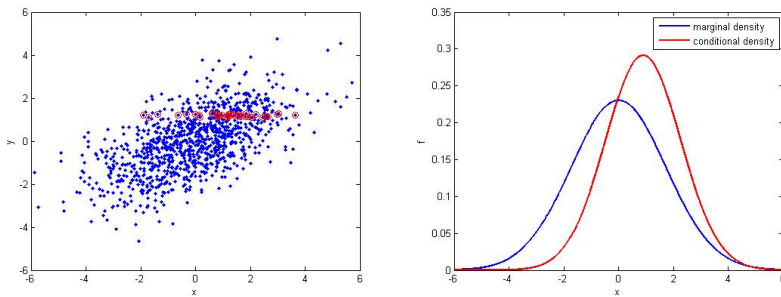
Figure A1. Scatter plot of 1000 random drawings of the RV's x and y (left); the values which satisfies the condition y=Y are indicated by red. Marginal and conditional densities (right).

From Eq. (A.1) and (A.2) it follows that the mean of the conditional density is 0.9 and the variance equals 1.9, see the figure at the right. In conclusion it can be said that in general the mean of a conditional density based on zero mean normal RV's is different from zero and the variance is smaller than the variance of the marginal density.

For random generation of the conditional RV the density (A.4) can be used directly. In practice it is often more convenient to generate random numbers of the unconstrained RV's **x** and **y** and calculate the following combination:

$$\mathbf{x}_c = \mathbf{x} + \mathbf{N}^\mathrm{T}\mathbf{Q}^{-1}(\mathbf{Y} - \mathbf{y}) \tag{A.5}$$

The RV x_c is again normal and it is not difficult to show that its mean and variance equals Eq. (A.1) and (A.2) resp.

Appendix B: Auto and cross correlation functions

The autocorrelation function (ACF) of the input u is given by:

$$R_{uu}(\tau) = \mathrm{E}[\mathrm{u}(t)\,\mathrm{u}(t+\tau)] \tag{B.1}$$

Likewise the ACF of the response r is:

$$R_{rr}(\tau) = \mathrm{E}[\mathrm{r}(t)\,\mathrm{r}(t+\tau)] \tag{B.2}$$

The cross correlation function (CCF) is defined by:

$$R_{ru}(\tau) = \mathrm{E}[\mathrm{r}(t)\,\mathrm{u}(t+\tau)] \tag{B.3}$$

The variance equals the ACF for $\tau = 0$, e.g. $\sigma_u^{\,2} = R_{uu}(0)$. Note: in expressions which also involve values of the ACF/CCF at other time values and/or time derivatives of the ACF/CCF, we will not use the symbol σ_u.

It is assumed that the involved stochastic processes are stationary so:

$$R_{ru}(\tau) = \mathrm{E}[\mathrm{r}(t)\,\mathrm{u}(t+\tau)] = \mathrm{E}[\mathrm{r}(t-\tau)\,\mathrm{u}(t)] \tag{B.4}$$

Via differentiation with respect to τ one obtains:

$$\dot{R}_{ru}(\tau) = -\mathrm{E}[\dot{\mathrm{r}}(t-\tau)\,\mathrm{u}(t)] = -\mathrm{E}[\dot{\mathrm{r}}(t)\,\mathrm{u}(t+\tau)] \tag{B.5}$$

and

$$\ddot{R}_{ru}(\tau) = \mathrm{E}[\ddot{\mathrm{r}}(t)\,\mathrm{u}(t+\tau)] = \ddot{R}_{ur}(-\tau) \tag{B.6}$$

So $\ddot{R}_{ru}(-\delta) = \ddot{R}_{ur}(\delta)$.

Combination of differentiation and application of the parameter shift, Eq. (B.4), leads to:

$$\ddot{R}_{rr}(\tau) = -\mathrm{E}[\dot{\mathrm{r}}(t)\,\dot{\mathrm{r}}(t+\tau)] \tag{B.7}$$

and

$$\dddot{R}_{rr}(\tau) = \mathrm{E}[\ddot{\mathrm{r}}(t)\,\ddot{\mathrm{r}}(t+\tau)] \tag{B.8}$$

In case a linear system is considered the CCF and ACF can be expressed in terms of the transfer function. Writing the input in terms of a Fourier series:

$$u(t) = \sum_k a_k \cos(\omega_k t) + b_k \sin(\omega_k t) \tag{B.9}$$

the response is given by:

$$r(t) = \sum_k h_k a_k \cos(\omega_k t + \phi_k) + h_k b_k \sin(\omega_k t + \phi_k) \tag{B.10}$$

with transfer function:

$$H(\omega_k) = h_k e^{i\phi_k} \tag{B.11}$$

The Fourier coefficients are zero mean normal RV's with variance $\mathrm{E}[a_k^{\,2}] = \mathrm{E}[b_k^{\,2}] = 2\dfrac{S_k}{T}$ with S_k the (double-sided) auto power spectral density of u (i.e. the Fourier transform of R_{uu}) and T the total length of the time signal. The ACF, of input and response, and the CCF can now also be expressed as (applying some goniometric identities):

$$R_{uu}(\tau) = \frac{2}{T}\sum_k S_k \cos(\omega_k \tau) \tag{B.12}$$

$$R_{ru}(\tau) = \frac{2}{T}\sum_k h_k S_k \cos(\omega_k \tau - \phi_k) \tag{B.13}$$

and

$$R_{rr}(\tau) = \frac{2}{T}\sum_k h_k{}^2 S_k \cos(\omega_k \tau) \tag{B.14}$$

The response of the linear system with the ACF as input, Eq. (B.12), is given by, see also Eq. (B.10):

$$r\_R_{uu}(t) = \frac{2}{T}\sum_k h_k S_k \cos(\omega_k t + \phi_k) = R_{ru}(-t) = R_{ur}(t) \tag{B.15}$$

Likewise the response on the CCF is given by:

$$r\_R_{ru}(t) = \frac{2}{T}\sum_k h_k{}^2 S_k \cos(\omega_k t) = R_{rr}(t) \tag{B.16}$$

so equals the ACF of the response.

Dealing with a linear system implies that the response on the time derivative of the CCF equals the time derivative of the response on the CCF:

$$r\_\dot{R}_{ru}(t) = \dot{R}_{rr}(t) \tag{B.17}$$

Appendix C: The statistics of B

In order to generate gusts with the required properties the statistics of B should be known. B is the 2nd time derivative of the response in case of the following event: a local maximum in the response, at time 0, and the input, at time $-\delta$, equals A. For convenience the following 3 RV's are introduced (zero mean normal): $x = u(-\delta)$, $y = \dot{r}(0)$ and $z = \ddot{r}(0)$. The probability of the above event to take place in time interval dt can be expressed by:

$$P(A) = \int_A^{A+dA}\int_0^{-z\,dt}\int_{-\infty}^0 f_{x,y,z}(x,y,z)\,dx\,dy\,dz \approx dA\,dt\int_{-\infty}^0 |z|\,f_{x,y,z}(A,0,z)\,dz \tag{C.1}$$

For a given second derivative z the first time derivative y should be in the range between 0 and $-z$ dt in order to obtain a local maximum inside the time interval dt. This explains the integration limits of y. The function $f_{x,y,z}(x,y,z)$ is a 3 variate normal density function with covariance matrix equal to Eq. (2.7).

According to Eq. (C.1) the probability of the event is obtained by integration over all possible values of the 2nd derivative z. In other words the density of B is given by the integrand of Eq.(C.1):

$$f_B(B) = \frac{|B|\,f_{x,y,z}(A,0,B)}{\int_{-\infty}^0 |B|\,f_{x,y,z}(A,0,B)\,dB} \tag{C.2}$$

By application of Eq. (A.4) twice the 3 variate density function can be written as:

$$f_{x,y,z}(A,0,B) = f_{z|x,y}(B\,|\,x=A, y=0)\,f_{y|x}(0\,|\,x=A)\,f_x(A) \tag{C.3}$$

With respect to the normalization of Eq.(C.2) the first term $f_{z|x,y}$ only have to be considered in Eq.(C.3). On basis of Appendix A the conditional density $f_{z|x,y}$ is again normal (univariate f_1) with mean and variance:

$$\mu_1 = A\frac{\ddot{R}_{ur}(\delta)}{R_{uu}(0)}; \quad \sigma_1{}^2 = \dddot{R}_{rr}(0) - \frac{\ddot{R}_{ur}{}^2(\delta)}{R_{uu}(0)} \tag{C.4}$$

So finally the density of B is given by:

$$f_B(B) = \frac{|B|\,f_1(B)}{\int_{-\infty}^0 |B|\,f_1(B)\,dB} \tag{C.5}$$

By e.g. means of special tools for formula manipulation like Maple it is possible to evaluate the integral in the denominator analytically:

$$I_1(A) = \int_{-\infty}^{0} |B| f_1(B)\,dB = -\mu_1 \Phi(-\frac{\mu_1}{\sigma_1}) + \sqrt{\frac{\sigma_1^2}{2\pi}} e^{-\frac{\mu_1^2}{2\sigma_1^2}} \tag{C.6}$$

with Φ the standard normal distribution function.
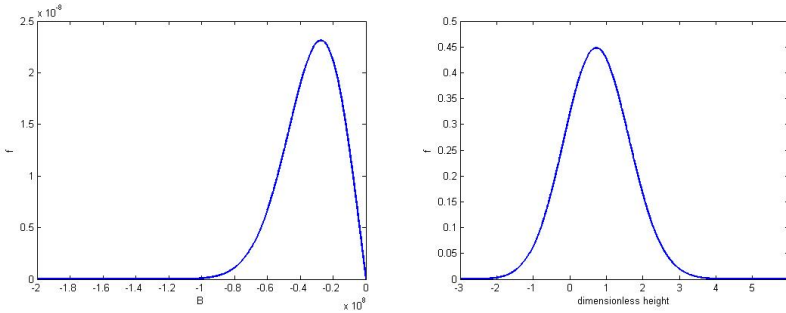
An example of the density is given in Fig. C.1.

Figure C.1: Example of the density of B; $A = 6\sigma_u$ Figure D.1: Example of the density of local maxima; $\varepsilon = 0.8$

Appendix D: The (conditional) density of the response

Similar as outlined in Appendix C the density of the response $r_c(0)$ can be determined by regarding the following event: a local maximum in the response of level C, at time 0, and the input, at time $-\delta$, equals A. The 4 involved normal (zero mean) RV's are: $w = r(0)$, $x = u(-\delta)$, $y = \dot{r}(0)$ and $z = \ddot{r}(0)$. The probability of this event is:

$$P(C,A) = \int_{C}^{C+dC} \int_{A}^{A+dA} \int_{0}^{-z\,dt} \int_{-\infty}^{0} f_{w,x,y,z}(w,x,y,z)\,dw\,dx\,dy\,dz \approx dC\,dA\,dt \int_{-\infty}^{0} |z| f_{w,x,y,z}(C,A,0,z)\,dz \tag{D.1}$$

with $f_{w.x.y.z}$ a 4 variate normal density with covariance matrix:

$$\mathbf{M} = \begin{bmatrix} R_{rr}(0) & R_{ur}(\delta) & 0 & \ddot{R}_{rr}(0) \\ R_{ur}(\delta) & R_{uu}(0) & 0 & \ddot{R}_{ur}(\delta) \\ 0 & 0 & -\ddot{R}_{rr}(0) & 0 \\ \ddot{R}_{rr}(0) & \ddot{R}_{ur}(\delta) & 0 & \ddddot{R}_{rr}(0) \end{bmatrix} \tag{D.2}$$

The mean frequency of the event, with specific values of C and A, equals:

$$N = \frac{P(C,A)}{dt} = dC\,dA \int_{-\infty}^{0} |z| f_{w,x,y,z}(C,A,0,z)\,dz \tag{D.3}$$

For the mean frequency of the event, for any value of C and A (i.e. all local maxima in the response), one has to sum up over all possible values:

$$N_{tot} = \int_{-\infty}^{\infty} \int_{-\infty}^{\infty} \int_{-\infty}^{0} |z| f_{w,x,y,z}(C,A,0,z)\,dz\,dC\,dA = \int_{-\infty}^{0} |z| f_{y,z}(0,z)\,dz = \frac{1}{2\pi} \sqrt{-\frac{\ddddot{R}_{rr}(0)}{\ddot{R}_{rr}(0)}} \tag{D.4}$$

In the above use is made (twice) of the identity:

$$f_y(y) = \int_{-\infty}^{\infty} f_{x,y}(x,y)\,dx \tag{D.5}$$

Furthermore Eq. (C.6) has been applied; note that:

$$f_{y,z}(0,z) = f_y(0) f_{z|y}(z\,|\,0) = f_y(0) f_z(z) \tag{D.6}$$

For the joint density of C and A, under condition that the event occurs, it holds (see also Eq. (A.4)):

$$f_{C,A}(C,A) = \frac{N}{N_{tot}\, dC\, dA} = \frac{\int_{-\infty}^{0} |z|\, f_{w,x,y,z}(C,A,0,z)\, dz}{N_{tot}} =$$

$$\frac{f_{w,x,y}(C,A,0)\int_{-\infty}^{0} |z|\, f_{z|w,x,y}(z)\, dz}{N_{tot}} = \frac{f_{w,x,y}(C,A,0)\, I_2(C,A)}{N_{tot}} \tag{D.7}$$

with

$$I_2(C,A) = \int_{-\infty}^{0} |z|\, f_2(z)\, dz = -\mu_2 \Phi\!\left(-\frac{\mu_2}{\sigma_2}\right) + \sqrt{\frac{\sigma_2^{\,2}}{2\pi}}\, e^{-\frac{\mu_2^{\,2}}{2\sigma_2^{\,2}}} \tag{D.8}$$

and f_2 a univariate normal density, representing the conditional density $f_{z|w,x,y}$, with mean and variance:

$$\mu_2 = \frac{C\{R_{uu}(0)\ddot{R}_{rr}(0) - R_{ur}(\delta)\ddot{R}_{ur}(\delta)\} + A\{\ddot{R}_{ur}(\delta)R_{rr}(0) - R_{ur}(\delta)\ddot{R}_{rr}(0)\}}{R_{uu}(0)R_{rr}(0) - R_{ur}^{\,2}(\delta)} \tag{D.9}$$

and

$$\sigma_2^{\,2} = \dddot{R}_{rr}(0) - \frac{R_{uu}(0)\ddot{R}_{rr}^{\,2}(0) - 2R_{ur}(\delta)\ddot{R}_{ur}(\delta)\ddot{R}_{rr}(0) + \ddot{R}_{ur}^{\,2}(\delta)R_{rr}(0)}{R_{uu}(0)R_{rr}(0) - R_{ur}^{\,2}(\delta)} \tag{D.10}$$

For the above the properties of a conditional density (see Appendix A) are again applied.

The density of A results from the joint density, according to Eq. (D.5):

$$f_A(A) = \int_{-\infty}^{\infty} f_{C,A}(C,A)\, dC = \frac{1}{N_{tot}} \int_{-\infty}^{\infty} \int_{-\infty}^{0} |z|\, f_{w,x,y,z}(C,A,0,z)\, dz\, dC$$

$$= \frac{1}{N_{tot}} \int_{-\infty}^{0} |z|\, f_{x,y,z}(A,0,z)\, dz = \frac{1}{N_{tot}} f_x(A) f_y(0) I_1(A) \tag{D.11}$$

Note: $f_{x,y,z}(x,y,z)$ is the same 3 variate density as in Eq. (C.3) and I_1 is the factor given by Eq. (C.6); the RV's x and y are uncorrelated (and thus independent) so:

$$f_{y|x}(0\,|\,A) = f_y(0) \tag{D.12}$$

Combination of Eq. (D.7) and (D.11) leads to the conditional density of the height C of a local maximum in the response, on observing x=A:

$$f_{C|A}(C\,|\,A) = \frac{f_{C,A}(C,A)}{f_A(A)} = \frac{f_{w,x,y}(C,A,0)\, I_2(C,A)}{f_x(A) f_y(0) I_1(A)} = f_3(C) \frac{I_2(C,A)}{I_1(A)} \tag{D.13}$$

With I_2 and I_1 given by Eq. (D.8) and (C.6) resp. and f_3 is a univariate normal density, representing the conditional density $f_{w|x,y}$, with mean and variance:

$$\mu_3 = A\frac{R_{ur}(\delta)}{R_{uu}(0)}; \quad \sigma_3^{\,2} = R_{rr}(0) - \frac{R_{ur}^{\,2}(\delta)}{R_{uu}(0)} \tag{D.14}$$

The conditional density (D.13) could also have been derived based on Eq.(2.10). This equation can be seen as the sum χ of a normal RV α (resulting from the sum of the factors involving $r(0)$, $u(-\delta)$ and $\ddot{r}(0)$) and the RV β (factor involving B, which statistics are presented in Appendix C):

$$f_\chi(\chi) = \int_{-\infty}^{\infty} f_\alpha(\chi - \beta) f_\beta(\beta)\, d\beta \tag{D.15}$$

From the conditional density the marginal density of level C is obtained via weighting with the probability of A (combination of Eq. (A.4) and (D.5)), use Eq. (D.7):

$$f_C(C) = \int_{-\infty}^{\infty} f_{C|A}(C\,|\,A)\, f_A(A)\, dA = \frac{1}{N_{tot}} \int_{-\infty}^{\infty} \int_{-\infty}^{0} |z|\, f_{w,x,y,z}(C,A,0,z)\, dz\, dA =$$

$$\frac{1}{N_{tot}} \int_{-\infty}^{0} |z|\, f_{w,y,z}(C,0,z)\, dz = \frac{f_w(C) f_y(0)}{N_{tot}} \int_{-\infty}^{0} |z|\, f_{z|w,y}(z)\, dz = \frac{f_w(C)\sqrt{2\pi}}{\sqrt{\dddot{R}_{rr}(0)}} I_4(C) \tag{D.16}$$

with

$$I_4(C) = \int_{-\infty}^{0} |z|\, f_4(z)\, dz = -\mu_4 \Phi\left(-\frac{\mu_4}{\sigma_4}\right) + \sqrt{\frac{{\sigma_4}^2}{2\pi}}\, e^{-\frac{{\mu_4}^2}{2{\sigma_4}^2}} \tag{D.17}$$

and f_4 again a univariate normal density, representing the conditional density $f_{z|w,y}$, with mean and variance:

$$\mu_4 = C\,\frac{\ddot{R}_{rr}(0)}{R_{rr}(0)}; \quad {\sigma_4}^2 = \dddot{R}_{rr}(0) - \frac{{\ddot{R}_{rr}}^2(0)}{R_{rr}(0)} \tag{D.18}$$

Equation (D.16) may be recognized as the (Rice) density of local maxima in a normal process, [2]; see also Fig. D.1. Via some manipulations it can be rewritten as (in agreement with the expression presented in [5]):

$$f_\eta(\eta) = \eta\sqrt{1-\varepsilon^2}\, e^{-\frac{\eta^2}{\varepsilon}} \Phi\left(\frac{\eta\sqrt{1-\varepsilon^2}}{\varepsilon}\right) + \frac{1}{\sqrt{2\pi}}\, \varepsilon\, e^{-\frac{\eta^2}{2\varepsilon}} \tag{D.19}$$

with dimensionless level of the local maxima:

$$\eta = \frac{C}{\sqrt{R_{rr}(0)}} \tag{D.20}$$

and bandwidth parameter:

$$\varepsilon = \sqrt{1 - \frac{{\ddot{R}_{rr}}^2(0)}{R_{rr}(0)\dddot{R}_{rr}(0)}} \tag{D.21}$$

Application of constrained stochastic simulation to determine the extreme loads of wind turbines

Wim Bierbooms
Wind Energy Research Group

Delft University of Technology, 2629 HS Delft, The Netherlands

w.a.a.m.bierbooms@tudelft.nl

Via so-called constrained stochastic simulation, gusts can be generated which satisfy some specified constraint. In this paper it is used in order to generate specific wind gusts which will lead to local maxima in the response of wind turbines. The advantage of constrained simulation is that any gust amplitude (no matter how large) can be chosen. By performing simulations for different gust amplitudes and mean wind speeds the distribution of the response is obtained. This probabilistic method is demonstrated on the basis of a generic 1 MW stall regulated wind turbine. By considering a linearised dynamic model of the reference turbine the proposed probabilistic method could be validated. The determined 50 year response value indeed corresponds to the theoretical value (based on the work of Rice on random noise). Next, both constrained and (conventional) unconstrained simulations have been performed for the non-linear wind turbine model. For all wind speed bins constrained simulation results in 50 year estimates closer to the real value. Furthermore, via constrained simulation a lower uncertainty range of the estimate is obtained. The involved computational effort for both methods is about the same.

1. Introduction

The objective of this paper is to find the extreme response of wind turbines under stochastic wind loading. In order to arrive at the 50-years extreme response it would be ideal to have available the wind data at the specific location of the wind farm over a period of say 500 year and unlimited computational power. The 50-years response could then be determined on the basis of simple statistical analysis of the simulated response. Both conditions do of course not apply in practice. Instead, in the IEC standard (IEC 61400-1 Ed. 3, 2005) some deterministic gust shape is provided which should represent the 50 years extreme *wind* situation. Only in case of linear systems one may assume that the 50-year *response* corresponds to the 50-year *input*. However, a wind turbine is a non-linear system, so the maximum response could well result from another wind situation. Other main disadvantages are that the gust shape is rather arbitrary, the deterministic approach in the standards does not reflect the stochastic nature of turbulence and that the particularities of specific design are not taken into account. An alternative is to do simulations, as long as practically feasible, and extrapolate the results to the desired return period of 50 years applying extreme value theory. Such an approach is followed in Ref. [6], [7] and [8].

1

In general, the uncertainty in the 50-year estimate decreases with the number of simulations. So in practice, the designer should do a trade-off between computational effort and required accuracy.

Here we will present another alternative. In Ref. 1 so called constrained stochastic simulation is treated which allow to generate wind gusts which satisfy some specified constraint. One may for example generate time series around a local maximum with specified amplitude, or wind gusts which contain a prescribed velocity jump in a specified rise time. These wind gusts are embedded in a stochastic background in such a way that they are in statistical sense not distinguishable from real wind gust (with the same characteristics of the constraint). It is also possible to put constraints on some specific load response, e.g. the flapping moment at the blade root.

Constrained stochastic simulation enables us to limit the simulation to situations which contribute to the extreme response and skip all others. This saves a lot of computational time and limit the required extrapolation (and accompanying uncertainty) to the required return period.

In this paper we focus on the application of the overall probabilistic method to come to the extreme response; the probabilistic method itself is treated in more detail in Ref. 5. See Ref. 1 and 3 for a full description of constrained stochastic simulation.

The proposed probabilistic method based on constrained simulation is treated in Section 3. The common way to arrive at the 50 years response, i.e. by means of normal, unconstrained wind simulations, is given in Section 4. In Section 5 the application of constrained simulations is covered. Both methods will be compared in Section 6. However, we start in Section 3, with the application of the probabilistic method to a linearised dynamic model of our reference wind turbine (Section 2). The reason of considering a linear system is that a theoretical analysis of the extreme loading is available which makes a validation of the probabilistic method possible.

2. Reference system

As reference system a generic fixed speed stall regulated wind turbine is taken. It is a 3-bladed 1 MW turbine with a rotor diameter of 51 m and a hub height of 55 m. For the determination of the extreme loads during power production all mean wind speeds between cut-in and cut-out should be considered. We have taken a bin size of 3 m/s resulting into 6 mean wind speeds as follows: 6, 9, 12, 15, 18 and 21. As example for the loading the blade root flapping moment is considered, but any other load signal could have been taken as well. Simulations with a random wind speed are performed with the Bladed software package (Garrad Hassan and Partners Ltd.). Just for convenience a uniform wind field, i.e. constant over the rotor disc (no shear or yaw), is taken.

In this paper constrained gusts are used which includes a constraint on the load. To this end, a linear system of the stall turbine, i.e. the transfer function between the wind input and the blade root flapping moment, is required. These transfer functions (one for each mean wind speed) are here obtained by application of a system identification toolbox, Ref. 4. For this purpose the periodic excitations (rotor imbalance, gravity, tower shadow, wind shear) are set to zero. Furthermore the turbulence intensity is set to just 2% to obtain linear behavior, see Fig. 1. The 2% is still sufficient to have enough response (compared to noise) for proper system identification.

The mean wind speed of 24 m/s is excluded since we were not able to determine a reliable linear model for this mean wind speed. This is perhaps due to a shortcoming in the dynamic model of the wind turbine (as implemented in Bladed), or its parameters, for this specific wind

2

turbine. Since we want to demonstrate the probabilistic method rather than to determine the extreme response of this particular wind turbine this phenomenon is not further investigated but instead the mean wind speed of 24 m/s is simply skipped.
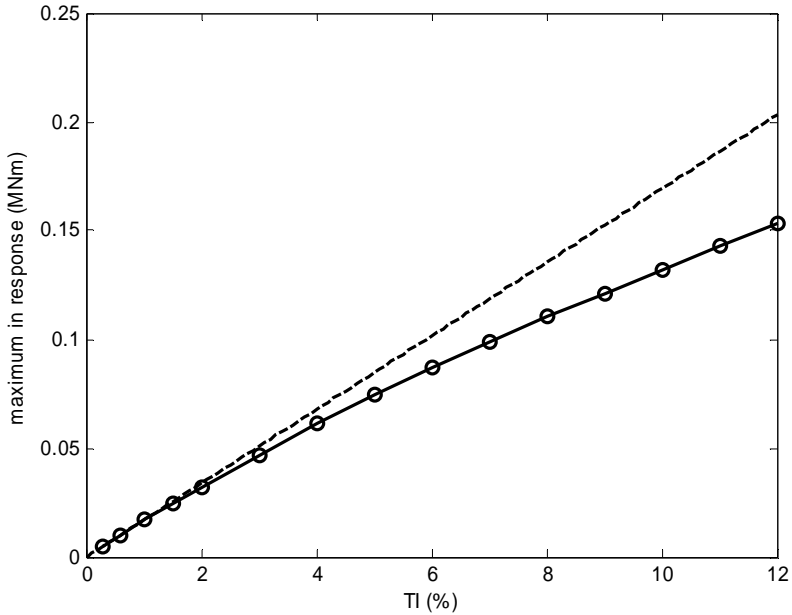

Figure 1. Relation between turbulence intensity and maximum in response with respect to steady value (for one particular turbulence time series).

3. A probabilistic method to find the extreme response using constrained simulations

3.1 Theory

The proposed probabilistic method is based on conditional distributions. The gust amplitudes of the stochastic wind input of the wind turbine will be denoted as random variable *x* and the local maxima of the response as random variable *y*. The marginal densities are $f_x(x)$ and $f_y(y)$; the joint density is $f(x, y)$ and $f_c(y) = f(y \mid x)$ is the conditional density of *y* upon observing *x=x*. The following well-known relations exist:

$$f_y(y) = \int_{-\infty}^{\infty} f(x, y)\, dx \tag{1}$$

$$F_y(y) = \int_{-\infty}^{y} f_y(\beta)\, d\beta \tag{2}$$

$$f_c(y) = \frac{f(x, y)}{f_x(x)} \tag{3}$$

$$F_c(y) = \int_{-\infty}^{y} f_c(\beta)\, d\beta \tag{4}$$

3

Combination leads to:

$$F_y(y) = \int_{-\infty}^{y} \int_{-\infty}^{\infty} f(\alpha, \beta) \, d\alpha d\beta = \int_{-\infty}^{y} \int_{-\infty}^{\infty} f_c(\beta) f_x(\alpha) \, d\alpha d\beta$$

$$= \int_{-\infty}^{\infty} F_c(y) f_x(\alpha) \, d\alpha \approx \sum F_c(y) n_x$$

(5)

with n_x the probability ('fraction of time') that a gust amplitude is within the discretized amplitude intervals of random input *x*

The distribution of response *y* can thus be obtained through a weighted summation (convolution) of the conditional distributions. The conditional distributions can be determined by simulations of wind gusts which are obtained by constrained stochastic simulations, say 100 simulations for each amplitude. The amplitude of the wind gusts may be varied from say 1σ to 5σ.

In order to apply the method one has to choose some constrained gust. For stall regulated wind turbines it can be anticipated that maximum amplitude gusts (in other words: local maxima) are governing the response. For pitch regulated wind turbines the proper gusts may be extreme rise time gusts. These maximum amplitude and extreme rise time gusts have been investigated in previous work, [1]. Surprisingly, the pitch control system was able to handle the extreme rise time gusts, even if the rise time was small, [11]. Based on this result a more fundamental approach is followed in [3] and applied in this paper. By putting a constraint on the response as well, it could be ascertain that the generated gusts would lead to a (local) maximum, of unspecified value, in the response (at time t=0). This approach can be used for both stall and pitch regulated wind turbines and for any load signal (in any wind turbine component). So, this solves the question of what kind of gusts should to be used.

In Fig. 2 an example of a constrained stochastic simulation is shown for the reference turbine; the maximum in the response, at t=0, is indicated by a circle. In total three constraints are applied: two on the response in order to obtain a local maximum (i.e. first time derivate equal to zero and second time derivative negative) and one on the wind input (which should be equal to some value A, which is considered to be the gust amplitude). Note that there are no constraints put on the time derivatives of the wind, so the constrained gust is in general not a local maximum. The expression of the constrained gust contains the auto- and cross correlation function (and time derivatives); see Eq. (2.9) from Ref. 3. So, in order to generate such gusts the turbulence spectrum as well as the transfer function of the linearized wind turbine model should be known. The generated gusts are equivalent with gusts (with the same gust amplitude) which would have been selected from wind time series. The advantage of the here presented method is that through constrained random simulation, gusts with any required high amplitude can be generated. To obtain similar gusts via selection from time series, very long time records are needed. So, by just a limited number of constrained stochastic simulations extreme responses can be obtained.
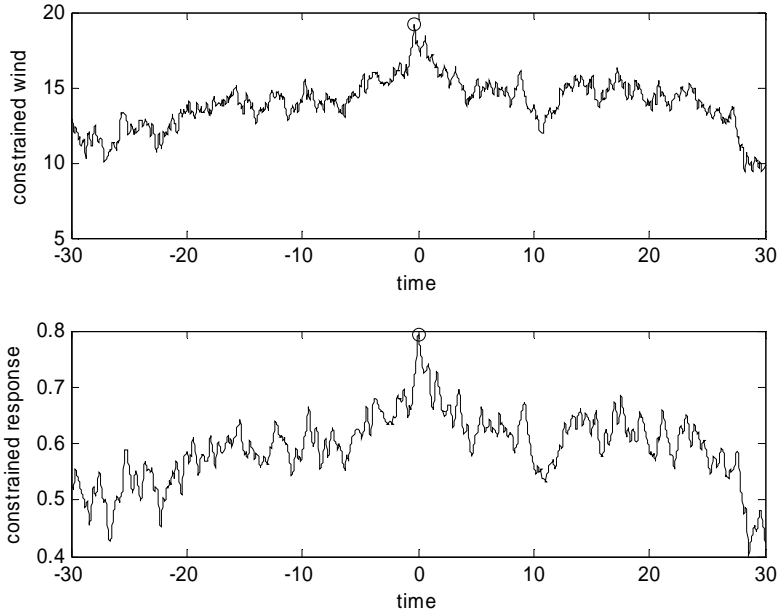
4

Figure 2. Example of constrained stochastic simulation; 5σ gust at t=0 s
Top: turbulence (input) in m/s (mean value of 12 m/s).
Bottom: blade root flapping moment (response) in MNm.

Eq. (5) is used to obtain the distribution of the local maxima in the response. To this end the conditional distributions F_c are fitted to some distribution, e.g. a generalized extreme value distribution (GEV) or three parameter Weibull. The long term response, say 50 year, is obtained via the following equation:

$$F_{50}(y) = F_y(y)^{N_{50}}$$
(6)

with N_{50} the number of local maxima in 50 years; it is assumed that the local maxima are independent. For response values in the order of the 50 year response this assumption is certainly true.

Application of Eq. (5) requires information on the gust probability n_x. For maximum amplitude gusts (i.e. local maxima) the gust probability is given by the Rice distribution, [2]. For the above mentioned gusts (with also a constraint on the response) an analytical expression for the gust probability is given in Ref. 3 (Eq. (D.11)).

3.2 Application
In Section 5 the above mentioned probabilistic method will be applied to the reference turbine. Here we will first demonstrate it with the aid of a linearised model (for each mean wind speed) of the same turbine. The reason to do so is that a theoretical expression exists for the

5

distribution of local maxima in a normal process, Ref. 2. So this makes the validation of the probabilistic method possible since the response of a linear system to a Gaussian input (turbulence) will also be Gaussian.

Gusts have been generated with 5 amplitude levels (from 3σ up to 7σ, turbulence intensity of 12%; 100 simulations for each amplitude with different random seeds). Constrained gusts can be short; to account for transient response a time interval of 30 s. before and after the gust is taken, see Fig. 2.

As explained in the Appendix, the maximum response (at t=0 s) can be considered as a 10-min. maximum. The theoretical advantage is that this establishes a one-to-one relation between the gust event and the maximum in the response. Such a one-to-one relation does not exist in case all wind gusts are considered (as done in previous work, Ref. 9 and 10) since in general the number of gusts (local maxima in the input) differs from the number of local maxima in the output. In other words, in that case it is not possible to relate each maximum in the response to one particular wind event (local maximum). A practical advantage of considering 10-min. maxima is that smaller amplitude gusts do hardly contribute to the 50-year estimate (see e.g. Fig. 8). This is convenient since the distribution of the response on constrained gusts with small amplitudes, say below 3σ, is not so easy to obtain. The reason for this is that then the response is dominated by the stochastic background rather than by the constrained gust. Another practical advantage of considering 10-min. maxima is that the maxima can be considered to be independent and that it is trivial to obtain the number of maxima in 50 year.

The results of the 100 constrained simulations for a mean wind speed of 12 m/s are depicted in Fig. 3. Please note that constrained simulation is still stochastic; i.e. 100 simulations leads to 100 different values of the maximum response (from which a distribution can be constructed). Since we are mainly interested in the tail of the distributions also a logarithmic scale has been used (bottom graphs). Via application of Eq. (5) the convolution (weighted average) can be obtained which is the overall distribution of the (10-min.) maxima in the response. In order to do this calculation it must be possible to evaluate the conditional distributions over the range of response level of interest. Here we apply a straightforward inter- / extrapolation scheme as follows: below the 90th percentile the empirical distribution ($F_e = i/(N+1)$ with i=1 to N and N=100) is used and above a Generalised Extreme Value (GEV) fit to the data. The GEV comprises all three possible limiting Extreme Value (EV) distributions with left endpoint, right endpoint or no endpoint at all, [13]. The latter one is also known as Gumbel distribution. For one amplitude the fit as well as the uncertainty ranges (dotted lines) are shown in Fig. 4. The uncertainty range taken here is the 68% confidence interval which corresponds to one standard deviation (plus and minus) assuming that the results are Gaussian distributed. A GEV has three parameters, namely a location, scale and shape parameter. The latter is also called the extreme value index. In case it is negative the distribution has a right endpoint. The fit, Fig. 4, is compared to the theoretical one (Eq. (D.13) from Ref. 3).
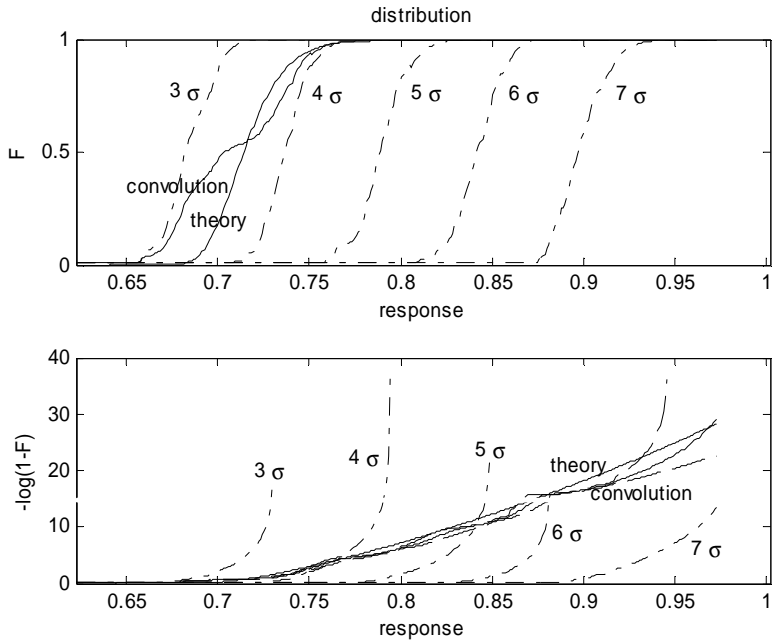
Figure 3. The distributions of the maxima in the response (linear model) obtained via constrained stochastic simulation for several gust amplitudes (for a mean wind speed of 12 m/s and turbulence intensity of 12%). In the bottom graph the uncertainty bounds of the convolution are given by dashed lines.
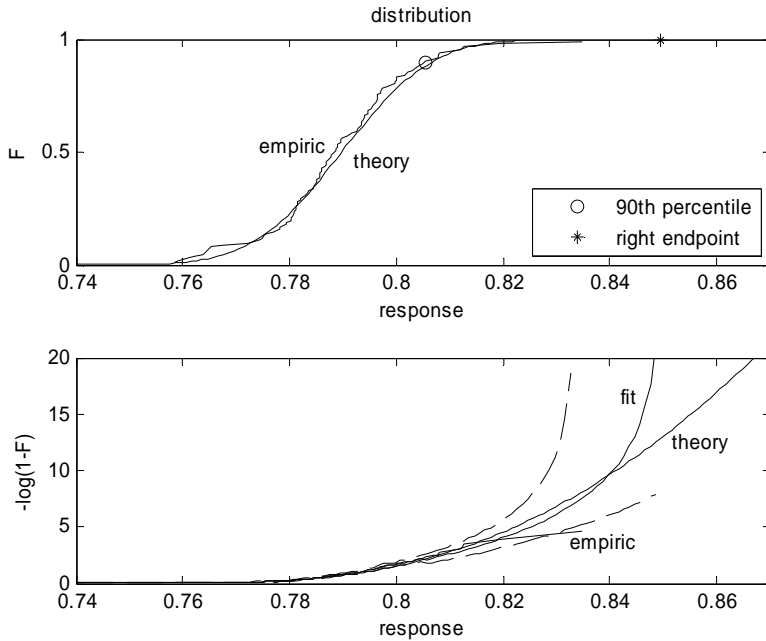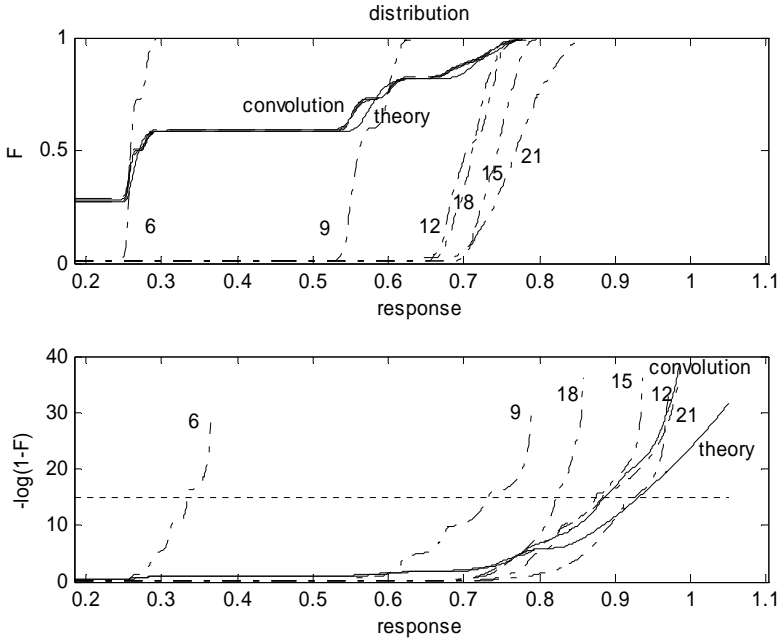
Figure 4. The (fitted) distribution of the maxima in the response (linear model) obtained via constrained stochastic simulation for 1 gust amplitude (5σ); mean wind speed 12 m/s and turbulence intensity of 12%. In the bottom graph the uncertainty range of the fit is indicated by dashed lines.

The convolution in Fig. 3 is compared to the theoretical Rice distribution, Ref. 2. As mentioned above, the convolution is a weighted average of the 5 distributions (for each gust amplitude), Eq. (5). This explains its stepwise behavior. At first sight one may think that the convolution is rather poor but that only holds for smaller response values (below 0.25 MNm). If one would be interested in this response range the result can be drastically improved by considering lower gust amplitudes (e.g. 1σ to 4σ with a step size of 0.3σ). Here we are interested in the (upper) tail and in that region the convolution is close to the theoretical one.

Please note that there is a strong correlation between gust amplitude and response, namely for higher amplitudes the distribution of the maxima in the response is shifted to the right. This substantiates the claim that by constrained stochastic simulation extreme situations can be obtained with a limited number of simulations.

The procedure outlined above is repeated for the other mean wind speeds and the results are depicted in Fig. 5. Again the agreement between the convolution (averaged over the probability of the mean wind speed bins, for which a Weibull distribution is taken with shape parameter 2 and scale parameter 8 m/s) and the theoretical one is excellent especially at the tail. For the reference turbine there is no simple relation between mean wind speed and response. Such a

8

simple relations does not to be the case due to the non-linear behavior of wind turbines (especially due to the aerodynamics, e.g. stall).

Figure 5. The distributions of the maxima in the response (linear model) obtained via constrained stochastic simulation for several mean wind speeds (turbulence intensity of 12%).

As can be seen, the convolution starts at about 0.3 instead of 0. This is due to considering mean wind speeds from 6 m/s (instead of 0) as well as gust amplitudes from 3σ (instead of 0). Furthermore, the convolution exhibits a stepwise shape; this is due to the discretized gust amplitudes used in Eq. 5. Both effects will not influence the determination of the 50-years value. The latter is obtained by the intersection of the distribution with $1-1/T_{50}$ with $T_{50}=2628000$ the number of 10-min. periods in 50 year (indicated in the graph by a horizontal line). The determined 50-years value $y_{50}=0.89\pm0.02$ MNm is close to the theoretical one: $y_{50t}=0.930$ MNm.

By considering the terms from Eq. (5) the contribution of each mean wind speed to the final result can be calculated, see Fig. 6. It appears that 21 m/s dominates the 50-year result. The obtained result for y_{50} can be improved by considering a finer amplitude range. With respect to Fig. 6 just the mean wind speeds of 12 m/s, 15 m/s and 21 m/s have to be taken into account. To this end the contribution of each gust amplitude to the result is determined, see Fig. 7.

9
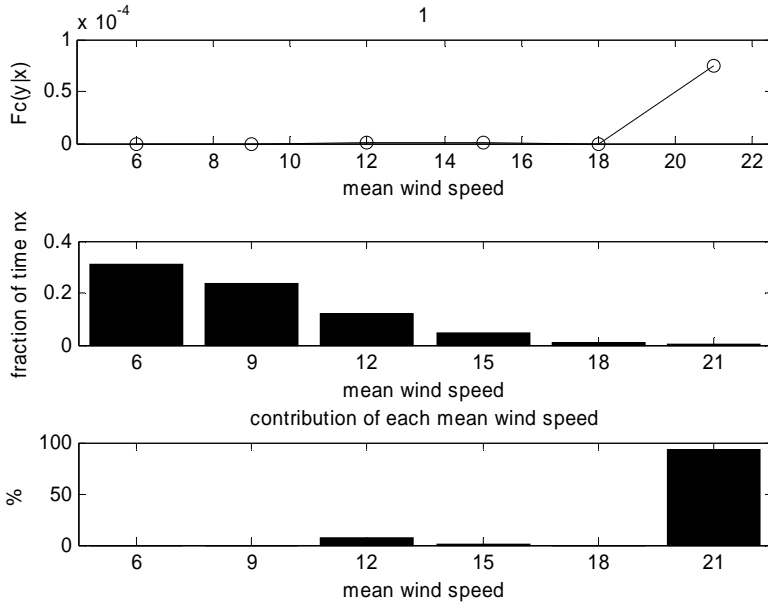
Figure 6. Top: The value of the conditional distribution (exceedance probalitity) for y=0.89 MNm (linear model) for mean wind speeds 6, 9, 12, 15, 18 and 21 m/s.
Middle: the fraction of time n_x for each mean wind speed.
Bottom: Contribution of each mean wind speed to the tail estimation of the response (i.e. the normalized product of the values of the top and middle graph).
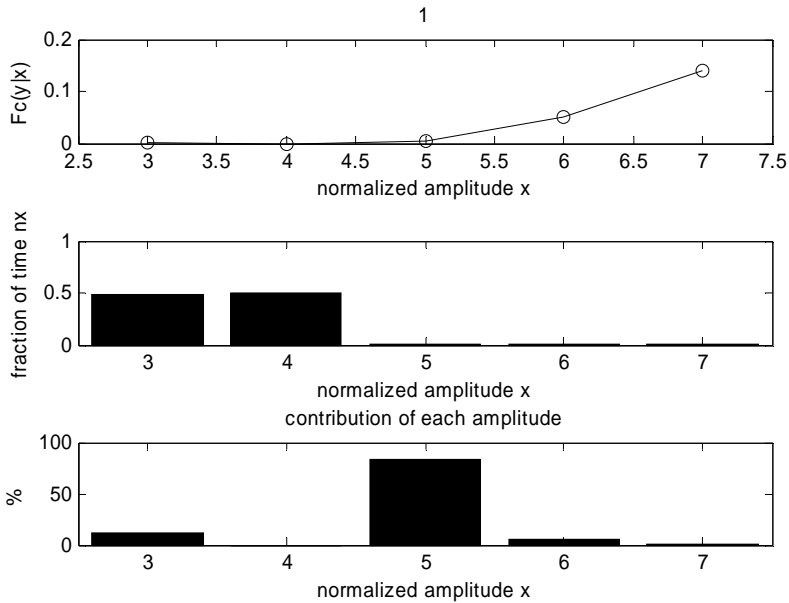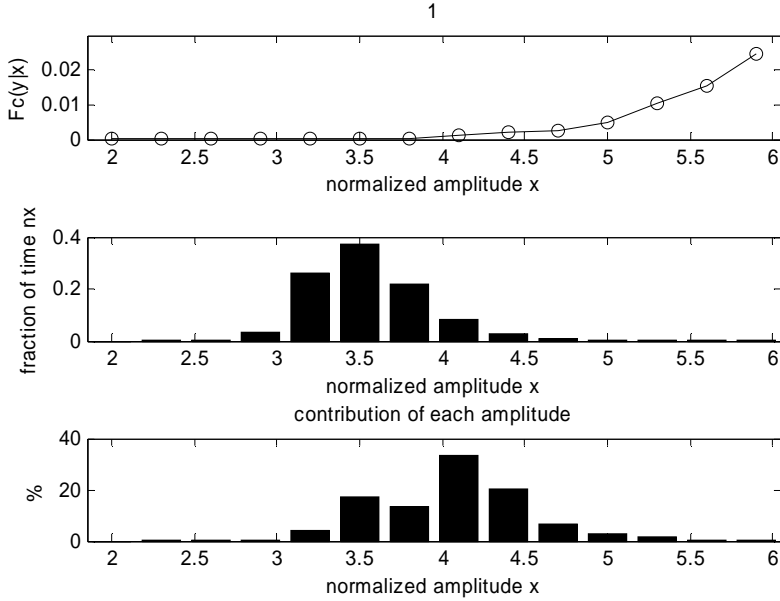
10

Figure 7. Top: The value of the conditional distribution (exceedance probalitity) for y=0.89 MNm (linear model), mean wind speed 21 m/s; gust amplitudes of 3σ to 7σ.
Middle: the fraction of time n_x for each gust amplitude.
Bottom: Contribution of each gust amplitude to the tail estimation of the response (i.e. the normalized product of the values of the top and middle graph).

On the basis of Fig. 7 new constrained simulations have been performed for gust amplitudes in between 2σ and 5.9σ (with steps of 0.3σ). This improves the calculated 50 years value to y_{50}=0.91±0.02 MNm. From Fig. 8 it can be concluded that the amplitude range, as well as discretization, is sufficient and much further refinement cannot be achieved. Without information as provided by Fig. 8 it is easily to consider too small amplitude ranges leading to wrong answers as occurred in [12].

11

Figure 8. Top: The value of the conditional distribution (exceedance probalitity) for y=0.91 MNm (linear model), mean wind speeds 21 m/s; gust amplitudes of 2σ to 5.9σ.
Middle: the fraction of time n_x for each gust amplitude.
Bottom: Contribution of each gust amplitude to the tail estimation of the response (i.e. the normalized product of the values of the top and middle graph).

4. Determination of the 50-years response based on normal (unconstrained) simulations

In the previously section the probabilistic method has been applied to a *linearised* dynamic model of a wind turbine in order to validate the method. In the next section we will apply it to our topic of interest, i.e. a regular (non-linear) dynamic wind turbine model. First, a traditional treatment of extremes based on normal simulations will be covered in this section. In the IEC annex F (informative) a statistical extrapolation of loads for ultimate strength analysis is described. How exactly such an extrapolation should be carried out, e.g. number of simulations and which distribution function(s) has to be used, is still under discussion. In order to have some reference for the results to be presented in Section 5, we have chosen to do 1000 10-min. simulations for each wind speed bin. This number varies in other studies from 10 only Ref. 6, 90 (Ref. 7) to 200 (Ref. 8). Just for ease a GEV distribution is again exploited for fitting a distribution to the simulation results.
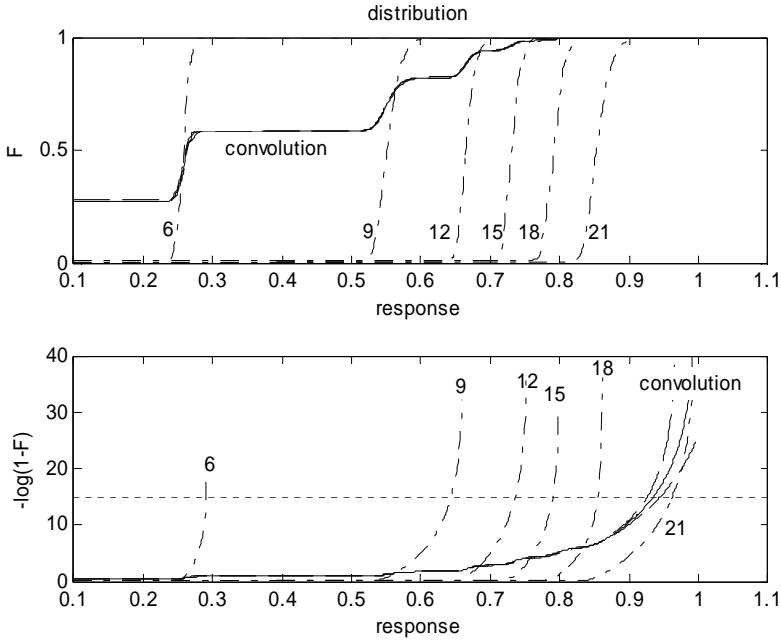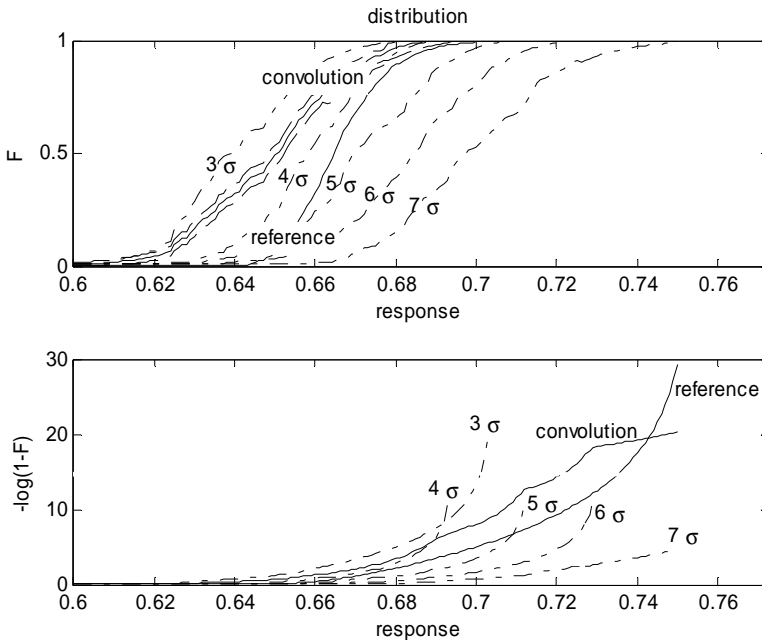
12

Figure 9. The distributions of the maxima in the response obtained via normal (unconstrained) stochastic simulation for several mean wind speeds (turbulence intensity of 12%).

The wind field simulation is based on a Fourier summation with random Gaussian coefficients (zero mean and variance related to the spectral value, [1]). By varying the seed of the random number generator different simulations are performed.

Similar to Section 3 the results per wind speed bin are fitted and afterwards averaged (convoluted), see Fig. 9. At a mean wind speed of 6 m/s the wind turbines has 2 operational rotor speeds; the rotor speed leading to the highest load have been considered.

As can be seen in the graph for the reference turbine the response increases with mean wind speed. This will not generally be true, esp. in case of pitch turbines.

The following 50-years value is obtained: y_{50}=0.934 MNm (with an uncertainty range of 0.925 to 0.943 MNm). This result is totally governed by the mean wind speed of 21 m/s (figure similar to Fig. 6 and not shown here). For the reference turbine the maximum wind speed taken into account (recall that the mean wind speed of 24 m/s was excluded from our analysis) is dominating the response. In general, this does not have to be the case.

This 50 year value is based on stochastic loading only. In practice one also has to take the deterministic loads (due to wind shear, gravity, etc.) into account.

13

5. Determination of the 50-years response based on constrained simulations

Constrained simulations will now be applied to arrive at the 50-year extreme. The same type of constrained gusts as used in Section 3 is taken. These gusts will lead to a local extreme in the response, of some unspecified level, at time t=0 s, see Fig. 2. However, this only holds for the linearized model as treated in Section 3. Here the gusts are applied as input to a non-linear wind turbine model so in general the extreme will not coincide with t=0 s. The local extreme in the response closest to t=0 s. is taken.

Since we are dealing with a non-linear model one may even question if these constrained gusts can be in fact used. From Fig. 10 it can be seen that the load response is related to the gust amplitude. In Section 6.3 it will be shown that it is worthwhile to apply constraint simulation in case such a relation exists.

Figure 10. The distributions of the maxima in the response obtained via constrained stochastic simulation for several gust amplitudes (for a mean wind speed of 12 m/s and turbulence intensity of 12%); in the upper graph the uncertainty bounds in the determination of the convolution are shown by dashed lines. For comparison the result obtained by unconstrained simulations (from Fig. 9) are shown as well.

The results for all mean wind speeds are displayed in Figure 11. From the graph a 50-years value can be read of y_{50}= 0.952 MNm (with an uncertainty range of 0.908 to 1.013 MNm). Again the fifty year value is dictated by the wind speed of 21 m/s (graph similar to Fig. 6 and not shown here). Next, on the basis of a figure similar to Fig. 7 a finer amplitude grid of A=3σ to 6σ is used to redo the constrained simulations leading to an improved estimate of y_{50}=0.935 MNm.
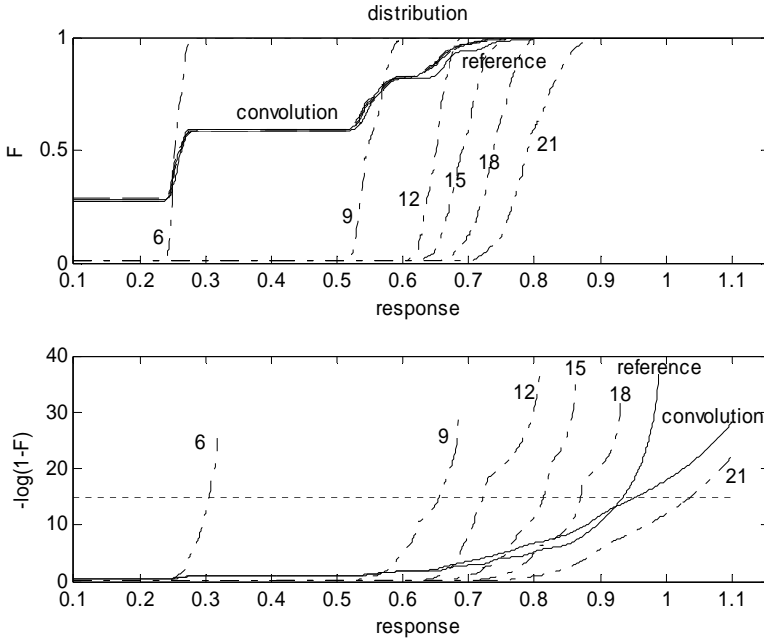
14

Figure 11. The distributions of the maxima in the response obtained via constrained stochastic simulation for several mean wind speeds (turbulence intensity of 12%); for comparison the result obtained by unconstrained simulations (from Fig. 9) are shown as well.

6. Discussion

In this section we will compare the results obtained by unconstrained simulations (Section 4) and constrained simulations (Section 5). Next, the differences between these results, obtained with a non-linear model and those from a linear dynamic model, Section 3, will be discussed. Finally, it will be investigated if it is possible to apply other kind of constrained gusts in order to arrive at the 50-year load level.

6.1 Comparison between constrained and normal simulations

We will first address the relation between the uncertainty range of the distribution fit and the number of simulations. In Section 4 1000 simulations have been performed for each wind speed bin. So we can redo the fitting of the results to a GEV distribution using 100 simulations only; in fact this can be done 10 times (simulation 1-100, 101-200, etc.). The resulting 10 fits are presented in Fig. 12. Furthermore, the uncertainty range (of about 0.1 MNm) of *one* of the 10 fits is shown (dashed lines). We recall from Section 3.2 that the uncertainty range taken equals the 68% confidence interval. Fig. 12 is in line with this since indeed 7 out of 10 of the fits are in the uncertainty range. As expected the uncertainty range (0.02 MNm, see Table 2) for the fit to the

15

1000 results is less but still considerable large. The particular range will depend on the specific case, wind turbine and load situation, as well as fit method (we have applied a built-in routine of Matlab). However it should be stressed that the occurrence of these (large) uncertainty ranges is inherent in fitting distributions on the basis of a limited number of simulations. This is due to the natural variations which will occur in case a limited number of random drawings are taken from a fixed distribution.

In the graph the 99th as well as the $1-1/T_{50}=99.99996^{th}$ percentile are indicated by (horizontal) lines (with $T_{50}=2628000$, the number of 10-min. periods in 50 year). The range of the 99th percentiles for the 10 fits is just 8% (normalized with the 99th percentile obtained from the 1000 simulations: 0.698 MNm). Often a convergence criteria or goodness of fit is taken considering the 99th percentile (or even lower in the tail). From Fig. 12 it is now instructive to notice that a rather small scatter at the 99th percentile will still lead to a large uncertainty range at the value of interest: the 50 year value (0.735 NMm determined from the fit using 1000 simulations). From the above it will be clear that it is good practice always to specify the uncertainty range in an estimate of a 50 year value.
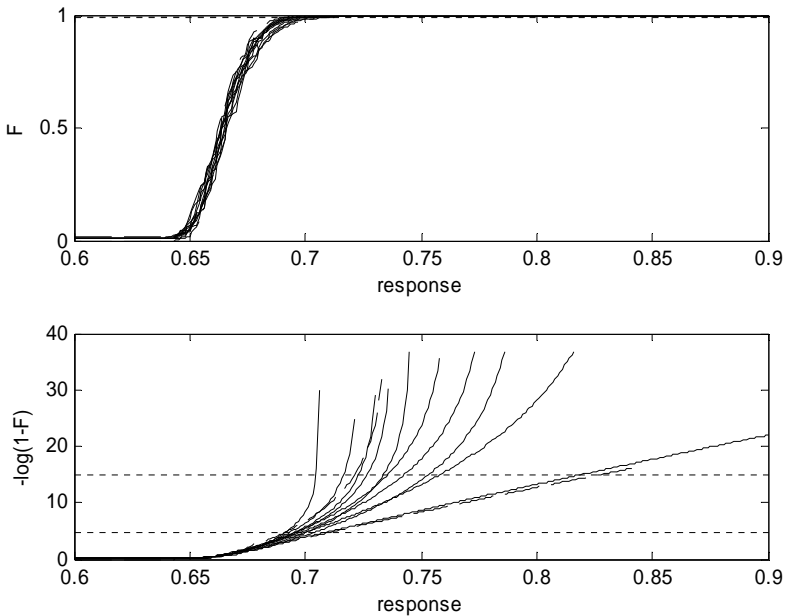

Figure 12. The distributions of the maxima in the response obtained via unconstrained stochastic simulation (for a mean wind speed of 12 m/s and turbulence intensity of 12%); obtained via 10 different sets of 100 simulations each.

16

Table 1: Unconstrained simulations
Nr: number of simulations
U: mean wind speed
R_{50}: the 50 year value
ΔR_{50}: the uncertainty range in R_{50} (corresponding with 2 times the standard deviation)

Nr (-)	U (m/s)	R_{50} (MNm)	ΔR_{50} (MNm)
100	9	0.688	0.165
100	12	0.757	0.104
100	21	0.980	0.132
100	overall	0.941	0.111
200	9	0.669	0.090
200	12	0.759	0.075
200	21	0.984	0.109
200	overall	0.942	0.058

Table 2: Unconstrained simulations

Nr (-)	U (m/s)	R_{50} (MNm)	ΔR_{50} (MNm)
1000	9	0.643	0.023
1000	12	0.735	0.021
1000	21	0.961	0.033
1000	overall	0.934	0.018

Table 3: Constrained simulations
A: amplitude range (lower value : step size : upper value)

Nr (-)	U (m/s)	R_{50} (MNm)	ΔR_{50} (MNm)	A (-)
100	9	0.645	0.010	5:0.2:7
100	12	0.739	0.040	4:0.2:6
100	21	0.976	0.094	3:0.2:6
100	overall	0.935	0.095	

The overall results for our reference turbine are given in the Tables 1 to 3 for the mean wind speeds of interest. With respect to the discussion above the given values for ΔR_{50} are more important than those for R_{50} since the latter depends on the particular set of 100 values which is taken (notice the variation of R_{50} in Fig. 12 for different data sets). Unlike the linear model (Section 3) there is no theoretical expression available for a non-linear model. So it is not known which of the results, obtained through constrained or unconstrained simulations, is best. Here we just take the values from Table 2 as reference. First it can be noticed that the R_{50} results from both Table 1 and 3 are in line with these reference values (taking the specified uncertainty ranges into account). Secondly, the results of the constrained simulations (Table 3) are (far) better than the unconstrained simulations (Table 1) for all mean wind speeds; the R_{50} values are closer to the reference ones and also the uncertainty ranges are smaller. The computational efforts are of the same order. A simulation length of 1 min. is taken for each gust amplitude in order to account for transient response. The amplitude ranges given in Table 3 have been chosen on the basis of

17

simulations using (normalized) amplitudes from 3σ to 7σ, so in total 16 or 21 amplitudes have been taken. Most probably 30 s. per gust is sufficient with respect to transient response so each constraint simulation can take about 10 min. simulation time. In case conservatively a length of 1 min. per gust is taken each constraint simulation of Table 1 corresponds to (16 to) 21 min. simulation time. Even then constrained simulation outperforms unconstrained simulation; compare Table 3 with the results for 200 10-min. simulations, Table 1.

On basis of Table 1 to 3 it can determined that the uncertainty range (per wind speed) decreases with the number of simulations:

$$\Delta R_{50} \propto Nr^{-b} \tag{7}$$

with b in between 1 and ½ (i.e. in order to halve the uncertainty range two to four times more simulations are required).

The uncertainty range for U=21 m/s for the constrained simulations (Table 3) is much larger than for the other wind speeds. A reason for this is that for this wind speed it happens that the 50 year value depends on a broader amplitude range; this weakens the advantage of constrained simulation compared to unconstrained simulation.

One of the aspects that needs further investigation is the choice of the extreme value distribution. In this paper the GEV is applied. This implies that it may happen that a GEV with some endpoint is fitted to the data even if this data is taken from a distribution without endpoint (or just the other way round). Due to the limited number of data and its randomness this may happen for some particular gust amplitudes and not for some other. As a consequence only the latter amplitudes will contribute to the 50-year estimate (assuming that all endpoints are less than this value). This phenomenon hinders the determination of the correct amplitude range. This may be solved by considering a distribution without endpoint, e.g. the three parameter Weibull distribution.

6.2 The effect of non-linearity

In this paper the extreme responses of both non-linear and linearised models are analyzed. By comparing the results some notion of the effect of non-linear behavior of wind turbines on the extreme loading can be obtained. The results presented below are of course just valid for our reference turbine.

In Section 3.2 the obtained (theoretical) 50-years response of the linearised model equals 0.930 MNm. The 50-years value of the original (non-linear) wind turbine model appears to be 0.934 MNm. As example of the differences for one particular mean wind speed we consider 12 m/s. The $1-1/T_{50}$ quantile for the linearised model equals 0.872 MNm. The same quantile of the non-linear model is much smaller: 0.735 MNm. It is in line with Fig. 1 that the extreme value of the non-linear model is lower.

6.3 Application of other constrained wind fields

In this paper gusts have been used which results in a local extreme in the response, Fig. 2. The expression of such gusts has been derived on basis of a linearized wind turbine model. In Ref. 3 the whole probabilistic method based on this kind of gusts has been validated. For non-linear models such a validation is not possible and it is open for discussion if these gusts are the proper ones. It will be shown below that as long as there is a correlation between gust amplitude and response (i.e. the larger the gust amplitude the larger the response) any gust shape can be used in the probabilistic approach. On basis of several simulations for different amplitudes it can be

easily determined if such a correlation exists. From Fig. 10 it is clear that a correlation is present for the considered gusts in this paper.

In fact, Eq. (5) is valid for every kind of gust. As example, maximum amplitude gusts (i.e. gusts which have a local maximum of some specified amplitude) are generated and afterwards used as input for the load calculations. The results are given in Fig. 13 (which is comparable to Fig. 10). It can be seen that the response is again related to the gust amplitude (in the range of the simulations, upper graph; not in the extrapolated tails, bottom graph). The result is not that good compared to the result from the unconstrained simulations but could again be improved by refining the range of gust amplitudes. We have not done so since we merely want to show that it is in principle possible to use some other gust shapes. Also gusts have been used with some maximum *negative* amplitude (i.e. maximum amplitude gusts multiplied by -1). The distributions for the different gust amplitudes appear more or less the same (not shown here) since there is hardly a correlation between negative gusts and response for a stalled regulated wind turbine. Still these gusts can in principle be applied but it makes no sense since it will not save simulation time compared to unconstrained simulations.

For stall regulated turbines it could have been anticipated that maximum amplitude gusts, as observed in Fig. 2, lead to extremes in the response. For pitch regulated wind turbines it is not straightforward which gust shape is relevant. So, for pitch turbines it is convenient to use the same gust model as we have used here from Ref. 3. It appears that the governing gusts for a typical pitch turbine are velocity dips, Fig 14.
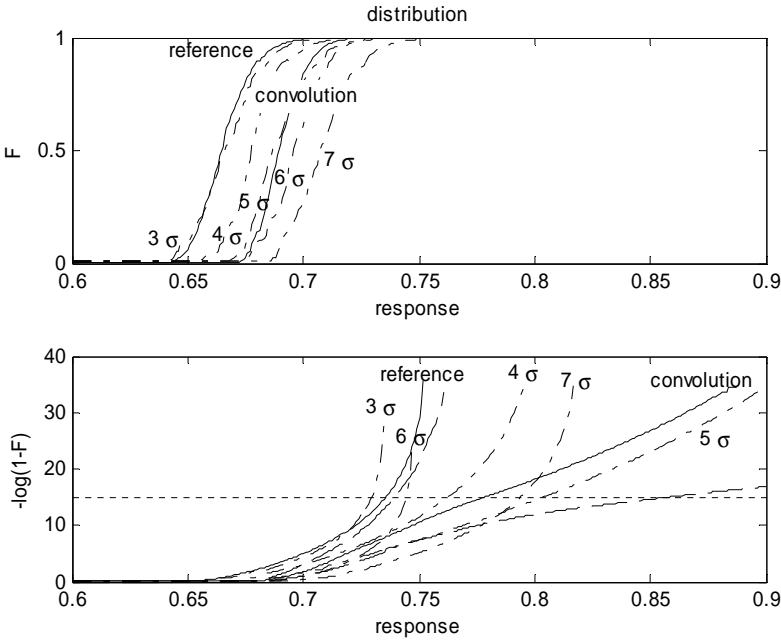

Figure 13. The distributions of the maxima in the response obtained via constrained stochastic simulation of maximum amplitude gusts (for several gust amplitudes and a mean

19

wind speed of 12 m/s and turbulence intensity of 12%); for comparison the result obtained by unconstrained simulations (from Fig. 9) are shown as well.
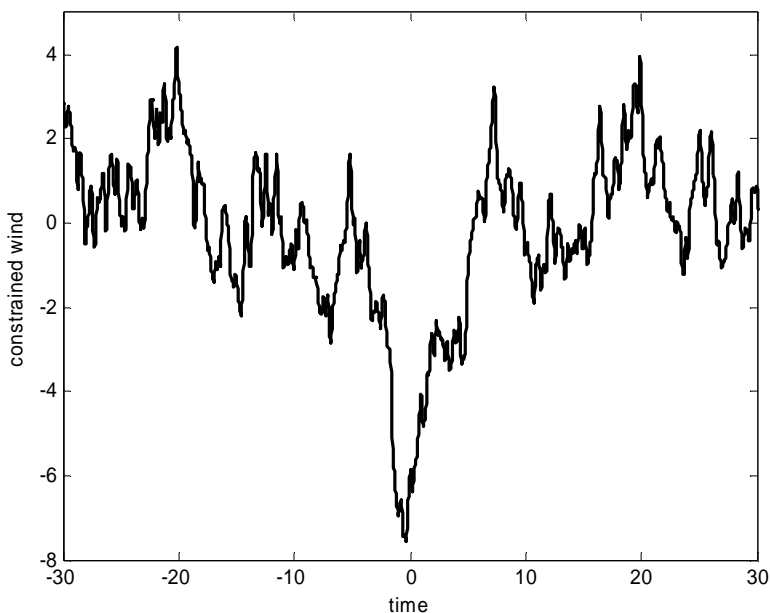

Figure 14. Example of a constrained gust (with respect to the mean value) for a pitch regulated wind turbine.

7. Conclusions

A probabilistic method has been presented to determine the 50 year value in the response of a wind turbine. The method relies on so-called constrained stochastic simulation. Through constrained simulation, gusts can be generated which satisfy some specified constraint. In this paper it is used in order to generate specific wind gusts which will lead to local maxima in the response of wind turbines. By performing many simulations (for given gust amplitude) the conditional distribution of the response is obtained. By means of a weighted average of these conditional distributions over the probability of the gusts the distribution for given mean wind speed is determined. The overall distribution of the response is obtained by a weighted average of the distributions for each wind speed bin taking into account the probability of occurrence of the wind speed bins.

The main advantage of constrained simulation is the reduction of the computational cost (or to increase the accuracy for the same computational effort). It is related to the ability of defining wind inflow series that lead to local load maxima based on linear modeling of the system.

20

As reference turbine a generic 1 MW stall regulated wind turbine is taken. By considering a linearized dynamic model of this turbine the proposed probabilistic method is validated. The determined 50 year response value corresponds indeed to the theoretical value based on Rice.

The 50 year values have been calculated on the basis of constrained and unconstrained (conventional) simulations with the non-linear dynamic model of the reference turbine. For each wind speed bin a number of 100 simulations are performed. For the governing wind speed bins the number of unconstrained simulations has been increased to 1000 to serve as reference result. For all wind speed bins the results obtained via constrained simulation are better than those using unconstrained simulations: the 50 year estimates are closer to the reference values and the uncertainty ranges are smaller. The involved computational effort for both methods is about the same.

The uncertainty range, inherent in the extrapolation from a limited data set to 50 year, is rather large even if 1000 10-min. simulations are performed. It is recommended to mention the uncertainty involved in a 50 year estimate.

In future research constrained simulations will also be applied to other current wind turbines and loads; for this purpose new constrained wind gusts should be generated. In this paper just a uniform turbulent wind field is taken into account. It should be possible to extent the method to a complete wind field covering all 3 turbulence components. A practical limitation can be the determination of the required transfer functions from wind field (i.e. many points in the rotor plane) to the load of interest. The required number of simulations for each gust amplitude as well as choice of the distribution function (with of without endpoint) may be further investigated. A final validation of any method to come to a 50 year response would be comparison with long term wind turbine load measurements. Combined wind and load measurements will also reveal if present turbulence simulators are good enough; do they provide the diversity of turbulent structures as encountered by real wind turbines operating in a range of environments?

References

[1] Wim Bierbooms, Constrained Stochastic Simulation – Generation of Time Series around some specific Event in a Normal Process, Extremes, Vol 8, p 207–224, 2006.

[2] Rice, S.O., Mathematical analysis of random noise, Bell Syst. Techn. J., 23, 282 (1944). [Reprinted in Wax, N. (ed.), Selected papers on noise and stochastic processes, Dover Publ., 1958].

[3] Wim Bierbooms, Specific gust shapes leading to extreme response of pitch-regulated wind turbines, The Science of making Torque from Wind, Lyngby, Denmark, 2007.
   http://www.iop.org/EJ/article/1742-6596/75/1/012058/jpconf7_75_012058.pdf?request-id=e4295526-bcda-432c-875e-1d7cd8dabce0

[4] Michel Verhaegen and Vincent Verdult, Filtering and System Identification: A Least Squares Approach, Cambridge University Press, 2007.

[5] Wim Bierbooms, Determination of the extreme value in the response of wind turbines by means of constrained stochastic simulation, 27th ASME Wind Energy Symposium, Reno, 2008.

[6] Rolf Genz, An investigation of load extrapolation according to IEC 61400-1 Ed. 3, European Wind Energy Conference, Athens, 2006.

[7] K. Freudenreich and K. Argyriadis, The Load Level of Modern Wind Turbines according to IEC 61400-1, The Science of making Torque from Wind, Lyngby, Denmark, 2007.

[8] Jeffrey Fogle, Puneet Agarwal and Lance Manuel, Towards an Improved Understanding of Statistical Extrapolation for Wind Turbine Extreme Loads, 27th ASME Wind Energy Symposium, Reno, 2008.

[9] Bierbooms, W., Cheng. P.W., Larsen, G., Pedersen, B.J., Modelling of extreme gusts for design calculations – *New*Gust FINAL REPORT JOR3-CT98-0239, Delft University of Technology, 2001.

[10] Taylor, P.H., Jonathan, P. and Harland, L.A., Time domain simulation of jack-up dynamics with the extremes of a Gaussian process, Journal of Vibration and Acoustics, 119, 624-628 (1997).

[11]   Wim Bierbooms, Investigation of spatial gusts with extreme rise time on the extreme loads of pitch regulated wind turbines, Wind Energy, Vol 8, p 17-34, 2005.

[12]   Léon A. Harland and Jan H. Vugts, Extreme responses of non-linear dynamic systems using constrained simulations, OMAE, 1996.

[13]   Samuel Kotz and Saralees Nadarajah, Extreme value distributions: theory and applications, Imperial College Press, London, 2002.

Appendix: Application of 10-min. maxima in the probabilistic method

In this appendix it will be investigated if 10-min. maxima, rather than all maxima, can be used in the probabilistic method outlined in main text. The gust amplitudes of the stochastic wind input of the wind turbine will again be denoted as random variable x and the local maxima of the response as random variable y. The joint distribution $F(x, y)$ corresponds to the joint density $f(x, y)$. The maxima during some period p (e.g. 10-min.) are indicated by x_p and y_p. The joint distribution F_p for these maxima is:

$$F_p(x, y) = F(x, y)^{N_p} \qquad (A.1)$$

with N_p the number of local maxima of the response in time period p.

We will now examine if we can express the marginal distribution $F_{yp}(y)$ in terms of conditional distributions like Eq. (5). The joint density f_p is given by:

$$f_p(x, y) = \frac{\partial^2 F_p(x, y)}{\partial x \partial y} \qquad (A.2)$$

From Eq. (A.1) we obtain:

$$\frac{\partial F_p(x, y)}{\partial x} = N_p F(x, y)^{N_p - 1} \frac{\partial F(x, y)}{\partial x} \qquad (A.3)$$

and

$$\frac{\partial^2 F_p(x, y)}{\partial x \partial y} = N_p (N_p - 1) F(x, y)^{N_p - 2} \frac{\partial F(x, y)}{\partial x} \frac{\partial F(x, y)}{\partial y} + $$
$$N_p F(x, y)^{N_p - 1} \frac{\partial^2 F(x, y)}{\partial x \partial y} \qquad (A.4)$$

The (first order) partial derivatives have an upper bound given by:

$$\frac{\partial F(x, y)}{\partial x} = \int_{-\infty}^{y} f(x, \beta) \, d\beta < \int_{-\infty}^{\infty} f(x, y) \, dy = f_x(x) \qquad (A.5)$$

and a similar expression for the partial derivative to y. For large x and y the densities $f_x(x)$ and $f_y(y)$ go to 0 while $F(x, y)$ is approaching 1, thus the 1st term at the right hand side of Eq. (A.4) can be neglected. So we have:

$$f_p(x, y) \approx N_p F(x, y)^{N_p - 1} f(x, y) \qquad (A.6)$$

Similar to Eq. (3) the conditional density for the maximum per period is given by:

23

$$f_{cp}(y) = \frac{f_p(x, y)}{f_{xp}(x)} \tag{A.7}$$

Assuming that the maxima per period are independent the marginal distribution F_{xp} equals:

$$F_{xp}(x) = F_x(x)^{N_p} \tag{A.8}$$

so the density f_{xp} is given by:

$$f_{xp}(x) = \frac{dF_{xp}(x)}{dx} = N_p F_x(x)^{N_p-1} \frac{dF_x(x)}{dx} = N_p F_x(x)^{N_p-1} f_x(x) \tag{A.9}$$

For large values of y, $F(x, y) \approx F_x(x)$, thus:

$$f_{xp}(x) \approx N_p F(x, y)^{N_p-1} f_x(x) \tag{A.10}$$

Finally, combination of Eq. (A.6), (A.7) and (A.10) leads to:

$$f_{cp}(y) \approx \frac{N_p F(x, y)^{N_p-1} f(x, y)}{N_p F(x, y)^{N_p-1} f_x(x)} = \frac{f(x, y)}{f_x(x)} = f_c(y) \tag{A.11}$$

So, the conditional densities obtained via constrained stochastic simulation can also be used for the determination of the distribution of the maxima of the response over some time period as long as we are interested in the tail of the distribution. For large y:

$$F_{yp}(y) = \int_{-\infty}^{\infty} F_{cp}(y) f_{xp}(\alpha) d\alpha \approx \int_{-\infty}^{\infty} F_c(y) f_{xp}(\alpha) d\alpha \approx \sum F_c(y) n_{xp} \tag{A.12}$$

with n_{xp} the probability ('fraction of time') that a maximum over period p is within the discretized amplitude intervals. This probability is given by:

$$n_{xp} = F_{xp}(x_{upp}) - F_{xp}(x_{low}) \tag{A.13}$$

with F_{xp} the distribution of the maximum of period p, Eq. (A.8), and x_{upp} and x_{low} the upper and lower bound resp. of the amplitude interval.

The contribution of modest gusts to the tail of the response distribution will be limited. It is therefore more natural to rewrite Eq. (A.12) in terms of the exceedance probability:

$$G_{yp}(y) = 1 - F_{yp}(y) = 1 - \int_{-\infty}^{\infty} F_{cp}(y) f_{xp}(\alpha) d\alpha = \int_{-\infty}^{\infty} (1 - F_{cp}(y)) f_{xp}(\alpha) d\alpha$$
$$\int_{-\infty}^{\infty} G_{cp}(y) f_{xp}(\alpha) d\alpha \approx \int_{-\infty}^{\infty} G_c(y) f_{xp}(\alpha) d\alpha \approx \sum G_c(y) n_{xp} \tag{A.14}$$

24

3

Time Domain Comparison of Simulated and Measured Wind Turbine Loads Using Constrained Wind Fields

Wim Bierbooms and Dick Veldkamp

Summary. By means of so-called constrained simulation, wind fields can be generated which encompass measured wind speed series. If the method of constrained wind is used in load verification, the low frequency part of the wind and of the loads can be reproduced well, which makes it possible to compare time traces directly. However from the three load cases for the reference wind turbine investigated here, it appeared that there was no clear improvement in fatigue damage equivalent load ranges.

3.1 Introduction

Comparison between wind turbine load measurements and simulations is complicated by the uncertainty about the wind field experienced by the rotor. Usually the wind speed is measured at just one location (hub height) which makes direct comparison between the measured and simulation load time histories impossible. Instead random wind fields are generated (with the same mean and spectrum as the measured wind) and the power spectra of the loads or the equivalent fatigue load ranges are compared. The next section will present a method of so-called constrained stochastic simulation. By means of this method wind fields may be generated which encompass measured wind speed series i.e. one or more measured wind speed signals are reproduced exactly. Subsequently the constrained wind fields as well as the resulting wind turbine loading will be dealt with. Comparisons of the results of actual load measurements and simulated loads, found by using constrained wind fields based on measured wind, are given in Sect. 3.5.

3.2 Constrained Stochastic Simulation of Wind Fields

For wind turbine load calculations an artificial wind field is needed. Here we use the description by means of Fourier series:

$$u(t) = \sum_{k=1}^{K} a_k \cos \omega_k t + b_k \sin \omega_k t \qquad (3.1)$$

The vector $u(t)$ represents the longitudinal velocity fluctuations in N points in the rotor plane (K frequencies). The Fourier coefficients a_k and b_k (row vectors) are independent for different frequencies and for the same frequency the following relation holds:

$$\mathrm{E}[a_k\, a_k^{\mathrm{T}}] = \mathrm{E}[b_k\, b_k^{\mathrm{T}}] = \frac{1}{T} S_k \qquad (3.2)$$

with T the total time of the sample and S_k the matrix of the cross-power spectral densities of the wind speed fluctuations in the different space points. They are found from the auto power spectral densities and the (root) coherence function γ.

In order to generate a spatial wind field we have to factorize the S_k matrix for each frequency component. In case the wind is measured at some location, it is straightforward to determine the set of Fourier coefficients for that space point. We can now improve the simulation of the wind speeds at the other space points on basis of the knowledge of the wind speed at that point. The accompanying equations can be found in the appendix of [1]. The wind fields which are simulated on basis of measured wind fields are called constrained stochastic simulations (they are generated under the constraint that at one or more points the measured wind speeds have to be reproduced). The generated wind fields may be considered to be wind fields which *could* have occurred during the measuring period; the actual wind field can never be reproduced in case of just a few measurement locations, since turbulence is a stochastic process.

3.3 Stochastic Wind Fields which Encompass Measured Wind Speed Series

With the method given in Sect. 3.2 several sets of wind time series are generated. As turbulence model the Kaimal spectrum and coherence function of IEC 61400-1 are chosen. Wind fields are created with mean wind speeds below, around and above rated wind speed of the reference turbines. Turbulence intensity is taken according to the IEC standard. For each situation at least 20 wind fields have been generated of 10 min length and a time step of 0.04 s. Nowadays it is common to generate all three velocity components; since the measurements (see Sect. 3.5) involved the longitudinal component only, the constrained simulations are restricted to that component.

The constrained simulations have been performed with two in-house packages. One uses a polar grid (30 azimuth by 5 radial, plus a point at the rotor

centre) and is used in combination with Flex5. The other applies a Cartesian grid (15 by 15) and produces wind fields which can be read by Bladed. In order to investigate the influence of the number of measuring points several configurations of anemometers (ranging from 1 to 11) have been considered. In Fig. 3.1 two of the considered configurations are shown.

One of the simulated wind fields can be appointed to be the "measured" wind field. The reduced scatter in the constrained wind time series is shown in Fig. 3.2. The shape of the time series gets more fixed (determined by the measured wind speeds). Unconstrained wind fields will average out to straight horizontal lines; the variance will be uniform over the rotor plane.
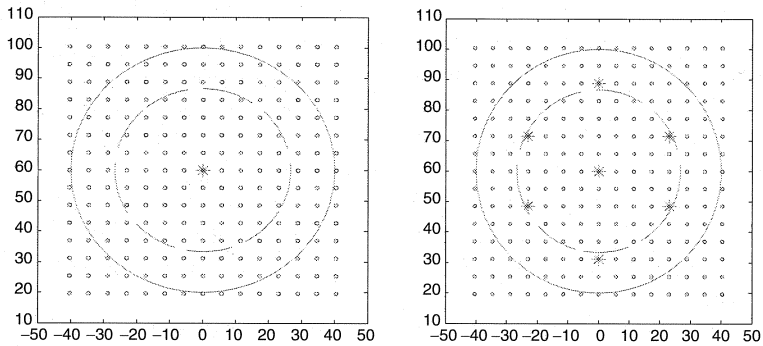
Fig. 3.1. The applied rectangular grid for the spatial wind fields and the locations of the anemometers of 2 of the considered configurations: 1 (left) and 7 (right); radius R and 2/3R are also indicated
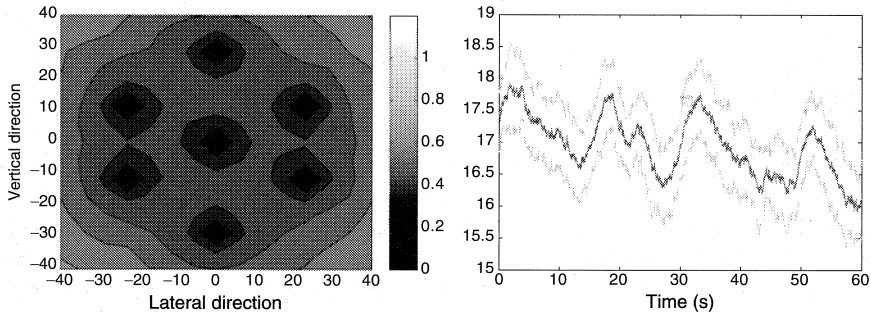
Fig. 3.2. Left: contour plot of the variance of the spatial constrained wind fields (averaged over time) over the rotor plane. Right: the mean (and plus/minus one standard deviation) of 30 constrained (7 anemometers) simulations; 17 m below the rotor centre

3.4 Load Calculations Based on Normal and Constrained Wind Field Simulations

The (un)constrained wind fields have been used as input for two standard wind turbine design tools: Flex5 and Bladed. Both packages feature among other things dynamic inflow, stall hysteresis and tip losses. Logarithmic wind shear is assumed and tower shadow is taken into account. In Flex5 the NEG Micon NM80/2750–60 is considered and in Bladed a generic 2 MW turbine. Both are pitch-regulated variable speed and have a diameter of 80 m, hub height of 60 m; the rated power is 2,750 kW and 2,000 kW respectively.

As example the time series of the calculated blade root flapping moment is shown in Fig. 3.3 based on the wind fields of Fig. 3.2. The response based on the "measured" wind is assigned "measured" load. The 1P (Ω=1.9 rad/s) response is clearly visible. The mean response of the constrained simulations gets more detailed, with increasing number of anemomenters / constraints, and the standard deviation decreases since the wind fields gets more fixed. Comparison with the filtered "measured" load shows that the constrained response captures the low frequency phenomena well.

In order to consider fatigue, the damage equivalent load ranges are considered of the blade root flapping moment (S–N slope 12). The load ranges and the frequencies of occurrence are found with the usual rain flow counting procedure.

It is anticipated that constrained simulation results into a smaller scatter of the obtained equivalent damage. As measure for the scatter the COV (coefficient of variation) is taken. The convergence of the COV has been checked by doing 100 simulations for a particular situation. It turned out that about 20 simulations are enough; the uncertainty in the COV is about 0.1 to 0.2.
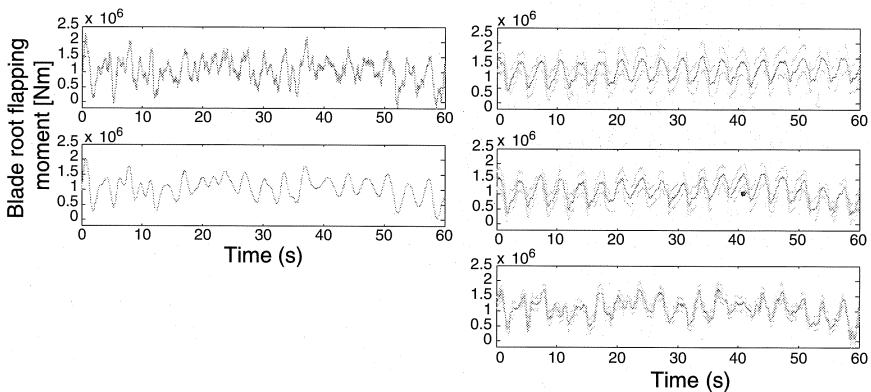

Fig. 3.3. Generic turbine: Left, top: "measured" flap moment; bottom: filtered flap moment. Right, from top to bottom: mean flap moment (plus/minus standard deviation) for 0, 1 and 7 anemometers/constraints. Note low frequency similarity
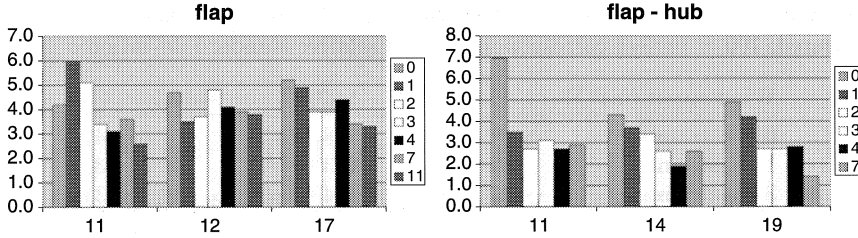
Fig. 3.4. COV of the blade equivalent flap moment range (left; generic turbine) and the flap moment range at the hub (right; NM80/2750). Mean wind speeds are indicated at bottom; legend indicates number of anemometers/constraints
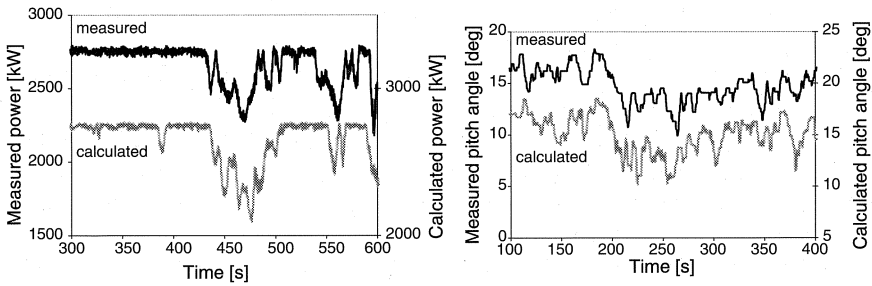

Fig. 3.5. Comparison between measurement and calculations (constrained wind in 1 point: rotor centre). Left: electrical power at $14.7\,\mathrm{ms}^{-1}$; right: pitch angle at $19.5\,\mathrm{ms}^{-1}$

In Fig. 3.4 (left) no clear trend can be observed; the reduction of the COV by constrained simulation is limited. Noticeable improvement is obtained however for the hub flap bending moment (right).

3.5 Comparison between Measured Loads and Calculated Ones Based on Constrained Wind Fields

Whether it is useful to use constrained wind in load verification can only be determined from a practical test. To this end we use the NEG Micon NM80 turbine in Tjæreborg (flat, open coastal terrain). The met-mast is located 200 m upwind of the turbine and has anemometers at 25, 41 and 60 m. Because the wind must come from a direction where the rotor sees the wind measured by the anemometer, only few measuring records could be used.

Two characteristic pictures are given in Fig. 3.5. It is clear that in both cases the low frequency behaviour is well captured (once the time delay from anemometer tower to wind turbine rotor has been incorporated, applying Taylor's frozen turbulence hypothesis), but that it is difficult to reproduce

Table 3.1. Relative mean equivalent flap moment range (calculated divided by measured; 100 = perfect correspondence) and relative standard deviation σ

Wind speed (ms^{-1})	11.4	14.7	19.5
0 constraints	87 (σ=4)	108 (σ=5)	107 (σ=4)
1 constraint	92 (σ=4)	103 (σ=4)	109 (σ=3)
3 constraints	92 (σ=3)	104 (σ=5)	112 (σ=3)

higher frequency phenomena. Even so, these comparisons are useful, for example it can be seen from Fig. 3.5 that apparently the pitch controller in the calculations is more "nervous" than the actual pitch system.

How good the load prediction is, is measured with the fatigue damage equivalent load. In Table 3.1 some results are given. Each selected measured 10 min. period was reproduced 20 times, respectively without constraint, and with wind constrained in 1 and 3 points. Mean and standard deviation of calculated load ranges are normalized by the measured load range. There is some improvement here and there, but on the whole it is not convincing. From the lack of improvement it must be concluded that the fatigue loads are mainly determined by high frequency wind variation, while the constraints only fix the low frequency wind (as can be seen in Figs. 3.3 and 3.5). We stress that at present it cannot be established whether this conclusion has general validity, because the limited number of load cases that were investigated.

3.6 Conclusion

If the method of constrained wind is used in load verification, the low frequency part of the wind and turbine loading can be reproduced well, which makes it possible to compare time traces directly. From the three load cases investigated here, it appeared that there was no improvement in predicted fatigue damage equivalent load ranges. However, more work is needed to verify this conclusion.

References

1. Wim Bierbooms, Simulation of stochastic wind fields which encompass measured wind speed series – enabling time domain comparison of simulated and measured wind turbine loads, EWEC, London, 2004

Recommendations with respect to standards and design

This dissertation deals with extreme loads on wind turbines due to turbulence. So, specific wind conditions like thunderstorms, front passages, downbursts and hurricanes are excluded. A probabilistic method has been presented to determine the 50 year value in the response of a wind turbine. The method relies on so-called constrained stochastic simulation. Through constrained simulation gusts can be generated which satisfy some specified constraint. It can be used in order to generate specific wind gusts which will lead to local maxima in the response of wind turbines. By performing many simulations (for given gust amplitude) the conditional distribution of the response is obtained. By a weighted average of these conditional distributions over the probability of the gusts the distribution for given mean wind speed is determined. The overall distribution of the response is obtained by a weighted average of the distributions for each wind speed bin taking into account the probability of occurrence of the wind speed bins.

Based on the performed research three recommendations can be formulated with respect to wind turbine standards.

In the IEC standard (IEC 61400-1 Ed. 3, 2005) an informative annex (annex F) is provided on the statistical extrapolation of loads for ultimate strength analysis. It is recommended that this annex becomes normative. If this is done, turbulence in the ultimate strength analysis will be treated in a stochastic rather than deterministic manner, just as is the case now for fatigue analysis. As a consequence the Extreme Operating Gust (EOG) will become obsolete. Also the use of the Extreme Turbulence Model (ETM) can be abandoned since through constrained stochastic simulation the specific gusts can be obtained which dominates the response.

A second recommendation is that the standard should focus on the 50-year response rather than the 50-year wind situation.

A practical bottleneck of a probabilistic approach is perhaps the required computational effort. Say, 100 simulations should be performed for each wind speed bin in order to obtain a reliable estimate of the response distribution function. Furthermore, suppose that in total 4 wind speed bins (between cut-in and cut-out) contribute to the 50 year response. So, in total 400 10-min. simulations should be carried out which will take in the order of 3 days on a PC (depending on design package and PC). This required computer time can be decreased significantly (a factor 2 or more) by the application of constrained stochastic simulation.

In the above mentioned IEC annex it is stated that one should consider at least 300 min. of time series (over the range of wind speed bins). The third recommendation is that not the simulation length is mentioned in the standard

but instead the required uncertainty range of the 50 year estimate, since the latter is of interest for a wind turbine designer.

Apart from a speed advantage the application of constrained stochastic simulation is profitable for a designer. As mentioned before, via constrained simulation the specific gust shape which dominates the response can be obtained. This information can be used in order to modify the design and/or the controller.

Furthermore, in this thesis analytical expressions for the conditional distribution of the response of linear models (for given gust amplitude) as well as the overall distribution (for given mean wind speed) are specified. These form an ideal test case of tools (e.g. fitting to an extreme value distribution) to be used for non-linear wind turbine models.

Appendix: Analytical expressions for the mean gust shape

In this thesis different expressions for the mean gust shape with amplitude A are mentioned which seem to contradict each other. For convenience they are here once more shown:

$$\bar{u}_{NewGust}(t) = A\,r(t) \tag{A.1}$$

$$\bar{u}_{ext_1}(t) = A\,r(t) - \frac{\sigma^2}{A}\;\{r(t) + \frac{\ddot{r}(t)}{\lambda}\} \tag{A.2}$$

$$\bar{u}_{max}(t) = A\,r(t) - E_{max}\,\frac{\sigma^2}{A}\;\{r(t) + \frac{\ddot{r}(t)}{\lambda}\} \tag{A.3}$$

with

$$E_{max} = \frac{e_{max}}{1 + e_{max}};\; e_{max} = \sqrt{2\pi}\,\gamma\,e^{\frac{\gamma^2}{2}}\,\Phi(\gamma) \tag{A.4}$$

and

$$\gamma = \frac{\lambda A}{\sqrt{\sigma^2(\mu - \lambda^2)}} \tag{A.5}$$

The auto correlation function is given by $r(t)$ and σ^2, λ and μ are the zeroth, second and fourth order spectral moment resp.

Eq. (A.1) follows immediately from the *New*Gust expression, Eq. (1) from Chapter 3 (with t_0 set to 0); Eq. (A.2) and (A.3) are resp. identical to Eq. (19), Chapter 3 and Eq. (3.12), Chapter 2. The mean gust shapes are depicted in Fig. A.1 and A.2.
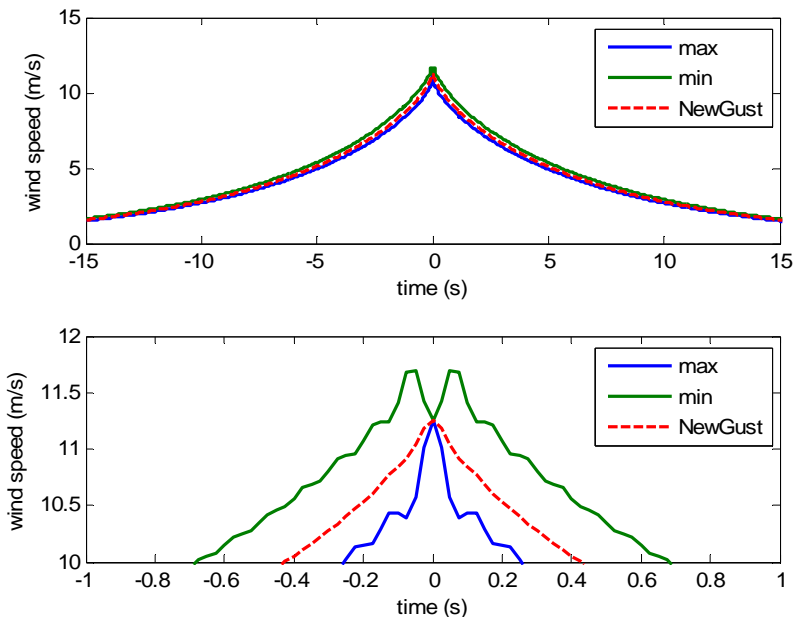
Figure A.1: Mean gust shapes of local maxima, Eq. (A.3), and local minima, Eq. (A.20), compared to NewGust, Eq. (A.1); U=10 m/s, σ=1.5 m/s and A=5. The graph at the bottom is a detail of the graph on top.

The reason for the differences is that the gusts have been defined dissimilar. Eq. (A.1) and (A.3) are based on the gust expression of constrained stochastic simulation. Eq. (A.3) is the mean shape of maximum amplitude gusts. By omitting the constraint that the extreme event has to be a local maximum leads to the *New*Gust simplification Eq. (A.1). For Eq. (A.2) local extremes have been considered but in a special way. To be more specific: both local maxima and local minima are taken into account but the latter are counted as -1. The idea behind this is the treatment of a peak with a small dip, which will regularly occur in a stochastic time series. Such a peak is counted as 2 maxima and 1 minimum thus in total as 2-1=1 extreme (instead of 2 maxima). In other words a peak with a small dip will have about the same effect on the average peak shape as a peak without a dip. Furthermore a dip (near the threshold *A*) in a flank of some higher peak will have a minor effect only on the mean gust shape as it is treated as 1 maximum and 1 minimum thus as 0 extremes.

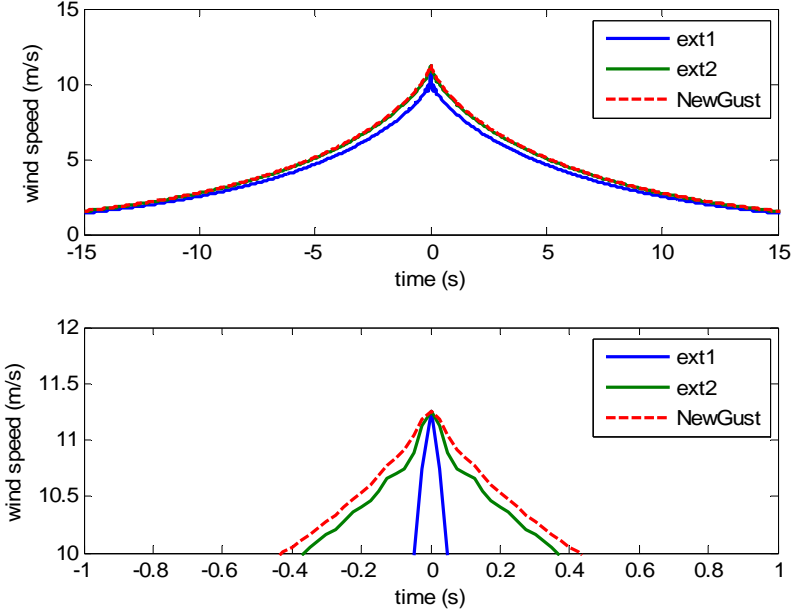Below it is shown that the three expressions are in line with each other.

Figure A.2: Mean gust shapes of local extremes, Eq. (A.2) and (A.27), compared to NewGust, Eq. (A.1); U=10 m/s, σ=1.5 m/s and A=5. The graph at the bottom is a detail of the graph on top.

Local maxima

We start with the expression for a maximum amplitude gust (Eq. (3.8), Chapter 2):

$$u_c(t) = u(t) + (\frac{\mu}{\mu - \lambda^2} r(t) + \frac{\lambda}{\mu - \lambda^2} \ddot{r}(t))(A - u(0)) + \frac{\dot{r}(t)}{\lambda} \dot{u}(0) +$$

$$(\frac{\lambda}{\mu - \lambda^2} r(t) + \frac{1}{\mu - \lambda^2} \ddot{r}(t))(B - \ddot{u}(0))$$

(A.6)

So the mean gust shape equals:

$$\overline{u_c(t)} = (\frac{\mu}{\mu - \lambda^2} r(t) + \frac{\lambda}{\mu - \lambda^2} \ddot{r}(t))A + (\frac{\lambda}{\mu - \lambda^2} r(t) + \frac{1}{\mu - \lambda^2} \ddot{r}(t))\overline{B}$$

(A.7)

In order to evaluate this expression the mean value of B has to be known. For the derivation of the statistics of B we use the method from appendix C, Chapter 5. For convenience the following 3 RV's are introduced (zero mean normal): $x = u(0)$, $y = \dot{u}(0)$ and $z = \ddot{u}(0)$. The probability of a local maximum

$$x = A, \ y = 0, \ z = B < 0$$

(A.8)

to take place in time interval dt can be expressed by:

$$P(A) = \int_A^{A+dA} \int_0^{-z\,dt} \int_{-\infty}^0 f_{x,y,z}(x,y,z)\,dx\,dy\,dz \approx dA\,dt \int_{-\infty}^0 |z|\,f_{x,y,z}(A,0,z)\,dz \qquad (A.9)$$

The function $f_{x,y,z}(x,y,z)$ is a 3 variate normal density function. According to Eq. (A.9) the probability of the event of a local maximum is obtained by integration over all possible values of the 2nd derivative z. In other words the density of B is given by the integrand of Eq. (A.9):

$$f_B(B) = \frac{|B|\,f_{x,y,z}(A,0,B)}{\int_{-\infty}^0 |B|\,f_{x,y,z}(A,0,B)\,dB} \qquad (A.10)$$

The denominator takes care of the normalization. The 3 variate density function can be written as:

$$f_{x,y,z}(A,0,B) = f_{z|x,y}(B\,|\,x=A,y=0)\,f_{y|x}(0\,|\,x=A)\,f_x(A) \qquad (A.11)$$

With respect to the normalization of Eq. (A.10) the first term $f_{z|x,y}$ only have to be taken from Eq. (A.11). The conditional density $f_{z|x,y}$ is again normal (univariate f_1) with mean and variance:

$$\mu_1 = -\lambda A; \quad \sigma_1^2 = \sigma^2(\mu - \lambda^2) \qquad (A.12)$$

So finally the density of B is given by:

$$f_B(B) = \frac{|B|\,f_1(B)}{\int_{-\infty}^0 |B|\,f_1(B)\,dB} \qquad (A.13)$$

The mean value of B is obtained through:

$$\overline{B} = \int_{-\infty}^0 B\,f_B(B)\,dB \qquad (A.14)$$

By e.g. means of special tools for formula manipulation like Maple it is possible to evaluate this expression analytically:

$$\overline{B} = \mu_1 + E_{\max}\frac{\sigma_1^2}{\mu_1} = -\lambda A - \frac{E_{\max}}{A}\frac{\sigma^2(\mu-\lambda^2)}{\lambda} \qquad (A.15)$$

Substitution in Eq. (A.7) leads to Eq. (A.3) the expression for the mean shape of local maxima as derived in Chapter 2; see also Fig. A.1.

Local minima
  Eq. (A.7) also holds for local minima
$$x = A, \; y = 0, \; z = C > 0 \qquad (A.16)$$
Similar to above the density of C equals:

$$f_C(C) = \frac{C\,f_1(C)}{\int_0^\infty C\,f_1(C)\,dC} \qquad (A.17)$$

The mean of C is given by:

$$\overline{C} = \int_0^\infty C\,f_C(C)\,dC = \mu_1 + E_{\min}\frac{\sigma_1^2}{\mu_1} = -\lambda A - \frac{E_{\min}}{A}\frac{\sigma^2(\mu-\lambda^2)}{\lambda} \qquad (A.18)$$

with

$$E_{min} = \frac{e_{min}}{1+e_{min}}; \; e_{min} = -\sqrt{2\pi}\,\gamma\, e^{\frac{\gamma^2}{2}}\, \Phi(-\gamma) \tag{A.19}$$

leading to the following mean gust shape for local minima (see also Fig. A.1):

$$\bar{u}_{min}(t) = A\,r(t) - E_{min}\,\frac{\sigma^2}{A}\,\{r(t) + \frac{\ddot{r}(t)}{\lambda}\} \tag{A.20}$$

Local extremes

For the mean shape of local extremes the mean gust shapes of local maxima and local minima have to be combined. For this purpose the number N_{max} of local maxima and N_{min} of local minima, in given time period, are required. From Eq. (A.9) we obtain:

$$N_{max} = \frac{P(A)}{dt} \approx dA \int_{-\infty}^{0} |z|\, f_{x,y,z}(A,0,z)\,dz \tag{A.21}$$

$$N_{min} \approx dA \int_{0}^{\infty} z\, f_{x,y,z}(A,0,z)\,dz \tag{A.22}$$

Further on, only the ratio of the numbers is needed so common factors can be ignored.

$$N_{max} \sim \int_{-\infty}^{0} |B|\, f_1(B)\, dB = (1+e_{max})\,\frac{\sigma_1}{\sqrt{2\pi}}\, e^{-\frac{\gamma^2}{2}} \tag{A.23}$$

and

$$N_{min} \sim \int_{0}^{\infty} C\, f_1(C)\, dC = (1+e_{min})\,\frac{\sigma_1}{\sqrt{2\pi}}\, e^{-\frac{\gamma^2}{2}} \tag{A.24}$$

The expression for the mean shape of extremes counting local minima as -1 equals:

$$\bar{u}_{ext_1}(t) = \frac{N_{max}\,\bar{u}_{max}(t) - N_{min}\,\bar{u}_{min}(t)}{N_{max} - N_{min}} =$$

$$A\,r(t) - \frac{N_{max}\,E_{max} - N_{min}\,E_{min}}{N_{max} - N_{min}}\,\frac{\sigma^2}{A}\,\{r(t) + \frac{\ddot{r}(t)}{\lambda}\} \tag{A.25}$$

The factor in the 2nd term can be evaluated by substitution of Eq. (A.4), (A.19), (A.23) and (A.24):

$$\frac{N_{max}\,E_{max} - N_{min}\,E_{min}}{N_{max} - N_{min}} = \frac{e_{max} - e_{min}}{e_{max} - e_{min}} = 1 \tag{A.26}$$

So, Eq. (A.25) indeed equals Eq. (A.2) the expression for the mean shape of local extremes as derived in Chapter 3; see Fig. A.2.

For completeness, also the expression is given for the mean shape of local extremes counting local minima as +1 (see also Fig. A.2):

$$\bar{u}_{ext_2}(t) = \frac{N_{max}\,\bar{u}_{max}(t) + N_{min}\,\bar{u}_{min}(t)}{N_{max} + N_{min}} =$$

$$A\,r(t) - \frac{N_{max}\,E_{max} + N_{min}\,E_{min}}{N_{max} + N_{min}}\,\frac{\sigma^2}{A}\,\{r(t) + \frac{\ddot{r}(t)}{\lambda}\} \tag{A.27}$$

The factor in the 2nd term can be rewritten as:

$$\frac{N_{max} E_{max} + N_{min} E_{min}}{N_{max} + N_{min}} = \frac{e_{max} + e_{min}}{2 + e_{max} + e_{min}} = \frac{\sqrt{2\pi}\, \gamma\, e^{\frac{\gamma^2}{2}} (2\Phi(\gamma) - 1)}{2 + \sqrt{2\pi}\, \gamma\, e^{\frac{\gamma^2}{2}} (2\Phi(\gamma) - 1)} \qquad (A.28)$$

One may wonder why Eq. (A.27) deviates (a little bit) from Eq. (A.1), see Fig. A.2. This is due to the fact that Eq. (A.1) is based on the condition

$$x = A, \ y = 0 \qquad (A.29)$$

This condition not automatically implies a local extreme. It may happen during a (almost) horizontal part of the time series (inflexion point), see Fig. A.3b. Vice versa, a local extreme does not always fulfill condition Eq. (A.29), see Fig. A.3c. In fact, a local extreme is determined by a zero crossing of y, the first time derivative of the wind speed. A zero crossing will occur, in a small time interval dt, in case y is in between 0 and $-z\, dt$ (with z the second time derivative). Note that the integration limits in Eq. (A.9) are taken accordingly. So, for a local extreme the specific range of y is depending on z in contrast to a fixed range to be taken in case of the condition according to Eq. (A.29).

The result of Eq. (A.1) can be obtained by considering Eq. (A.7) as the mean shape of the event given by
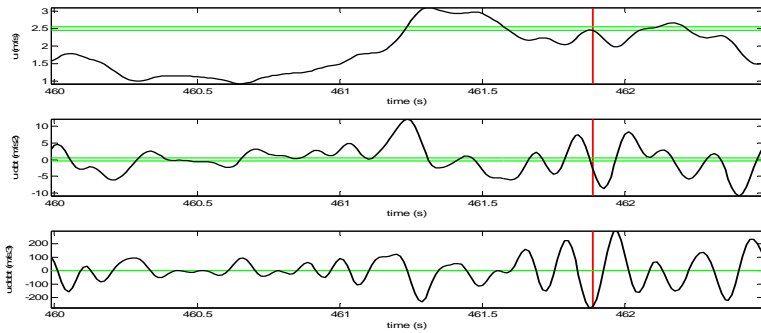
$$x = A, \ y = 0, \ z = D \qquad (A.30)$$

(i.e. it is left open if it is a local maximum or local minimum or even an inflexion point). So, D is the 2nd derivative of the wind speed on condition Eq. (A.29). As mentioned previously, the corresponding conditional distribution equals f_1 and its mean is given by Eq. (A.12). Substitution into Eq. (A.7) indeed leads to Eq. (A.1).
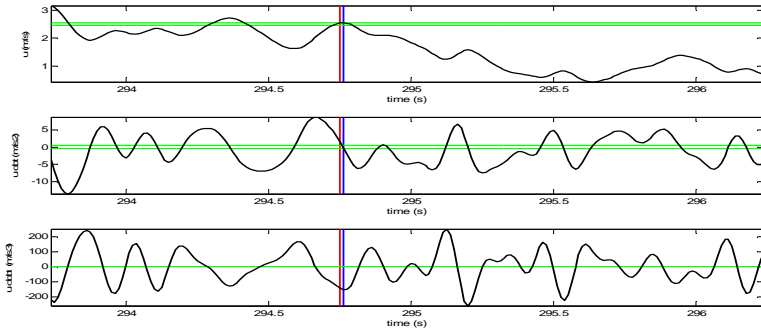
a)
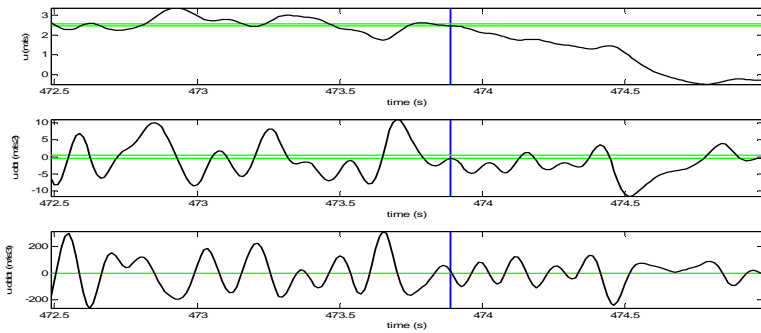
b)

c)

Figure A.3: Three different wind speed time series. Two conditions are considered:

- *vertical red line:* $2.45 < u < 2.55$ *; zero crossing in* $\dot{u}$ *(local extreme)*
- *vertical blue line:* $2.45 < u < 2.55$ *;* $-0.5 < \dot{u} < 0.5$

The mean wind speed (on top) as well as its first (middle) and second (at the bottom) time derivative is shown.

Curriculum Vitae

Wilhelmus Anna Adrianus Maria Bierbooms was born on 7 December 1959 in Eindhoven, The Netherlands.

He obtained his diploma Atheneum B (1978) at the Lyceum Augustinianum in Eindhoven. He graduated in 1986 at the Technical University Eindhoven at the faculty of Applied Physics. He joined the Section of Wind Energy of the Technical University of Delft later that year as research assistant. He has been involved in projects concerning the design and dynamics of wind turbines (Indymo, Duwecs, Focus, WindSim) as well as offshore wind energy (Opti-Owecs, Dowec, WE@Sea). Currently, as assistant professor at the Wind Energy Research Group he is focusing on wind field simulation (Swing, *New*Gust) and is responsible for the courses *Introduction to Wind Energy* and *Wind and Site Conditions*.

In his spare time he likes to run, cycle and skate.